FACULTY OF MEDICINE AND DENTISTRY

PALACKÝ UNIVERSITY OLOMOUC

Effect of subtractive machining of lithium disilicate glass dental ceramic on strength and the possible improving mechanisms

MDDr. Kristýna Hynková

Olomouc 2023

TABLE OF CONTENTS

1.	**PREFACE**	**6**
2.	**STATE OF THE ART**	**7**
2.1.	**History**	**7**
2.2.	**Introduction to dental ceramic**	**10**
2.3.	**Composition of dental ceramic**	**11**
2.3.1.	Glass	11
2.3.2.	Crystals	12
2.4.	**Classification of dental ceramic**	**13**
2.4.1.	Classification by microstructure	13
	2.4.1.1. Predominantly glassy ceramic	13
	2.4.1.2. Particle – filled glasses	13
	2.4.1.3. Polycrystalline ceramics	14
2.4.2.	Classification by manufacturing process	15
	2.4.2.1. CAD/CAM	15
	2.4.2.2. Hot pressing	22
	2.4.2.3. Conventional method	24

2.5. CAD/CAM dental ceramic 27

2.5.1. Feldspar ceramic 27

2.5.2. Leucite ceramic 31

2.5.3. Lithium disilicate glass ceramic 33

2.5.4. Lithium disilicate glass ceramic reinforced by zirconia 36

2.5.5. Zirconia ceramic 37

2.5.5.1. 3Y – TZP zirconia 44

2.5.5.2. Cubic zirconia 45

2.5.6. Additional group 46

2.6. Mechanical properties of dental ceramic 47

2.6.1. Strength 49

2.6.2. Elasticity 50

2.6.3. Plasticity 51

2.6.4. Hardness 52

2.6.5. Toughness 52

2.6.6. Brittleness 54

2.6.7. Stiffness 56

2.6.8. Ductility 56

2.6.9. Measurement methods 56

2.6.9.1. Strength 56

2.6.9.1.1. Uniaxial strength 57

2.6.9.1.2. Biaxial strength 58

2.6.9.2. Hardness 59

2.6.9.3. Fracture toughness 60

2.6.10. Limiting factors of strength of dental ceramic 62

2.6.11. Defects caused by subtractive machining 64

2.6.11.1. Negative factors 65

2.6.11.1.1. Use 66

2.6.11.1.2. Heat 66

2.6.11.2. Remedies 68

2.6.11.2.1. Crystallization process 68

2.6.11.2.1.1. Crystallization process of lithium disilicate glass ceramic 69

3. The effect of pre-crystallization defect size on strength limitation lithium silicate glass ceramic 72

3.1. Objective 72

3.2. Hypothesis 72

3.3. Brief Introduction to the study 72

3.4. Materials and methods 73

3.4.1. Test specimen manufacture 73

3.4.2. Controlled defect generation 74

3.4.3. Crystallization process 76

3.4.4. Optical microscopy 76

3.4.5. Atomic force microscopy 78

3.4.6. Bi – axial flexural strength (BFS) determination 79

3.4.7. Statistical analysis 81

3.5. Results 81

3.6. Discussion 85

3.7. Conclusion 88

4. REFERENCES 89

5. LIST OF FIGURES 101

6. LIST OF TABLES 104

7. LIST OF EQUATIONS 105

8. CONTRIBUTIONS 106

9. ACKNOWLEDGMENTS 108

10. UNDERTAKING 109

1. PREFACE

Failure of ceramic prosthetic reconstructions in the form of cracks, fractures or chipping is unfortunately an integral part of the prosthetic surgery. While the use of modern technologies in dental surgeries and laboratories makes our work easier and saves us time, little is known that these modern technologies can introduce strength limiting defects in brittle materials such as ceramics. These defects can affect the durability and success of the work. Even if such defects are not caused by the dentist, they can negatively affect the patient's view of the dentist and the whole dental surgery. Good understanding of ceramic materials and their properties is an integral part of a positive treatment result for the doctor and the patient. This dissertation brings information about dental ceramic, its mechanical properties, defects caused by manufacturing methods and possible help to mitigate these strength limiting defects.

2. STATE OF THE ART

The word “ceramics” now represents a wide range of materials with varying structure, chemical composition, and usage [1]. It is used in the production of jewellery, tableware, in the construction industry, in sculpturing and last but not least - in dentistry. This chapter introduces its origins and the first applications in dentistry. We will also provide a fundamental classification based on its composition.

2.1 History

The word” ceramics" comes from the Greek word "ceram, ceramos", which can be translated as "potter or pottery"[2] The history of ceramics dates back to the Palaeolithic age, circa 28000 BC. The oldest discovery from this age is a ceramic statue called “Venus of Dolní Věstonice”, found in the Czech Republic [3]. Over the centuries, the use of ceramics has increased, and its chemical composition and types of production processes have changed.

Chinese porcelain was already known in the 7th century AD. Thanks to the voyages of the famous seafarer Marco Polo, Europeans learned about the existence of Chinese porcelain. Because of the glitter of the Chinese porcelain, Marco Polo described the beauty of porcelain by the pearly luster of a seashell; he used the Italian word porcellana - “seashell”. Great interest in porcelain then boomed in Europe during the 17th century. Wealthy rulers bought pottery from China and Japan as a proof of their prestige and wealth. Thus, China became known as the "Bleeding Bowl of Europe" [4]. The largest collection in Europe was owned by August II of Saxony (also known as August the Strong), and today is part of the museum's permanent exhibition at the Zwinger castle in Dresden [4,5]

Due to its aesthetic properties that imitate very well dental hard tissues, experts started to speculate about the use of porcelain in the field of dentistry.

Use in Dentistry

In the second half of the 18th century, Parisian pharmacist Alexis Duchateau was very unhappy with the use dental dentures due to malodour and unsatisfactory aesthetic and mechanical properties after a long-term wear. He searched for Parisian dentist Dubois de Che´mant, to ask him for help with manufacturing of the porcelain dentures. After a long research and cooperation with porcelain factory Guerhard & Dahl, they succeeded and the first porcelain denture was made in 1774 [2,4,6,7]. Previously, the technicians needed to use human or animal teeth to make dentures, so the use of porcelain was a huge achievement for dentistry as well as an improvement in personal oral hygiene [7].

After this huge development Dubois de Che´mant further improved its parameters, such as translucency. Initially, teeth were baked in a single block together with the gums. In 1808, Fonzi introduced his invention of single teeth with platinum pins (History of dentistry; a practical treatise for the use of dental students and practitioners). In 1890, Land then introduced jackets crowns, which were very fragile, and their indication was only for frontal teeth.

Substantial development in ceramic dentistry came in 1962 by Weinstein, when a new composition of dental ceramic allowed to fire ceramics using classic casting alloys [4,6,8]. It was found that melting feldspar rock followed by immediate cooling results in a special glass mass. This process is then referred to as incongruent melting. Thanks to a new leucite crystals component in material composition, his glass has a higher coefficient of thermal expansion. The higher coefficient of thermal expansion then allows to create a ceramic mix suitable for firing on any classic casting alloys [4].

A come-back of an all-ceramic restoration came in the second half of the 20th century, when McLean and T.H. Hughes developed a new version of the porcelain jacket crown with an inner core of aluminous porcelain (40% to 50% alumina crystal). This porcelain was made

by adding industrial aluminous porcelain (>50%) to feldspathic porcelain manufacturing. This ceramic was very opaque, and it had higher strength in comparison to traditional jacket crowns (previously developed by Land), but it was still only used in the anterior region as the low mechanical properties did not favour lateral reconstructions [4,8–11].

In the 1950s, the lost wax manufacturing technique of Dicor ceramic (used for all crown reconstruction) was very popular. In the 1980s, pressing technique further improved the lost wax technique. The ingots of Empress 1 (leucite reinforced glass ceramic) were heated and pressed into the special mold in the pressing furnace [11].

In the late 20th century, the infiltrated glass ceramic was favoured as this ceramic achieved good mechanical properties. This ceramic has then been replaced by modern CAD-CAM and zirconia ceramic.

Between the 1950s and 1960s, CAD/CAM technology (Computer aided design/Computer aided manufacturing) was initially used in the automotive and aircraft industries. Dr. Duret was the first, who presented the use of CAD/CAM technology in dentistry in 1971, and the first to make dental restoration with CAD/CAM technology in 1983 [12–15]. The same year, dr. Andersson and Odén introduced the Procera system, which allowed them to make highly precise prosthetics restorations [12,15]. The process consisted of scanning models in the laboratory with a sapphire ball and then sending this information to the Procera working station. After that, a second control enlarged model (15-20% larger to compensate for the alumina oxide shrinkage during the sintering process) was made. The alumina oxide powder was pressed on the enlarged model to form a highly dense mass, and then milled to the required shape before sintering [8,16].

The year 1987 marks a revolution in the use of CAD/CAM in dentistry - Dr. Mörmann and Brandestini introduced the CEREC system (Sirona). CEREC was the first system which connected scanning and milling device. It was the first practical chair-side system used by

dentists. Since its introduction, the system has undergone many upgrades - from wheels to different types of diamond burs and software improvements. Nowadays, it is possible to produce inlays, onlays, veneers, crowns, three-unit bridges and also implant abutments [12– 15,17–19].

2.2 Introduction to the dental ceramic

Material for dental restorations ideally mimics the dental hard tissues such as dentin and enamel. Critical properties include biocompatibility, chemical resistance, good optical properties (i.e. similar to hard dental tissues), mechanical properties akin to dental tissues, easy production and reasonable price.

Dental ceramics currently provide the best available properties - biocompatibility, long-term colour stability, wear resistance, chemical durability, strength in compression and their very good look thanks to optical properties close to dental hard tissues [20–22]. Dental ceramics is of course not perfect, and (as any other dental material) comes with compromises. It is brittle, it is harder than dentin (7x) and enamel (0.3x) and thus wears antagonal teeth [21] and it is weak in tension. Moreover, expensive manufacturing machines are often needed for fabrication, and a skilful dental technician is required to create the restoration [6,20–22].

2.3 Composition of dental ceramic

Ceramics are inorganic materials, generally composed of metallic and non-metallic components. Atoms or oxide groups of molecules are linked by a covalent or ionic bond. Most are semi-crystalline in nature and are composed of crystalline and amorphous glassy phases (Fig.1) [7,23].

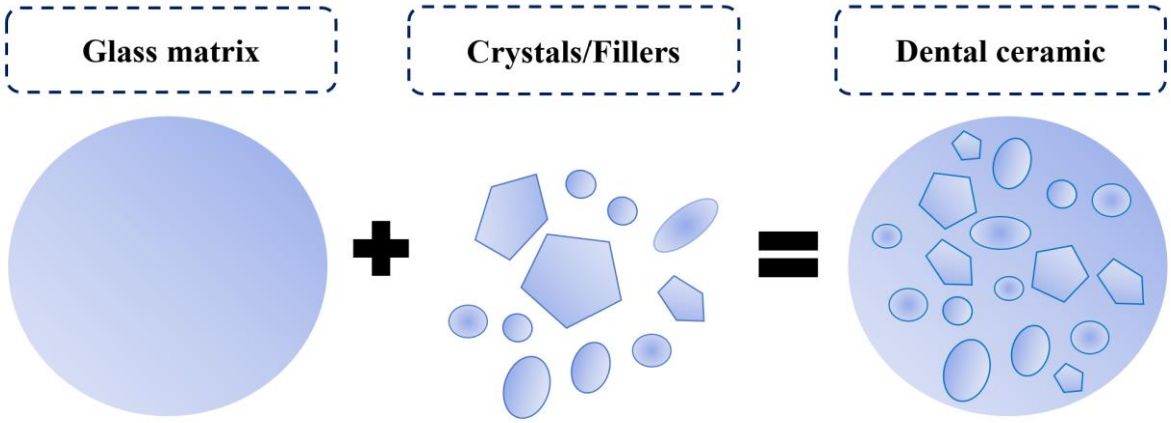

Figure 1: Composition of dental ceramic.

2.3.1 Glass

Glass is an amorphous solid without definite lattice pattern. The molecules are not organised. Dental glasses are based on silica (SiO_2) network and potash feldspar (K_2O-$Al2O_3$-$6SiO_2$), soda feldspar (Na_2O-Al_2O3-$6SiO_2$), or both. These feldspathic glasses fall into a family called “aluminosilicate glasses” [4,7,10,23]. The silicon-oxygen-silicon bond is occasionally broken by natrium or potassium. These modifying cations can help to change the firing temperature or coefficient of thermal expansion of the glass.

2.3.2 Crystals

Crystal's function is to alter mechanical properties of dental ceramic. Glass has perfect optical properties but is very fragile. The more glass content the better optical properties - the ceramic is more translucent and mimics better the optical properties of dental hard tissues (such as dentin and enamel).

Increasing the content of crystals results in improved mechanical properties such as toughness, but decreases the optical properties (e.g. by increasing opacity). The crystals work as buffers and stop or slow the crack propagation. The crystals can be formed in a glass matrix by crystallization process or can be added artificially to the glass matrix to increase the mechanical properties (Fig.2). In some cases, high melting glass fillers are added to the glass matrix instead of crystals.

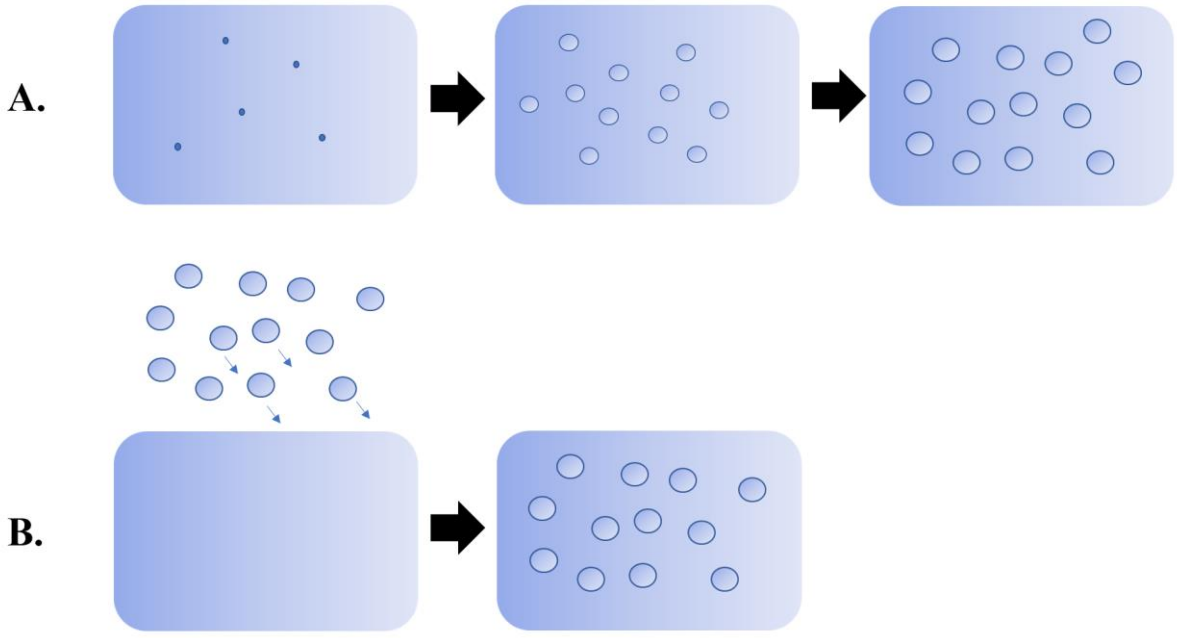

Figure 2: Creation of crystals in glassy matrix. A - Crystals are formed naturally in the glassy matrix by ceraming or control crystallization process. B - Crystals/glass fillers are added to the glass matrix artificially.

2.4 Classification of dental ceramic

There are multiple classifications available in the dental literature, making it somewhat confusing for the readers. These classifications are typically based on microstructure, chemical composition, firing temperature, clinical application, manufacturing process and indications [4,6,21]. The classification used in this dissertation thesis is based on microstructure and manufacturing process. We believe this type of classification helps dental clinicians in their practice to choose the right ceramic material for their specific needs.

2.4.1 Classification by microstructure

A common classification categorizes the materials based on their microstructure composition. The concrete categorization chosen in this work is based on (Kelly).

Based on the microstructure (glass/crystal content), the ceramic can be divided into three groups: predominantly glass ceramic, particle filled ceramic, polycrystalline ceramic (Fig.3) (Classification by Kelly [4]).

2.4.1.1 Predominantly glassy ceramics

This ceramic has a large amount of glass and is highly aesthetic, best mimicking optical properties of enamel and dentine. As was previously mentioned (see 2.3.1), glasses in dental ceramic are usually based on aluminosilicate glasses. These glasses are relatively resistant to crystallization during firing.

2.4.1.2 Particle-filled glasses

Compositions based on two or more phases are formally known as “composites”.

As discussed, the crystalline fillers or high melting glass fillers are added to the glass matrix to improve the mechanical properties and to control optical properties (such as translucency, opacity, opalescence, and fluorescence effects). Modern fillers are mainly leucite crystals ($KAlSi_2O_6$), lithium silicate ($Li_2Si_2O_5$), zirconia (ZrO_2), fluorapatite ($Ca_5(PO_4)_3F$) crystals, nepheline (Na, K) $AlSiO_4$, albite $NaAlSi_3O_8$ and high melting glass. Most of the ceramics available on the market fall to this group. These include glass ceramic with low content of leucite (referred to as feldspathic porcelain), high leucite containing glass, lithium disilicate glass ceramic, lithium disilicate ceramic reinforced by zirconia, fluorapatite glass ceramic and others.

2.4.1.3 Polycrystalline ceramics

Polycrystalline ceramics are very strong as there are no glassy components, and all the atoms are densely packed into regular arrays. Due to no content of glass, the ceramic has the lowest aesthetics properties and is very white and opaque. The mechanical properties such as strength and fracture toughness are the highest within the group, so this ceramic is indicated in parts that are under heavy load. A representative of this group is zirconia dental ceramic [4,24].

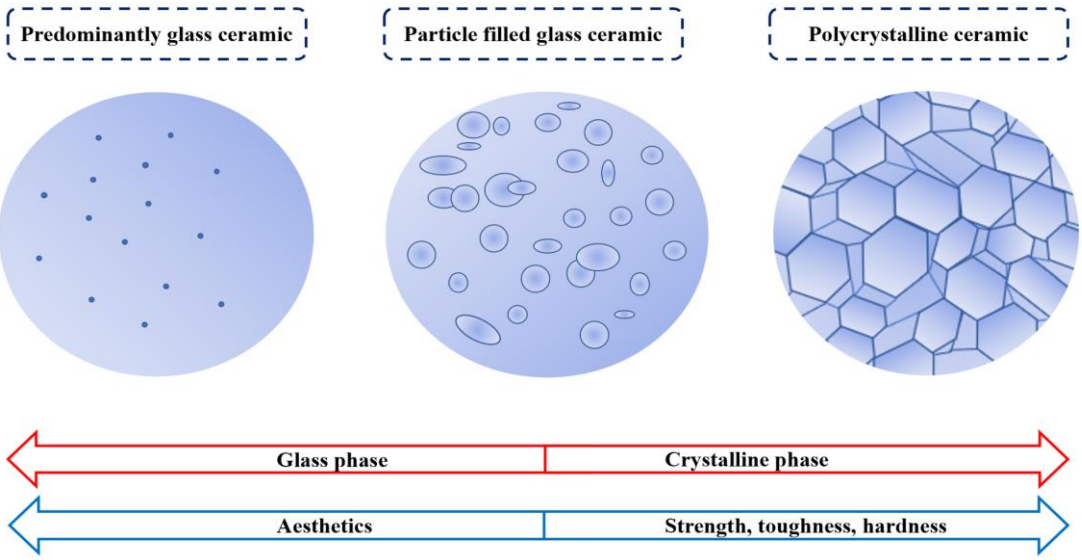

Figure 3: Classification of dental ceramic by glass/crystalline content.

2.4.2 Classification by manufacturing process

Given a dental ceramic material, one needs to create the required dental restoration - and there are multiple manufacturing processes to choose from. Different ceramics are then designed to be used in different manufacturing processes.

2.4.2.1 CAD/CAM (computer aided design/computer aided manufacturing)

CAD/CAM manufacturing is a three-step process consisting of i) scanning the tooth ii) creating and adjusting a 3D model of the restoration iii) computer manufacturing process (either 3D printing or CNC). CAD/CAM system thus consists of three parts: scanner, software and manufacturing device [12,13,15,19].

Data acquisition - Scanners

Scanners are used to collect data about the situation of the oral cavity. The scanners can be divided according to the place of use - intraoral scanners and extraoral scanners. The intraoral scanners scan the oral cavity directly and the scanning procedure is commonly performed by the dentist. The extraoral scanners are a combination of analog-digital processes. This process is performed in a dental laboratory and the 3D data are derived by scanning the plaster models or impressions. The photo of the intraoral scanner is demonstrated in figure 4.

The advantages of intraoral scanners mean that no additional materials and devices such as impression tray, impression material or plaster are needed. The intraoral scanners are smaller

and handier for dentists. On the other side the extraoral scanners are more accurate and are faster.

Figure 4: Photo of intraoral scanner (CEREC Omnicam AC).

The scanners can also be divided according to different scanning techniques to mechanical (contact) and optical scanners (non-contact). Mechanical scanning is now obsolete - the master 3D structure was read manually by ruby ball. This process was then very slow and complicated.

Optical scanning or non-contact digital scanning is a method which uses light to capture the surface of a 3D structure. Scattered signal is captured by a scanner, and the analogue signal is digitized and processed with software, resulting in a digital image. The optical image acquisition can be divided into active and passive processes. Passive processes use non-coherent light sources such as ambient light. For example, the passive triangulation

process belongs to this group. The active process uses structured coherent light. This light is usually generated by lasers or LED diodes that project stationary or oscillating codes (patterns like dots, stripes, …) on the surface of the scanning surface. For example, the active triangulation, accordion fringe interferometry and confocal laser scanning microscopy processes and more belong to this group [12,19,25].

Software

Computer aided manufacture software (CAD) allows designing a virtual restoration. Dentists or lab technicians can see a 3D model of the scanned teeth on a screen of the computer. The CAD software then leads users step by step. Material can be selected, type of required restoration (inlay, onlay, crown, veneer etc.), mark the preparation boundaries and design future restoration. After designing the restoration, the dentist can virtually fit the restoration into a ceramic block and send the data to the milling machine (Fig.5) [12,18].

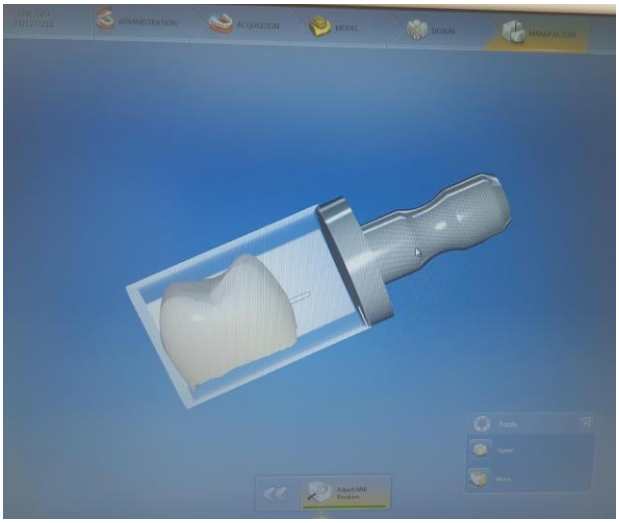

Figure 5: Virtual crown fit in virtual software block.

Machining device - Machining process

Final step is the computer manufacturing process (CAM), which can be classically divided into 3D printing or CNC (computer numerical control) manufacturing.

- ***Additive manufacturing***

The 3D printing uses an additive process - the object is built layer by layer. Additive processes for dental ceramic include methods such as powder bed fusion (SLS - Selective laser sintering), material jetting (NPJ - Nanoparticle jetting), binder jetting (BJ - Binder jetting) [25]. To the best of the author's knowledge, these processes are not yet commonly used for manufacturing of ceramic restorations in dental offices. As the next step we give a brief explanation of these processes.

SLS - Selective laser sintering is classified as a powder bed fusion process. SLS consists of a vat filled with powder and a laser beam. The laser beam selectively sinters powder layer by layer and builds the required object (Fig.6). The selective sintering is very similar to the most famous 3D printing method called SLA (Stereolithography), which uses a resin bath instead of the powder.

BJ - This method uses a bonding agent to stick particles together, forming the required shape of restoration layer by layer (Fig.7).

NPJ - Nanoparticle jetting, falls into the material jetting group of 3D printing process. This process uses nanoparticles of ceramic suspended in liquid. When the nanoparticles are jetted by layers to the build platform, any excess liquid is evaporated by high temperature in the chamber. This stage of product (after the evaporation) is called the green stage. The green stage does not have final mechanical properties and needs to be sintered to get the final product (Fig.8) [25].

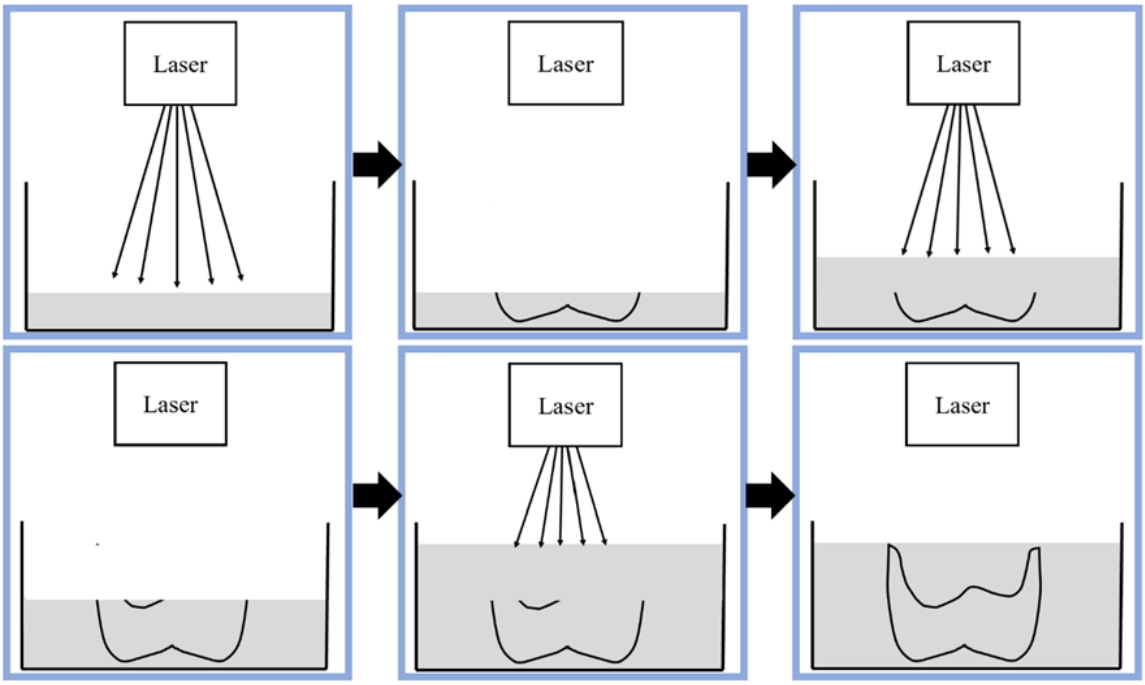

Figure 6: Graphical demonstration of selective laser sintering.

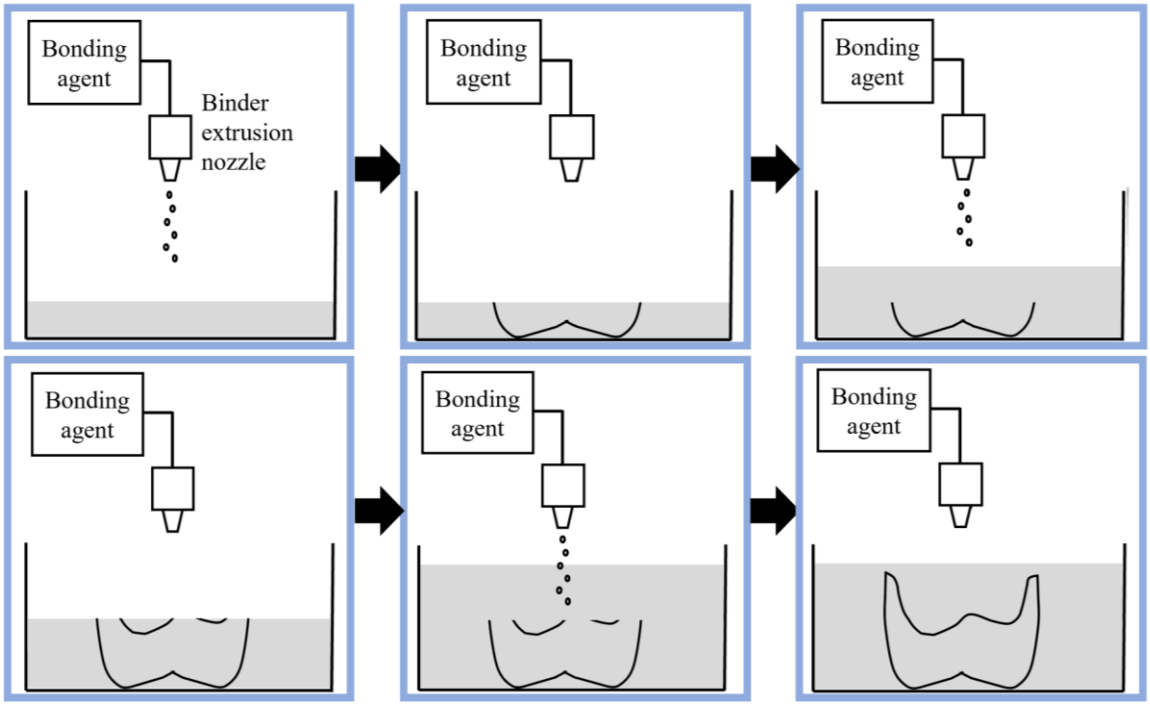

Figure 7: Graphical demonstration of binder jetting.

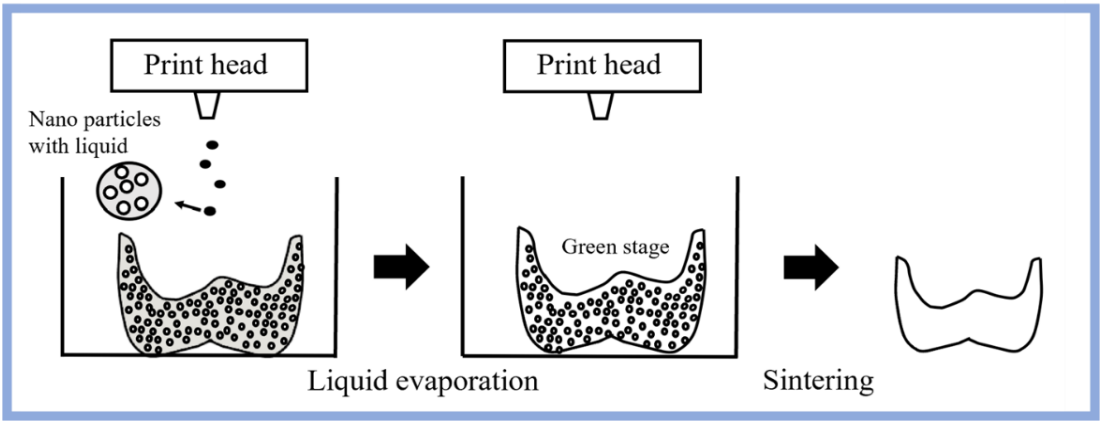

Figure 8: Graphical demonstration of nanoparticle jetting. Comment: the subject is printed in several layers which is not denoted in the picture.

- ***Subtractive manufacturing***

The subtractive machining process is usually applied for manufacturing dental ceramic reconstructions, where the CNC (computer numerical control) - milling machines are used. The milling devices can be divided based on the number of milling axes: 3-axes (XYZ), 4-axes (XYZA), 5- axes (XYZAB) devices. Most chair side machines are 4-axes. The difference between the different axis machines is the size area which can be milled. The axis directions are demonstrated in figure 9 [12,26].

There are two terms used for the subtractive machining process - grinding and milling. The process is referred to as grinding when diamond-coated burs are used, and referred to as milling when carbide burs are used (especially for machining zirconia ceramic).

The block or disc of dental ceramic of the required colour and size are fitted into the milling unit. For the manufacturing process, burs of different shapes are used. Contact of the bur with the ceramic causes local stress, resulting in micro-fractures, chipping, and consequent material loss. This material loss is how the final shape of the restoration is achieved (Fig.10) [12,14,15,18,27]. Usually, the restoration is still attached with a sprue to the rest of the dental

ceramic block/disc, and it needs to be removed (Fig.10). The restoration in a non-fully sintered (green stage, partially sintered stage) or partially crystallized stage then undergoes additional firing process (crystallization, sintering). All restorations in fully crystallized and fully sintered stages are then finally attached with veneering, polishing, glazing or staining procedure.

- ***Chair side system***

A very popular system used nowadays in dental offices is called Chair side CAD/CAM. Chair side CAD/CAM system is a sophisticated system that allows dentists to i) intraorally scan the treated tooth, ii) design, iii) fabricate and iv) also fixation of prosthetics restoration in a single appointment. Thanks to this system, dentists are not dependent on dental technicians. One the other hand, the system is quite expensive as the dentist needs to own an intraoral camera, software and the manufacturing machine [13,18].

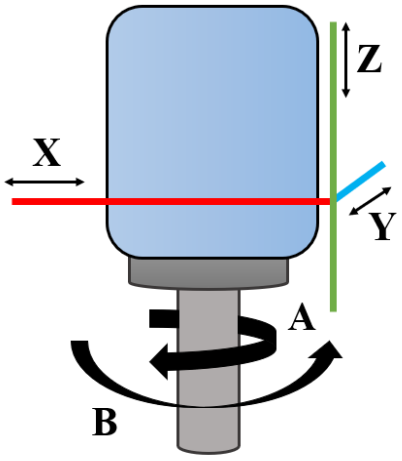

Figure 9: Milling axis. X axis - moves from left to right. Y axis - moves back to front. Z axis - moves up to down. A axis - rotate around X axis. B axis - rotate around Y axis.

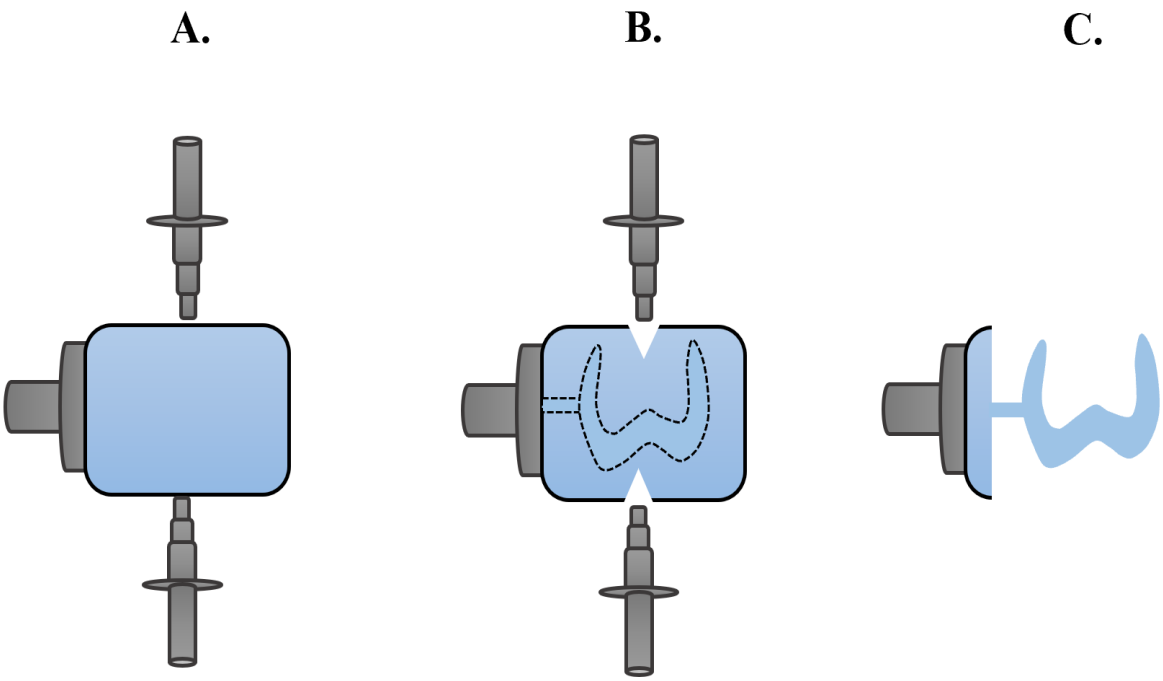

Figure 10. Graphical demonstration of subtractive machining. A - Ceramic block with diamond or carbide burs ready for grinding/milling process B - Start of grinding/milling process. C - Grinded/Milled required shape of dental ceramic restoration still attached with sprue to the rest of the dental ceramic block.

2.4.2.2 Hot pressing

Hot pressing manufacturing process is very similar to casting alloys. First, the technician needs to create wax patterns of dental restoration. The press wax sprues are then attached to the wax patterns and to the crucible former of the press moulding ring. The silicone ring with the wax patterns in the middle is then invested with phosphate bonded investment material. After setting of the investment material, the silicon ring and cylinder crucible former are removed. The invested mold is placed into a burnout furnace, where the wax patterns of reconstruction are burned out without any residue. The cylindrical entrance to the mold is then filled with ceramic ingot and preheated to a specific temperature. The dental ceramic is then pressed into basic the empty dental reconstruction mold in the furnace (Fig.11). After the

cooling process, the dental reconstructions are removed from the investment mold and further adjusted. The copping is veneered with compatible veneering porcelains to build up the final restoration. The monolithic restoration is polished/stained/glazed directly. There are available pressable dental ceramics for copping, full crown restorations but also dental pressable ceramic for veneering [28].

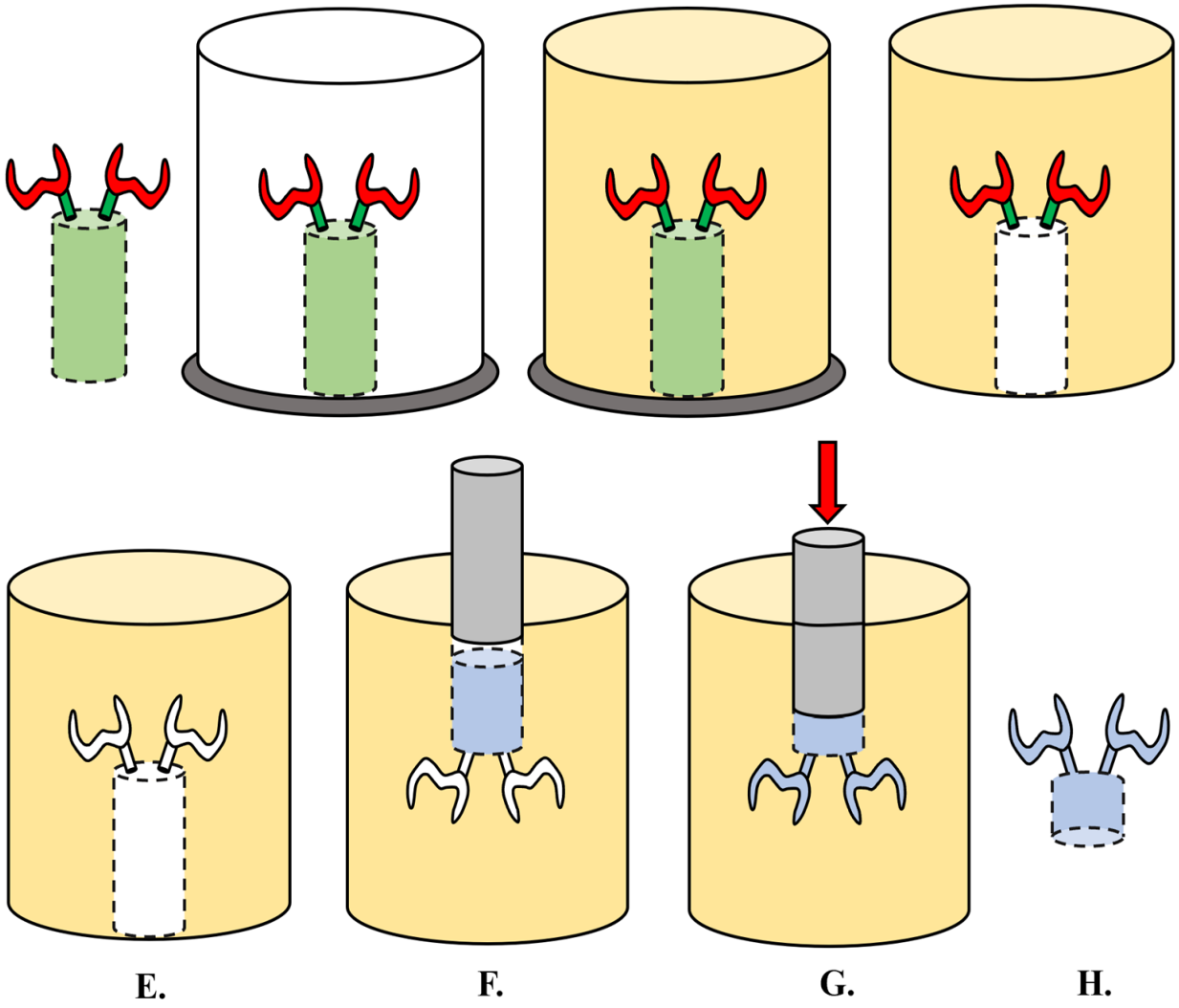

Figure 11: Graphical demonstration of hot-pressing process. A - Wax patterns crowns with press wax sprues are attached to the cylinder crucible former. B - Connection of silicon ring - to help to create the mold. C - Investment. D - After setting of investment material, the cylinder crucible former is removed to create the space for ceramic ingot. E - Burning wax patterns without residue. F - Melting of the ceramic ingot. G - Pressing melted ceramic material into crown mold created by burning wax patterns. H - Ceramic pressed crowns attached by sprues to the rest of ceramic ingot.

2.4.2.3 Conventional method

The conventional technique (also called stacking-sintering technique) consists of application of ceramic slurry and building the ceramic restoration. The ceramic slurry is applied manually using a special brush, and the ceramic restoration is built using a special refractory cast. Another option is to model only the outer aesthetic coat of restoration on a ceramic or metal coping.

The ceramic powder is put with spatula into depressions in a special desk and then the powder is saturated by liquid. The mixture of ceramic powder and liquid is referred to as the slurry. The slurry is applied with a Chinese or Kolinsky sable brush (brush manufactured from tail hairs of red Sable - the finest brush for an artist and lab technicians) by several dentin, enamel layers on the substrate (Fig.12,13). The condensation of ceramic slurry is performed using vibration movements, causing the particles to be packed closer together and consequently excluding water onto the surface (Fig.14). The excess water is then carefully removed using paper towels. Resulting condense stage is called the green stage (Fig.14). The restoration in green stage can be carved and shaped and is then fired under the vacuum to the specific temperature. This firing process is called sintering, during which the surface of powder particles melts and fuses with the other particles (Fig.14). The ceramic then gets substantially denser while losing its volume. This volume change needs to be accounted for by the technician during the slurry modelation. As even under the best conditions the condensation is imperfect,

the water intake after firing results in air bubbles. Therefore, the resulting ceramic is very porous, which negatively influences its strength [2,23,29,30].

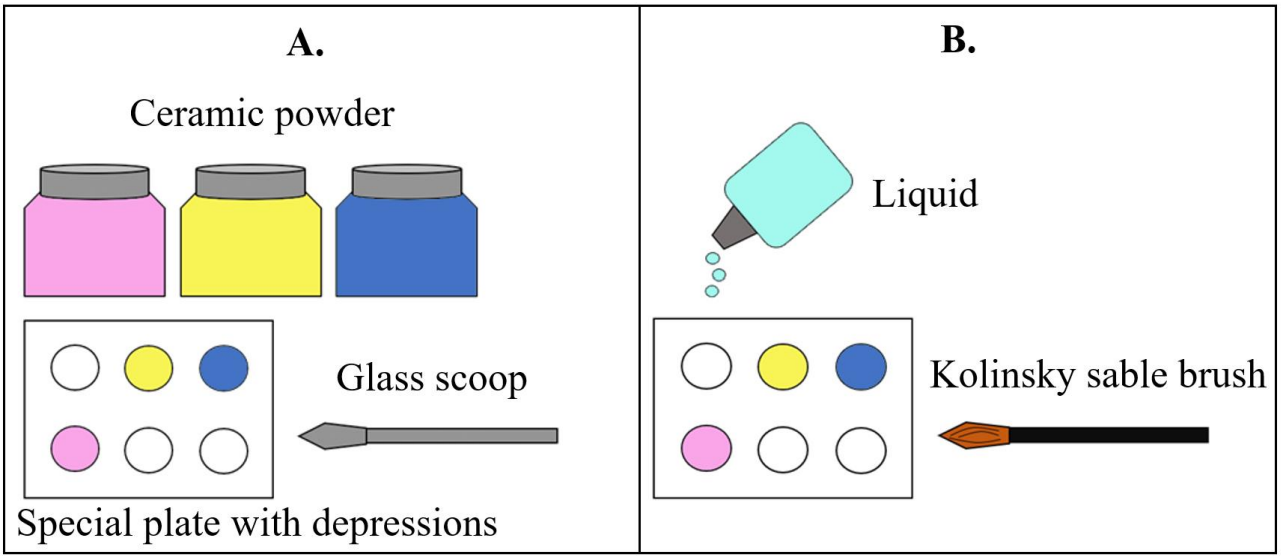

Figure 12: Preparation of ceramic slurry. A - The ceramic powder is put with spatula into depressions in a special desk. B - Saturation of ceramic powder by liquid.

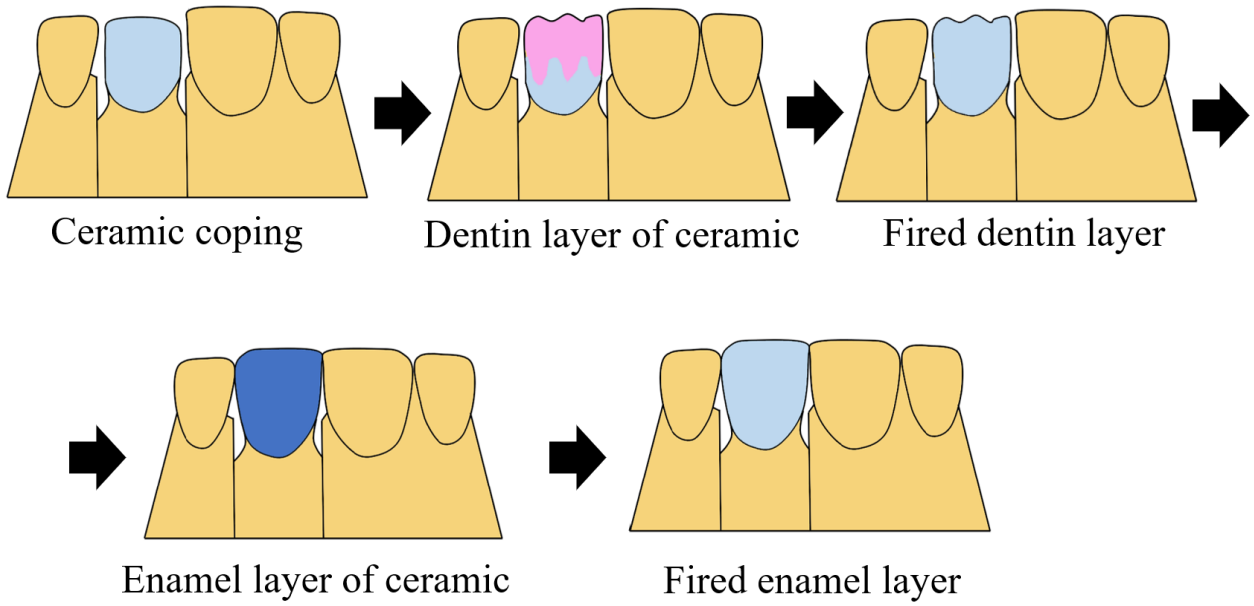

Figure 13: Application of dental ceramic layers.

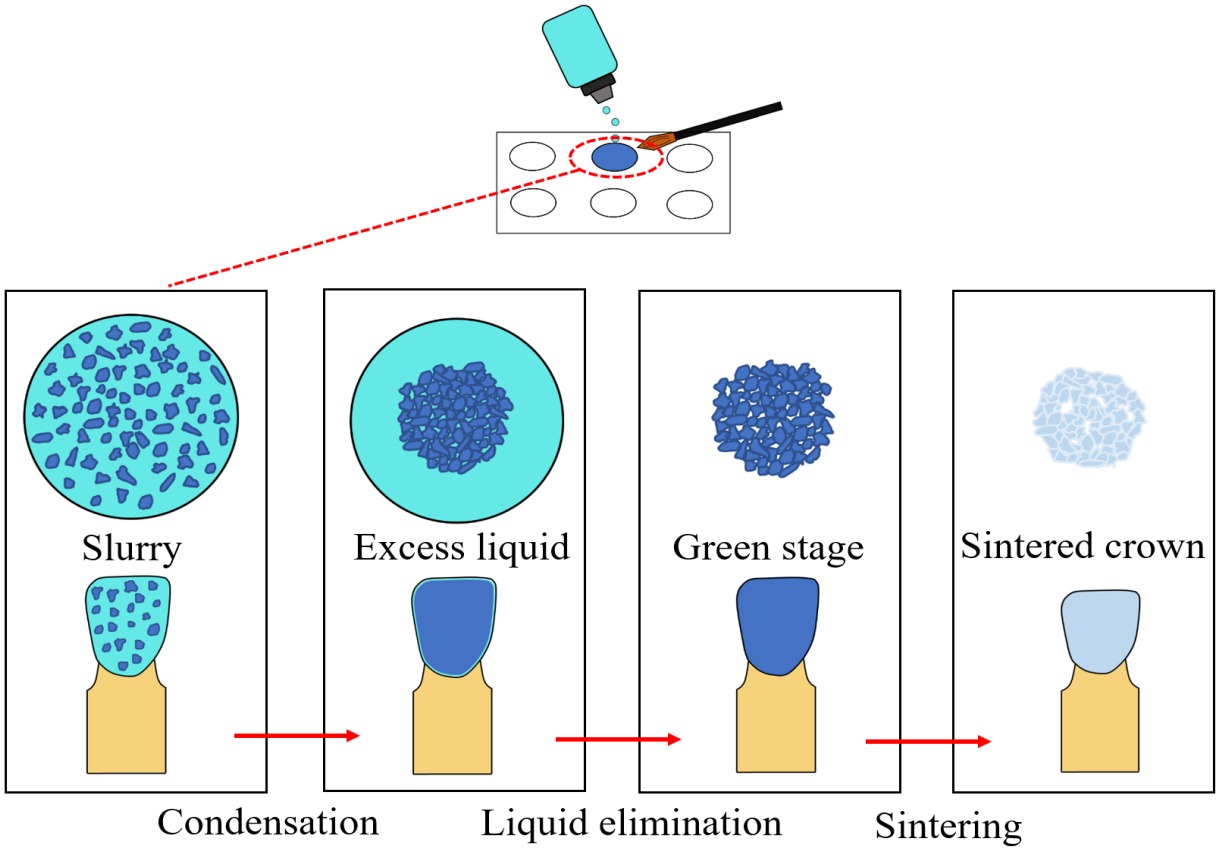

Figure 14: Graphical demonstration of stacking-sintering process.

2.5 CAD/CAM dental ceramic

This chapter is devoted to the topic of dental CAD/CAM ceramics. The reader will get acquainted with the relevant types of ceramic materials that are available on dental market in this form, their advantages, disadvantages, and possible indications. This chapter derived from paper Compendium of current ceramic materials used for the CAD/CAM dentistry [31].

As the popularity of CAD/CAM machining in dentistry increases, there is an increasing variety of new dental ceramics with good optical and mechanical properties available in the market.

CAD/CAM ceramics are available in blocks or discs of different sizes, colours, optical features and sintered stage. These blocks or discs are ground/milled with diamond embedded burs or carbide burs to the desired shape of the restoration - this is called subtractive machining process. Based on the sintered stage of block the manufacturing can be divided to soft or hard machining. Presently CAD/CAM machining materials can be categorized as:

- Glass ceramics reinforced with crystals/fillers: Feldspar ceramics, Leucite reinforced ceramics, Lithium disilicate ceramics, Zirconia reinforced lithium disilicate ceramics.
- Polycrystalline ceramics: Zirconia ceramic [32].

2.5.1 Feldspar ceramic

Representative of this group is the very famous CAD/CAM feldspar ceramic called Vita Mark II (Vita Zahnfabrik) (Fig.15). The proper definition is sanidine reinforced feldspar ceramic with two types of crystals nepheline and microlin. The crystallinity is around 30% and the average size of the particles is 4 micrometres [33–35]. These ceramics' optical properties best mimic the dental hard tissues. Due to their aesthetic properties and utilization of this

material for frontal restorations, ceramic blocks are produced with 3D layer structure or integrated shade gradients to best reproduce the natural look of teeth (Fig.16) [36,37].

Figure 15: Photo of VITA Mark II block.

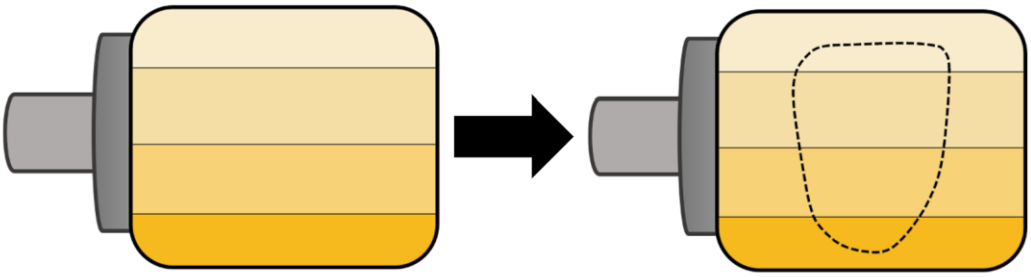

Figure 16: Graphical demonstration of ceramic block with integrated shades gradients. Left- block with integrated shades - cervical part is darkest and incisal part is lightest. Right- virtually positioned ceramic crown in polychromatic block.

Figure 17 depicts the range of flexural strength measured by the three-point bending test [33,35,38–46], figure 18 shows the range of elastic modulus [39,44,47–50] and figure 19 demonstrate the range fracture toughness [39,44,46,51,52] of feldspar ceramics (Vita Mark II).

The indications for this type of ceramic are:

- Inlay, onlay, veneer, partial crown, anterior crown, and veneering material for oxide ceramic substrate [18,46,49,53].

The advantages are:

- Aesthetics, translucency, and a wide range of block shades.

The disadvantages include:

- Fragility and translucency [47].

The ceramics are ground in a fully sintered stage (hard machining). Cooling water is used to protect overheating of the grinding material [51,54]. The restoration can be finally treated by polishing, glaze, stains or personalized with cut back technique [47]. Due to the high content of glass and poor mechanical properties, this ceramic material is recommended to be fixed by adhesive fixation to increase the restoration resistance to fracture [55]. Examples of representative CAD/CAM ceramics that can be found on the market are described in table 1.

Table 1 - Example of market representatives of CAD/CAM dental ceramic.

Feldspar ceramic	**Vita Mark II** (Vita-Zahnfabrik); **Cerec blocs** (Sirona Dental Systems); **Vita TriLuxe forte** (Vita Zahnfabrik); **Vita RealLife (**Vita Zahnfabrik)
Leucite ceramic	**IPS Empress CAD** (Ivoclar – Vivadent); **Initial LRF Block Universal** (GC); **Initial LRF Block CEREC/InLab Blocks** (GC).
Lithium disilicate glass ceramic	*IPS e.max CAD* (Ivoclar-Vivadent); **Amber Mill** (Hass); **Obsidian** (Glidewell Laboratories); **Suprême.cad** (Suprême); **Rosetta SM** (Hass); **MAZIC Claro CAD** (Vericom).
Lithium disilicate glass ceramic reinforced by zirconia	**Vita Suprinity** (Vita Zahnfabrik); **Celtra Duo** (Sirona Densply)
3Y-TZP zirconia	***Framework zirconia*** – **Vita YZ T** (Vita Zahnfabrick); **In-Ceram Classic Zirconia** (VITA North America); **In-Ceram YZ** (VITA North America); **inCoris ZI (**Dentsply Sirona); **IPS E.max ZirCad LT MO** (Ivoclar Vivadent). ***Monolytic zirconia*** – **IPS E.max ZirCad LT** (Ivoclar Vivadent); **Lava Plus** (3M ESPE); **Katana HT, ML** (Kuraray Noritake); **Cercon HT** (Dentsply Sirona); **Vita YZ HT** (Vita Zahnfabrick); **inCoris TZI, TZI C** (Dentsply Sirona**); BruxZir Full-Strength** (Glidewell Laboratories); **Pretau Zirconia** (Zirkonzahn).
Cubic zirconia	***4Y-TZP – IPS* e.max ZirCAD MT** (Ivoclar Vivadent); **Katana ST/STML** (Kuraray Noritake); **Zpex 4** (Tosoh). ***5Y-TZP* – Lava** esthetics (3M ESPE); **Katana UT/UTML** (Kuraray Noritake); **BruxZir Anterior** (Glidewell Laboratories); **Pretau Anterior** (Zirkonzahn); **Zpex Smile** (Tosoh).

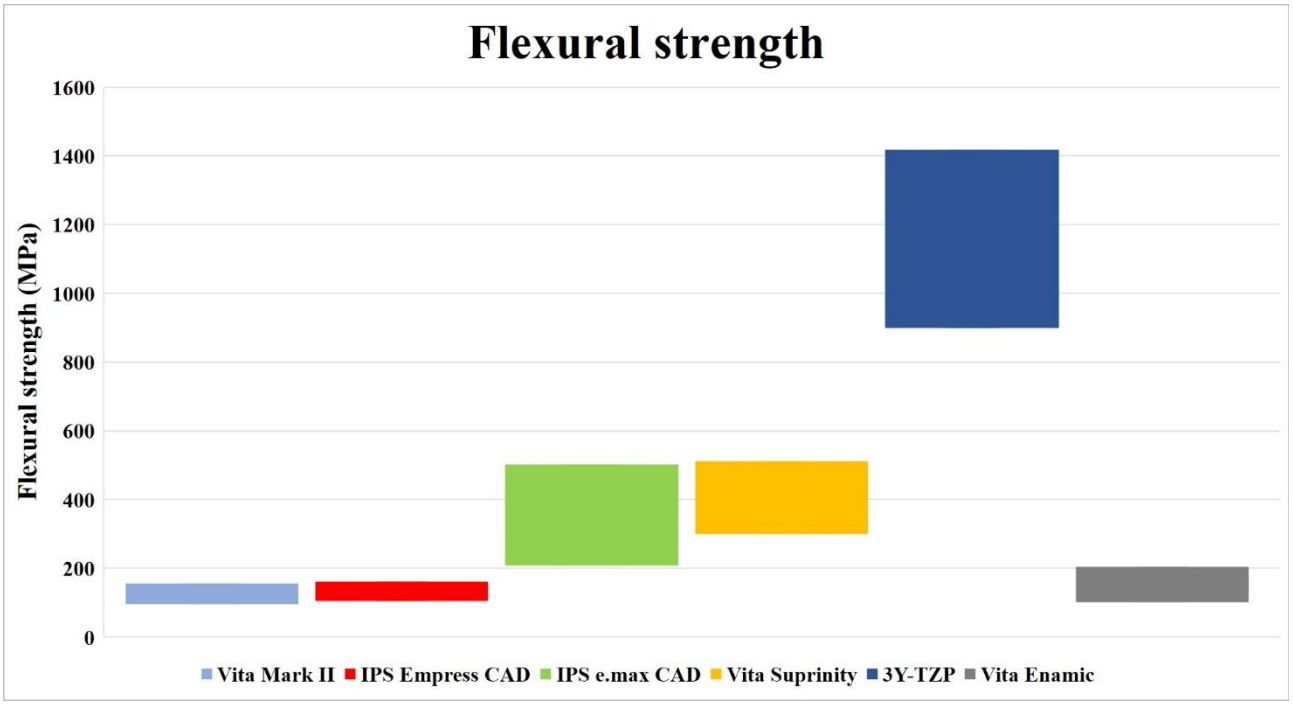

Figure 17: Boxing graph - flexural strength. Graph shows the range of flexural strength in MPa for each ceramic group.

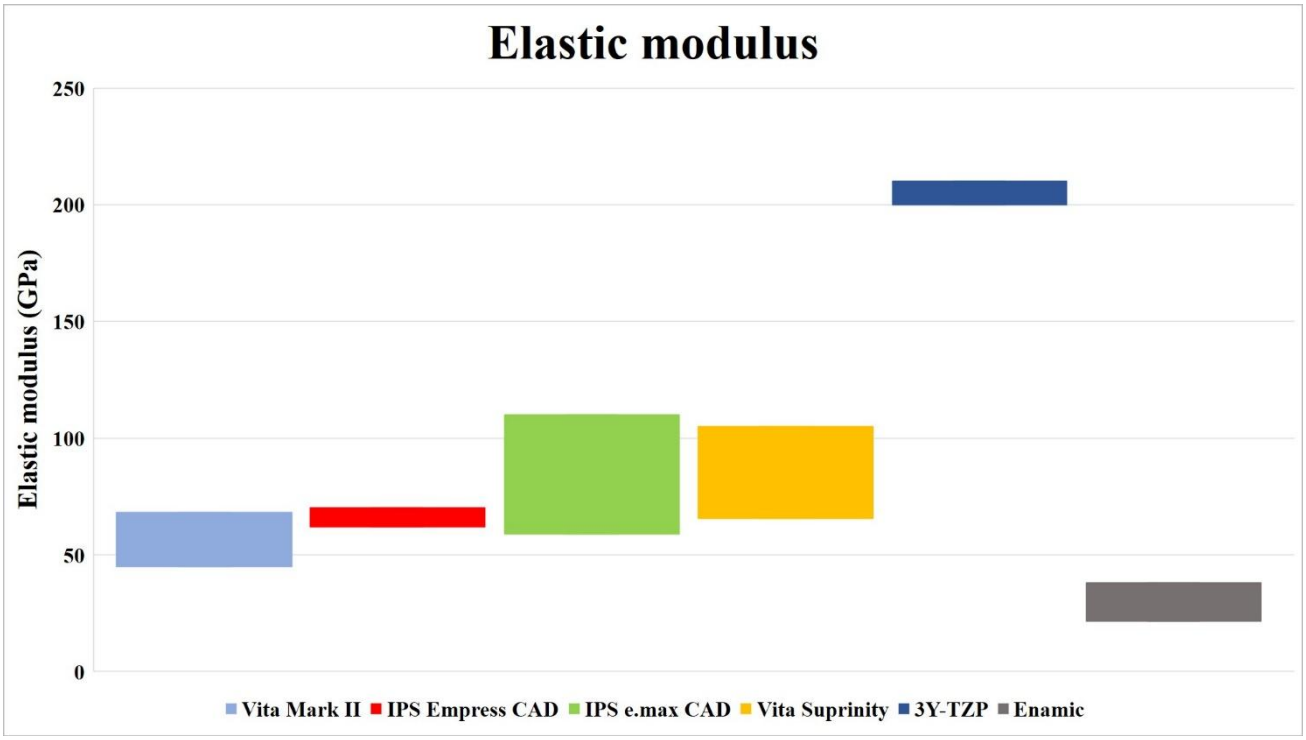

Figure 18: Boxing graph - elastic modulus. Graph shows the range of elastic modulus in GPa for each ceramic group.

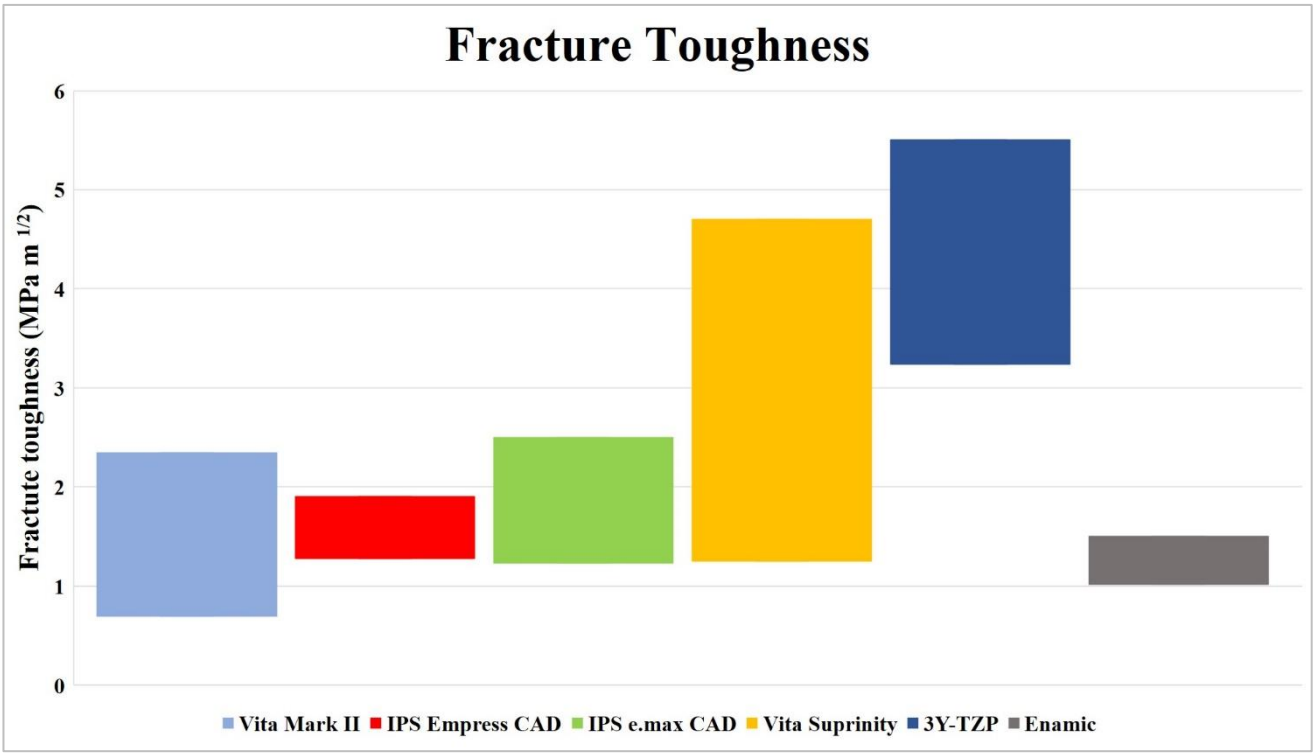

Figure 19: Boxing graph - fracture toughness. Graph shows the range of fracture toughness in MPa $m^{1/2}$ for each ceramic group.

2.5.2 Leucite reinforced glass ceramic

The leucite glass ceramics consist of leucite crystals and glass matrix. For example, IPS Empress CAD (Ivoclar -Vivadent) (Fig.20) is 30-45% by volume leucite crystals ($KAlSi_2O_6$) which are approximately 1-10 micrometres in diameter [2,51,56]. It was found by Weinstein in 1962 leucite crystals have high coefficient of thermal expansion (CTE, greater than $20 \times 10{-}6/^\circ$ C) thus influencing the thermal expansion of material and eliminating the propagation of cracks if the fracture energy is absorbed by crystals (Fig.21).

Leucite has polymorphic crystal structure, at room temperature the leucite present in tetragonal phase and during the heating process (after reaching the 625 C), it transfers to cubic crystalline phase. This transformation includes volumetric increase. During the cooling

transformation from C to T phase (volume - decrease) occurs. The combination with greater contraction of leucite crystals in comparison to glass matrix due to larger CTE mismatch, causes tangential compressive stresses around leucite crystals. Compressive stresses are positive, act as crack deflectors [18,21,22].

Figure 20: Photo of Empress CAD.

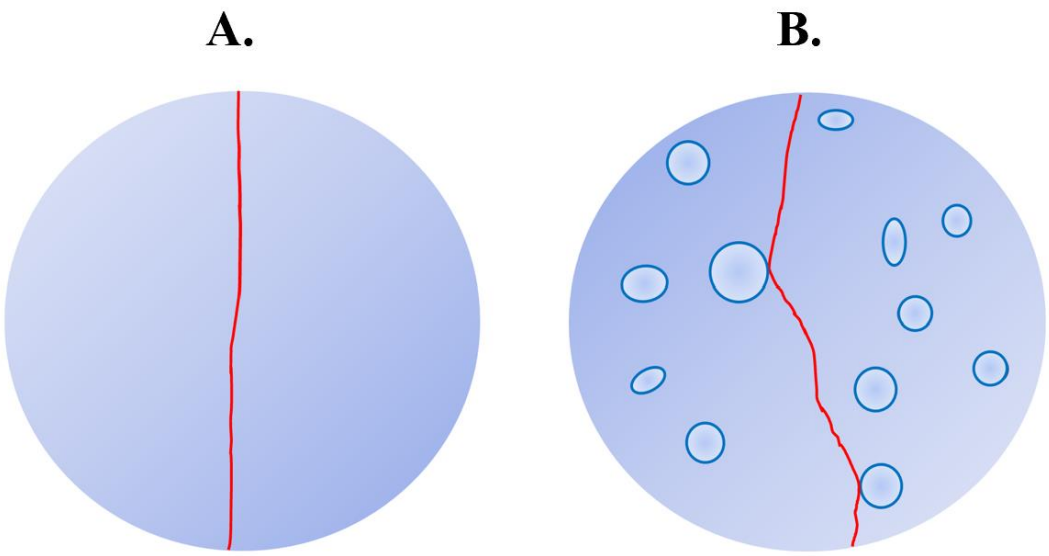

Figure 21: Propagation of crack. The material A is an amorphous glassy matrix, material B is composite consisting of crystals and a glassy matrix. In material B fracture propagation is partially suspended by presence of crystals. In material A (amorphous glassy matrix) there is no presence of crystals (bumpers/stoppers) and the fracture goes straight through the material.

Figure 17 depicts the range of flexural strength values which were measured by three-point bending test [18,35,39,42,46,51,57], figure 18 shows range of elastic modulus [39,47,49,58–60] and figure 19 demonstrates the fracture toughness [39,46,58,60] of leucite reinforced glass ceramics (IPS Empress CAD).

Indications for leucite glass ceramics are:

- Inlay, onlay, partial crown, veneer, and anterior crowns [18,46,53].

The advantages include:

- Good aesthetics, translucency, and a wide range of block shades.

The disadvantages are:

- Fragility and translucency [47].

The ceramics blocks are also present and ground in a fully sintered stage (hard machining) and cooled by water during the grinding process to prevent overheating [21,51,54]. The final surface treatment is the same as for feldspar ceramics [47]. This ceramic has a high content of glass, and the adhesive fixation is also recommended to increase the strength of final restoration [55]. Examples of representative CAD/CAM ceramics on the market are described in table 1.

2.5.3 Lithium disilicate glass ceramic

The most famous lithium disilicate glass ceramics are on the market under the name IPS e.max CAD (Ivoclar-Vivadent) (Fig.22). These ceramics provide good mechanical and aesthetic properties. Lithium disilicate glass ceramics consist of 70% lithium disilicate crystals (Li_2SiO_5) and retain relatively high translucency [51]. Translucency is achieved due to the low refractive index of lithium disilicate crystals[2]. Crystal's dimensions are 1.5-5 micrometres [10,51]. The large amount of crystals helps to increase the strength [18]. IPS e.max CAD is

produced in partially crystallized stage and is called blue stage because of the colour of partially crystallized block of ceramic.

Figure 22: Photo of IPS e.max CAD. Different sizes, translucencies and types of blocks.

The blue/violet colour is controlled by colouring ions such as vanadium, which are dissolved in the glass matrix. During the heat treatment, the primary crystalline metasilicate structure changes to lithium disilicate and the final restoration gets the natural colour of tooth due to change of vanadium from valency +4 to +3. Blue stage consists of 40% of the meta-silicates crystals (Li_2SiO_3), around 0.2-1 micrometres in diameter. This composition enables easier milling and less deterioration of grinding tools. The restoration after milling is still in the partially crystalline state and has to undergo a crystallization process. During this process, the meta-silicate crystals are dissolved and the lithium disilicate crystals are formed.

After the crystallization process, the ceramics obtain the shade, translucency, and the mechanical features described above [33,51,61,62].

Figure 17 depicts the range of flexural strength measured by the three-point bending test [10,33–35,41,42,46,49,51,57,63–67], figure 18 demonstrates range of elastic modulus [47,49,50,58,59,63,66–70] and figure 19 shows the fracture toughness [46,49,52,58,64–71] of lithium disilicate glass ceramics in fully crystallized stage (IPS e.max CAD).

These ceramics are sold in a fully sintered, partially crystallized stage [21], representative examples are mentioned in table 1. After the hard milling by water cooling, the restoration needs to undergo the crystallization process to achieve final crystallinity, strength and optical features. The final surface treatment for monolithic restoration includes polishing, staining, glazing or cut back technique, and the restoration can also be veneered with conventional ceramic [47]. Both cementation types (conventional/adhesive) are reported, but to maximize strength, adhesive cementation is usually preferred to reinforce the present ceramics [34,54,72,73].

Indications are:

- Inlay, onlay, veneer, partial crown, anterior and posterior crown [18], endocrowns [47], three-unit bridges up to premolar, anterior and posterior implant abutments and implant crowns, and veneering material [46,53].

The advantages include:

- Good aesthetics, mechanical strength, wide range of block shades and good optical properties.

The disadvantage of lithium disilicate ceramics is usually less translucency[47].

2.5.4 Lithium disilicate glass ceramic reinforced by zirconia

Lithium di-silicate ceramics reinforced with zirconia could also be classified as a subgroup of lithium disilicate glass ceramic. This dental ceramic consists of a fine-grain crystalline phase of lithium metasilicate and lithium disilicate with an average size of crystals of 0.5-0.7 micrometres. These lithium disilicate ceramics are reinforced with 8-10 wt% of zirconia, which is dissolved in the amorphous glassy matrix [61,63,73–75]. This leads to higher flexural strength. An example of the lithium disilicate zirconia ceramics on the market is the Vita Suprinity (Vita Zahnfabrik). This material is sold in the partially crystallized form, so it is easier to mill the restoration [61].

Figure 17 shows range of flexural strength values measured by the three-point bending test [35,38,49,57,66–68], figure 18 refers to the range of elastic modulus [49,66–70] and figure 19 depicts range of fracture toughness [49,66–70,76] of zirconia reinforced lithium disilicate glass ceramic in fully crystallized stage (Vita Suprinity).

Lithium disilicate zirconia reinforced ceramics are sold in partially/fully crystallized state. After water-cooled hard machining, the restoration in a partially crystallized state has to undergo a thermal heating process called crystallization. During this thermal process, the ceramic will reach the final crystallinity and increase its strength. Vita Suprinity blocks also change colour from honey-transparent to the natural colour of the tooth. The machined restoration from fully crystallized blocks (Celtra Duo, Sirona Densply) skips the final crystallization process, because they are already fully crystallized. Final surface treatment is identical to the lithium disilicate ceramics [47], and adhesive fixation is recommended [73,75].

The indications are:

- Veneers, inlays, onlays, anterior and posterior crowns [18], endocrowns, bridges of small extent in anterior region [47].

The advantages are:

- Good aesthetics, mechanical strength, wide range of block shades and their optical properties.

The disadvantage is typically less translucency [47].

Available products on the market are mentioned in table 1.

2.5.5 Zirconia ceramic

Zirconia is a polycrystalline ceramic. It is a highly crystalline ceramic without an amorphous glassy matrix. Chemically it is zirconium dioxide [10]. Zirconia is available in three crystalline forms: monoclinic, tetragonal and cubic.

- The monoclinic form is stable from room temperature to 1170°C and the density is 5.6 g/cm^2.
- Tetragonal phase is stable from 1170°C to 2370°C. This form has good mechanical properties with a density of 6.1 g/cm^2.
- The cubic phase is stable at over 2370°C and its density is 6.27 g/cm^2. Due to the low mechanical properties of the monoclinic phase, it is good to eliminate this phase in the composition of the ceramics [51,77].

Tetragonal/cubic zirconia can be partially stabilized at room temperature by adding smaller amounts of oxide dopants such as yttria (Y_2O_3), ceria (CeO_2) or magnesia (MgO) [21,51]. For fully stabilized zirconia, it is necessary to add 8 mol% Y_2O_3 or 16 mol% MgO. Nowadays, the most common dopant is yttria (Y_2O_3), where lower valence dopants Y^{3+} ions replace Zr^{4+} in the lattice. This substitution leads to oxygen vacancies, which are responsible for the metastability of the tetragonal phase. The metastability and therefore the stabilization of zirconia is mostly attributed to the existence of these oxygen vacancies. These vacancies

allow relaxation of cations and anions depending on their distance to the vacancies (Fig.23) [78].

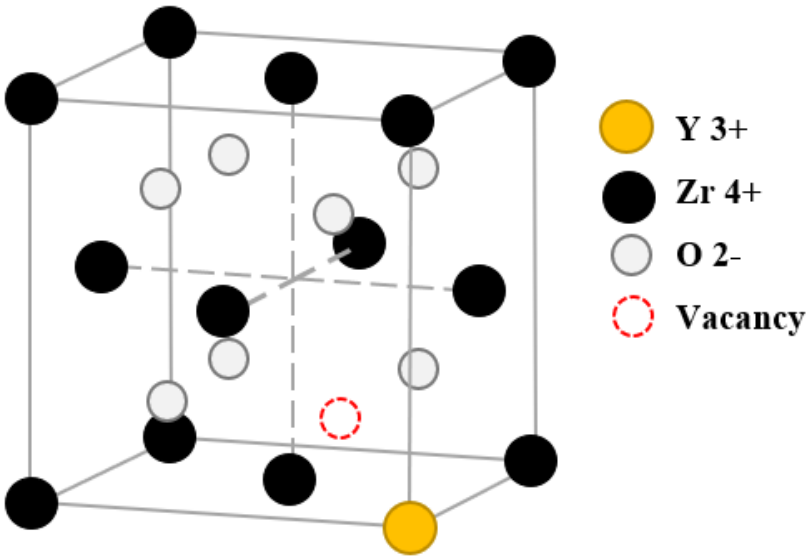

Figure 23: Illustration of yttria stabilized zirconia, picture inspired by Vágner, P., Guhlke, C., Miloš, V. et al. A continuum model for yttria-stabilized zirconia incorporating triple phase boundary, lattice structure and immobile oxide ions. J Solid State Electrochem 2019; 23:2907–2926 [79].

Zirconia ceramics have a unique feature called transformation toughening. Transformation toughening occurs when the propagation of the crack induces stress, which results in a phase change from tetragonal phase to monoclinic phase. Due to this phase transformation, there is a volume increase of 3-5 %, causing compressive stress around the walls of the crack. This closes the crack in the transformation zone, decreases crack propagation and increases the toughness of material (Fig.24) [10,21].

Zirconia ceramics suffer from low temperature degradation (LTD). This process is also called aging of zirconia ceramic. Combination of water and relatively low temperatures cause the surface of the reconstruction to transform from tetragonal to monoclinic phase. The process

starts from single grain and then propagates. The pull out of grains and microcracks cause degradation of the surface and lead to degradation of mechanical properties [78].

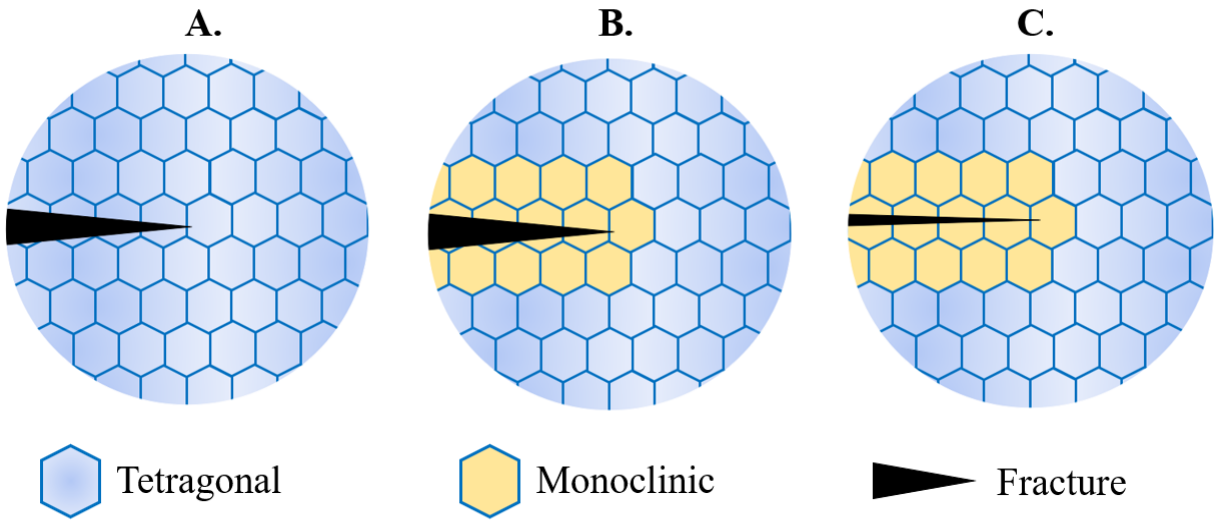

Figure 24: Transformation toughening mechanism. A - Propagation of the crack induces stress. B - The stress results in a phase change from tetragonal phase to monoclinic phase (blue to yellow). C - Compression stress induced due to volume change T to M phase, causes closure of crack. Phase transformation T to M, causes volume increase which results in compressive stress, which mitigate propagation of crack.

The manufacture of zirconia restorations can be divided into soft machining process and hard machining manufacture [21]. The zirconia blocks or discs for CAD/CAM technique are sold in three states: i) chalk or green state (non-sintered), ii) pre-sintered and iii) fully sintered state [20]. The first two states are softer and easier for milling, causing less wear of milling burs. Milling of non-sintered and pre-sintered blocks is called a soft machining process and has to be followed by a sintering process. The green stage is very porous and could absorb a lot of water - thus dry milling is required to avoid a long period of drying before sintering. The restorations from non-sintered and pre-sintered zirconia ceramics are milled in larger sizes to

allow for a shrinkage during the sintering process (about 20-25%) [47,54,77]. The fully crystalized blocks are manufactured by grinding with diamonds burs with water cooling. The disadvantages of the hard machining process of fully crystallized blocks are higher wear of grinding burs and longer grinding time. The advantage is that the material does not shrink [54].

How are the zirconia blocks and discs manufactured before delivery to the dental laboratory? There are two ways: Uniaxial dry pressing and Cold isostatic pressing.

Uniaxial dry pressing

In this method the zirconia ceramic powder is poured to the mold and pressed in uniaxial direction, to the green stage. The big disadvantage of this method is the varying degree of density of the green stage zirconia block, due to the friction effect between zirconia particles and walls of the mold. This can lead to different mechanical properties of dental ceramic restoration, depending on which zone of dental block the restoration was ground (Fig.25).

Cold isostatic pressing

Cold isostatic pressing is a very similar process to a meat processing technique called sous-vide. The zirconia ceramic powder is placed into a deformable form, and then an external pressure acts uniformly from all directions (isostatic) (Fig.26). These produced blocks/discs in green stage have uniform density. They are in a green stage and could be sintered (partially densified) by an additional heating process (without using pressure). This stage is called a partially sintered block. To remove redundant porosity, a pressure and additional heat is used to partially sintered blanks and the blocks, achieving the final density. The resulting blocks are marked HIP blocks because the final compression heat process is called Hot Isostatic Postcompaction (HIP) [77].

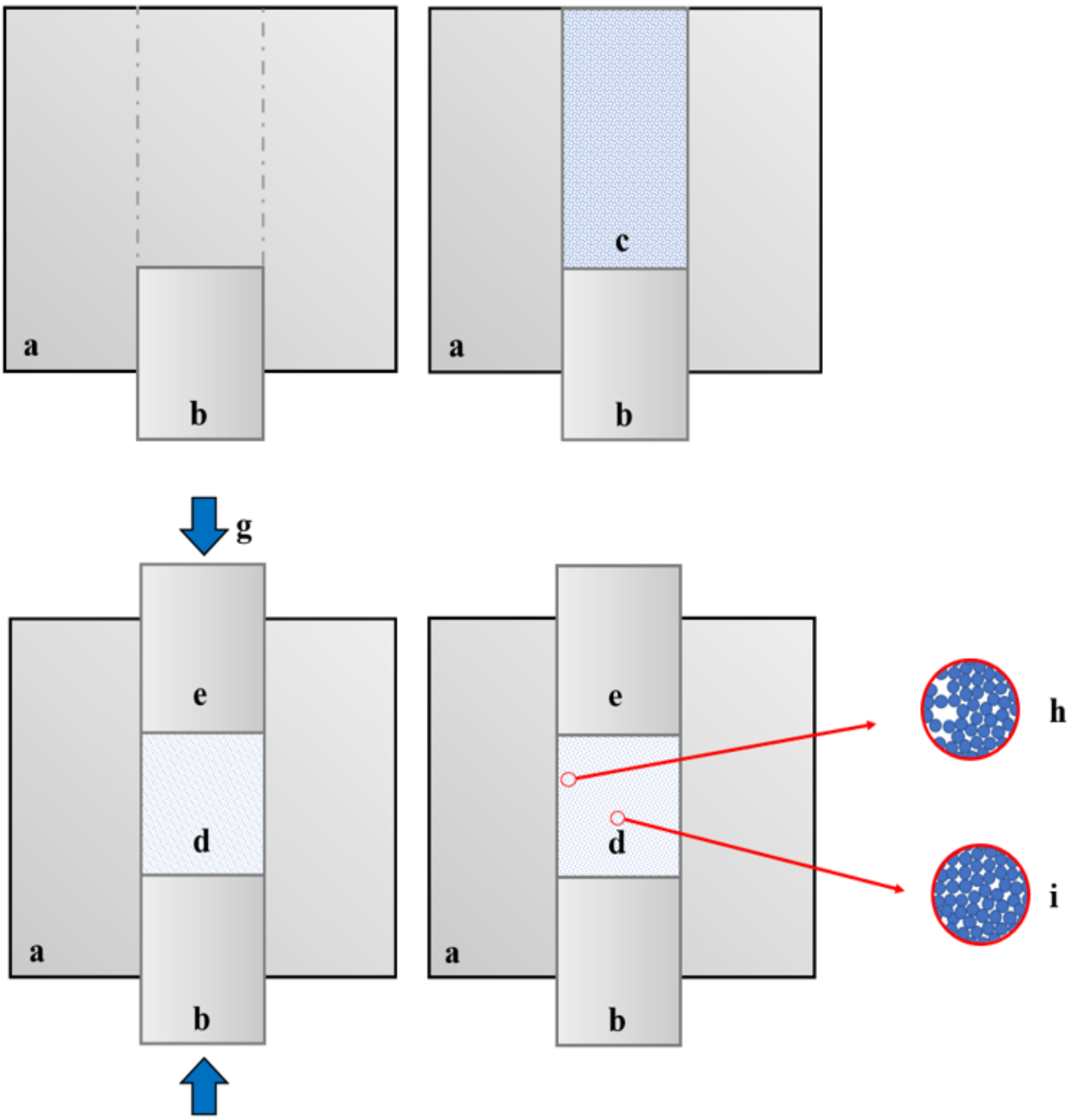

Figure 25: Uniaxial dry pressing. a - mold, b - lower plugger, c - zirconia powder, d - zirconia powder pressed to green stage, e - upper plugger, g - uniaxial loading, h and i - varying degree of density

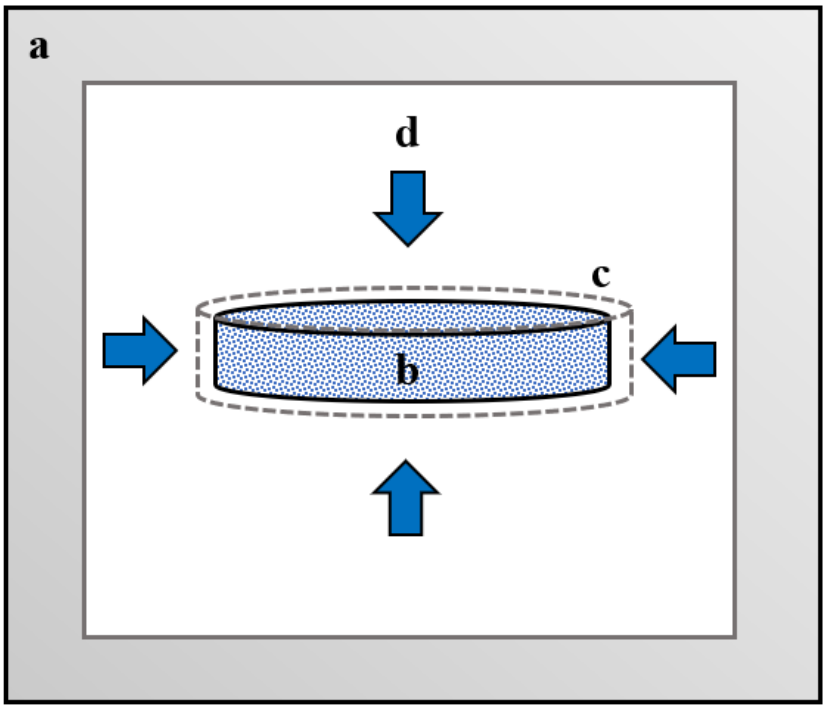

Figure 26: Cold isostatic pressing. A - high pressure vessel, b - zirconia powder, c - deformable mold, d - isostatic pressure.

The fixation of zirconia ceramic is mostly done with conventional cementation, but adhesive fixation is also possible. The zirconia is not etched by hydrofluoric acid due to the absence of glass, and it does not contain silica to achieve chemical bond with silane coupling agent. To achieve micro retention, air abrasion with alumina particles or tribochemical silica coating is used to increase surface roughness. The surface is then treated with adhesive with MDP monomer (methacryloxydecyl dihydrogen phosphate monomer) to achieve chemical bond between dental surface and resin cement. MDP's phosphate groups bond strongly with metal oxides such as zirconium oxide (ZrO_2) (Fig.27). If the surface is air abraded with silica coated alumina particles, it can be treated with the silane coupling agents for glass ceramics [55,80].

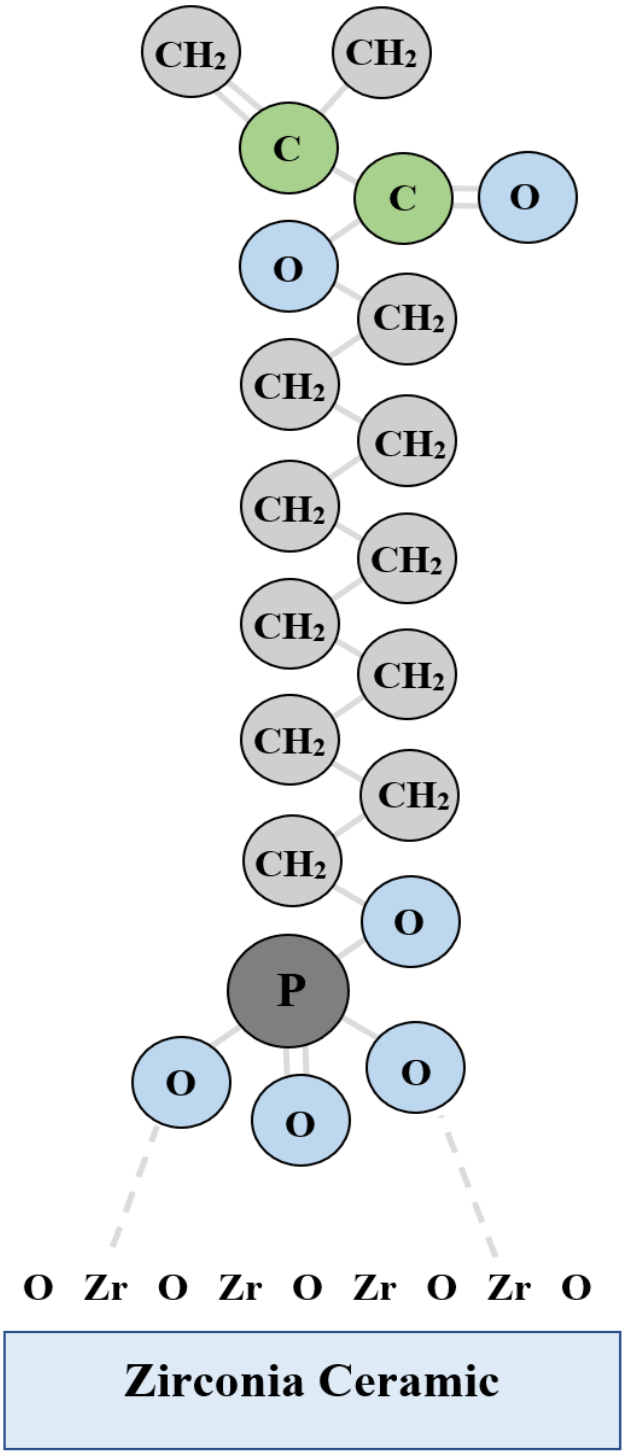

Figure 27: Graphical description of MDP monomer bond with zirconia ceramic. MDP's phosphate groups bond strongly with exposed zirconium oxide (ZrO_2) on zirconia ceramic surface. Adjusted from Guide to All-Ceramic Bonding.

2.5.5.1 3Y-TZP zirconia

3Y-TZP (yttria tetragonal zirconia polycrystals) frameworks are very opaque due to the high content of alumina. It requires veneering with glass ceramics to achieve an improved aesthetic result [81]. Manufactures later introduced a dedicated monolithic zirconia, having lower content of alumina. While this increases translucency, it is still quite opaque compared to glass ceramic. 3Y-TZP is commonly stabilized with 3 mol% of yttria [3Y-TZP] and the tetragonal phase is stabilized at room temperature. Both forms exhibit transformation toughening. The mechanical properties of these forms are similar [47,70,77]. Zirconia causes wear of the antagonist enamel that can be improved with a surface finishing and polishing technique [81].

Figure 17 depicts the range of flexural strength measured by three-point bending test [35,42,67,70,77,82], the range of elastic modulus is demonstrated in figure 18 [39,67,82] and figure 19 shows the fracture toughness [39,58,67,70,83] of 3Y-TZP ceramics. Since the mechanical properties for 3Y-TZP zirconia are predominantly reported for a whole group rather than for individual brands of this material, the mechanical properties for the whole group are shown here.

Indications are:

- Crowns, bridges, implants abutments, implants, orthodontic brackets, endodontics posts [51].

The advantages of 3Y-TZP ceramic are:

- High flexural strength

The Disadvantages include:

- Worse aesthetics, less translucency and implementation [47] and antagonist wear [81].

2.5.5.2 Cubic zirconia

Currently, a more translucent zirconia form is available on the market, namely cubic zirconia or 4Y-TZP/5Y-TZP (yttria stabilized zirconia) zirconia. It is zirconia stabilized with 4 or 5 mol% yttria and contains a higher percent of cubic phase. 4Y-TZP contains more than 25% of cubic phase and 5 Y-TZP zirconia up to 50 % of cubic phase. This increases the translucency of the material [47,67,84]. The translucency is also achieved by reduction of light scattering due to larger size of grains and less grains boundaries. The size of the grains is around 1.5 micrometres while 3Y-TZP has the size of grains around (0.5-1 micrometres) [47,67]. The main disadvantages of these materials are that they have a smaller amount of tetragonal phase, and the cubic phase does not undergo transformation toughening [84]. Thus, the mechanical features such as strength and toughness decrease in comparison with conventional zirconia. The flexural strength is denoted around 500 to 700 MPa [47].

Suitable indications are:

- Veneer, inlay, onlay [47], single crown and anterior three-unit bridge [84].

The advantages are:

- Aesthetics, higher translucency in comparison with conventional zirconia

The disadvantages are:

- Low mechanical properties.

Examples of representative CAD/CAM ceramics on market are included in table 1.

2.5.6 Additional group

There is very specific material on the market which can be included in the CAD/CAM dental ceramic and composite dental materials. It is called Polymer Infiltrated Ceramic Network (PICN). PICN is a ceramic network which is infiltrated by polymers. It contains ceramic (75 % v/v, 86% w/w) and polymer (25% of v/v, 14% w/w)[33,46,61,85]. Combining the properties of ceramic and polymer, the material has mechanical properties closer to dental hard tissues [86]

Indication:

- Inlay, onlay, veneer, anterior and posterior crown can be made from this type of ceramics [18,46,53].

The advantages of PICN are:

- The mechanical properties, rapid milling, implementation, and low antagonists' wear.

Disadvantages are:

- Less aesthetics and sustainability [47].

2.6 Mechanical properties of dental ceramic

This chapter is focused on selected mechanical properties of dental ceramics which are important for dental technician, dentist and everyone who works with these materials. This will enlighten readers as to why ceramic work sometimes fails unexpectedly and what we can expect from these materials. This chapter is derived from work Dental Ceramic - Mechanical properties [87].

Mechanical properties express the ability of a material to withstand mechanical stress [1]. The mechanical properties of the material represent durability, the resistance of the material to mechanical stress - chewing. Furthermore, the resistance of the material to damage - abrasion by hard particles from food [6].

The “ideal” replacement material is a material that fully mimics the properties of the replaced tissues. As we have not yet found the ideal material that fully replaces hard dental tissues, materials which replace the lost dental hard tissues try to get as close as possible to its mechanical, physical, chemical, and biological properties [88].

The mechanical properties of materials are typically described by stress-strain curve [88]. The x-axis shows the deformation of the material under this force and y-axis expresses the force acting on the surface (stress). The curve can then be divided into two sections, namely the elastic and plastic deformation section, which are explained in section elasticity and plasticity (Fig.28).

Point A

Point A - proportional limit, is the limit within which Hooke's law is valid, where the stress is linearly proportional to the deformation of the material [89]. For linearly elastic materials, the limit of proportionality is the same as the limit of elasticity [21,90].

As it is often difficult to determine the exact proportional limit, the yield strength is sometimes given. Yield point is the stress at which permanent deformations occur. This transition from elastic to plastic changes is not clearly apparent for most materials, so the contractual yield strength is often used. The contractual yield strength is the stress at which the relative plastic deformation reaches a prescribed value e.g. 0.2 percent of the permanent deformation.

Point B

Point B - ultimate strength is the maximum stress that a material withstands before it fails [21]. Depending on the strength test we use, the ultimate strength can be called the maximum flexural, compressive, and tensile strength, etc.

Point C

Point C - fracture strength is the stress at which the material fails (fractures). Fragile material fails at maximum load. Therefore, on the stress-strain curve of the brittle material, these points are identical. For ductile materials such as metals or alloys, the breaking point and strength limit differ. For tensile materials, the fracture stress is not necessarily the maximum value [21]. After the action of the maximum force acting on the body, a significant constriction of the cross-section of the tensile material occurs, so-called necking, and only then does a rupture occur, so-called ductile fracture.

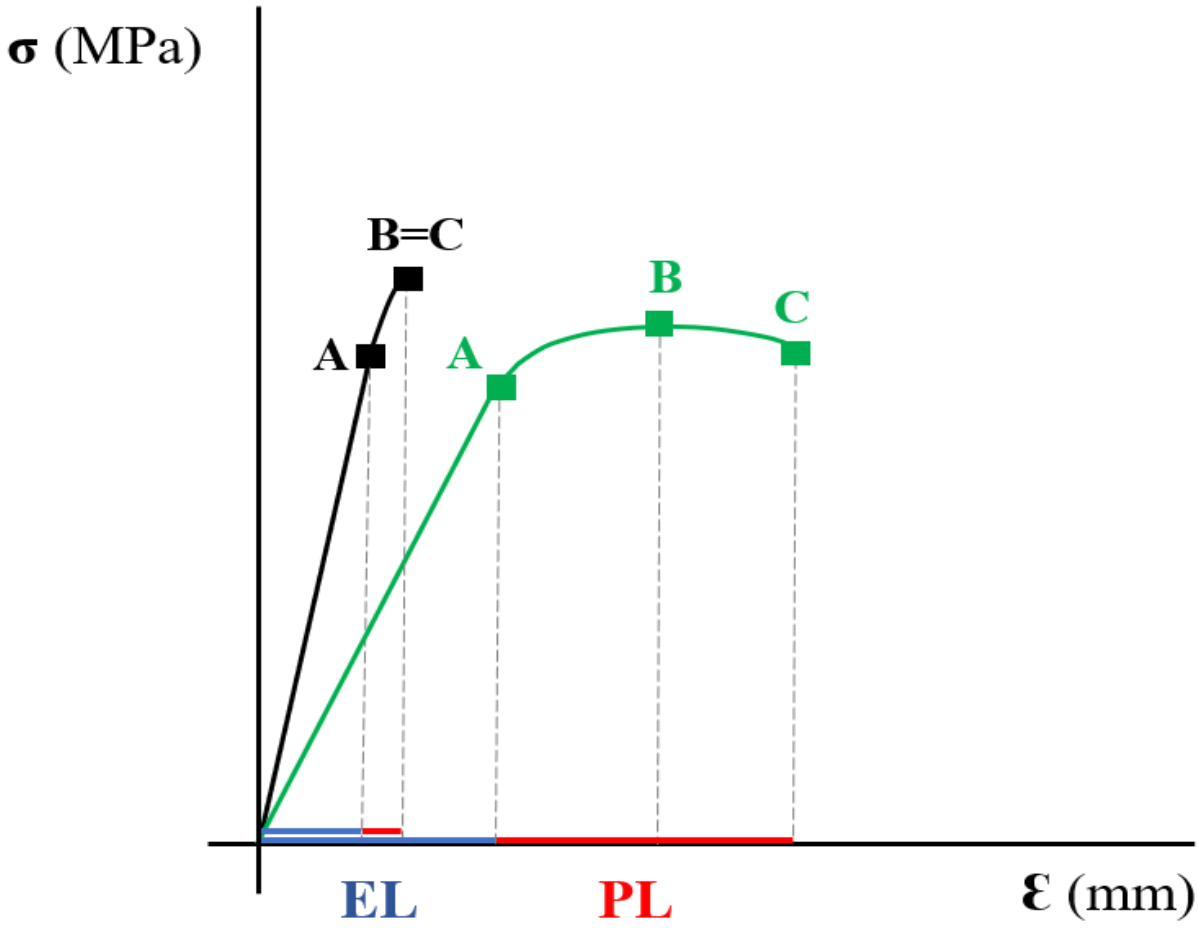

Figure 28: Stress (σ) – strain (ε) curve of hypothetical material. Where σ is the stress applied to the material, ε is the material deformation. The red section shows elastic deformation (EL). The blue section shows plastic deformation (PL). Point A - represents Proportional limit, B – Yield point, C – Ultimate stress, D – Failure stress. Adjusted from: Sakaguchi R, Powers J. Craig's Restorative Dental Materials. Fourteenth edition. Missouri: Elsevier; 2019 [21].

2.6.1 Strength

Strength is defined as the ability of a material to withstand external forces that seek to deform and disrupt material's integrity [91]. Strength of dental material (ceramic) is very

important, because the reconstructions are frequently under chewing forces in the range of 150 N to 800 N in the lateral segment. The ceramic material thus must be strong to withstand these forces [21,91].

For brittle materials such as ceramics, the ultimate strength is the same as the fracture stress [21]. This means that the material cracks at the maximum load.

2.6.2 Elasticity

Elasticity or elastic modulus characterizes the rigidity or stiffness of the material. It characterizes how stiff the material is to resist plastic/permanent deformation. The slope of the linear segment of elastic deformation on the stress-strain curve corresponds to the elastic modulus [E]. The stronger the interatomic bonds are, the higher the elastic modulus is and the stiffer is the material.

Elastic deformation of a material is defined as a temporary state. It is a segment on the stress-strain curve, where the stress and strain are in linear relationship; and as already noted, the slope of this linear segment corresponds to the elastic modulus [E].

When external forces act on the material, the atoms shift from the equilibrium position, which externally manifests itself as a change in the shape of the body. However, it is a reversible process, and the material retains its original body shape after the external force ceases to exist (Fig.29) [1].

Its limit is the elastic limit, which is defined as the maximum possible stress at which permanent plastic deformation has not occurred. Ceramic materials are typically linearly elastic [90]. For a linearly elastic material, the yield strength is the same as the proportionality limit [21]. The zone of plastic deformation then begins after the elastic limit

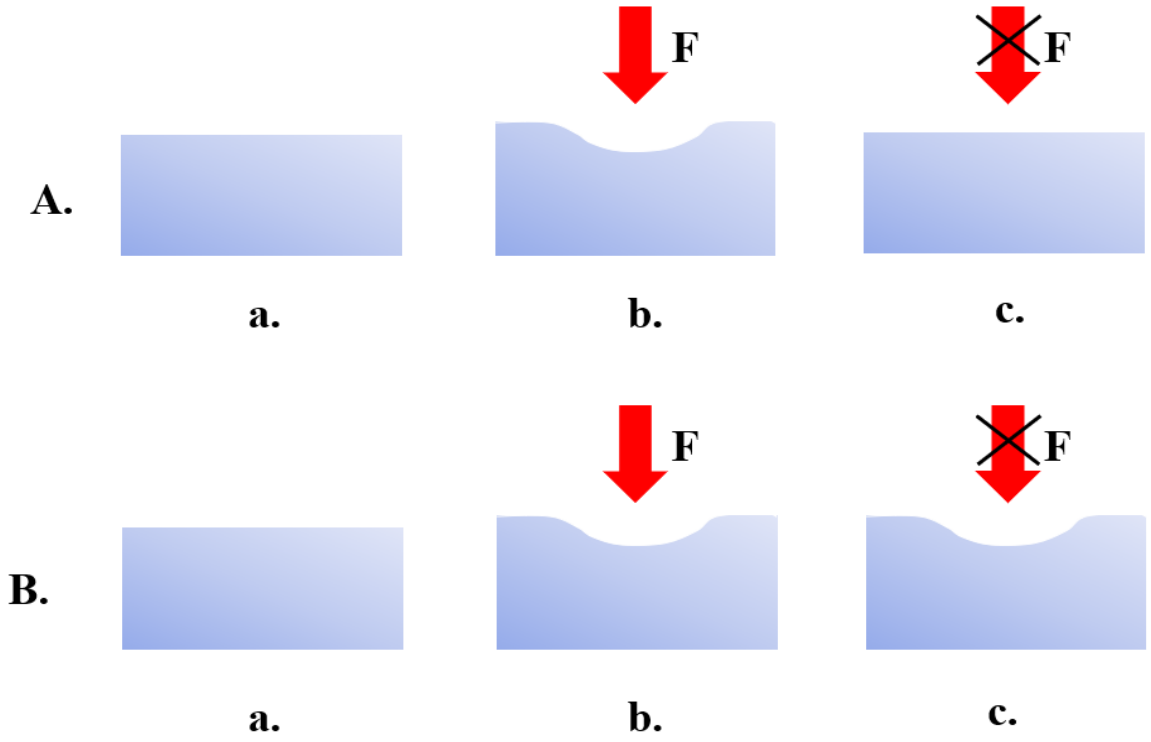

Figure 29: Elastic and plastic deformation. A - Description of elastic deformation. Ad a – sample of testing material, ad b – the force acting on sample causes deformation, ad c – after removal of the applied force, the body returns to its original state before deformation. B - Description of plastic deformation. Ad a – sample of testing material, ad b – the force acting on sample causes deformation, ad c – after removal of applied force, permanent deformation of the material persists.

2.6.3 Plasticity

Plasticity is a mechanical property when the material is deformed permanently. It is defined as a permanent change in the shape of the body after removal of an external force (Fig.29) [21]. The brittle material such as dental ceramic is not subject to significantly visible plastic deformation compared to tensile materials such as metals.

2.6.4 Hardness

Hardness is the ability of a material's surface to resist foreign body intrusion. It is tempting to assume that the harder the material, the better. But as already mentioned, ideal material should mimic as closely as possible properties of replaced tissues. If the material would be too hard, abrasion of the antagonist may occur. On the other hand, low hardness of the material (e.g. such as in for some resins) is also not preferred, as it can lead to rapid wear of the dental material and failure of the entire work. The hardness of ceramics is, however, higher when compared to dentin and enamel - or surprisingly even compared to chromium-cobalt alloys. According to the available literature, the hardness of feldspar ceramics ranges from 400 to 800 HV, and for polycrystalline ceramics based on zirconia from 1100 HV to 1300 HV [6,29,92–94]. For better illustration the hardness of ceramic: the hardness of the enamel in the literature is given around 270 to 400 HV [6,29,48,92,95,96], dentin from 50 HV to 75 HV [6,29,48,92,95,96], the Cr-Co alloy ranges from 330-465 [6,21,95]. Due to its high hardness, ceramic restoration can cause abrasion of its antagonist [97]. Hardness of dental ceramics is thus often stated as a negative property of the material.

2.6.5 Toughness

Ceramic dental reconstructions sometimes fail unexpectedly under very low loads. Unexpected failures at relatively low loads can be caused by the existence of surface and internal defects in the material.

Fracture toughness is the mechanical property of the material describing the resistance of the material to the propagation of existing cracks/defects. It is the amount of energy needed to propagate a crack, resulting in failure of the material.

Brittle material is then not subject to significant plastic deformation, so its ability to resist the spread of defects is very low.

The presence of defects and microcracks in the ceramic material is critical especially in the area of tensile stress. The largest amount of tensile stress accumulates in the area of the crack tip (Fig.30). In the case of ductile materials, the crack tip widens and rounds thanks to large plastic deformation - loosening the stress accumulation (Fig.30). A large amount of energy is required for the failure of ductile/tough material. Brittle material is not subject to significant or any plastic deformation, so the stress accumulates in the area of the crack tip -until the stress exceeds the critical limits, and the crack propagates, and the material fails [20,21].

Defects or microcracks on the surface of ceramic work are subject to substantially higher stress than defects inside the material. Therefore, the final surface treatment of ceramic work is a critical part of the production process [20].

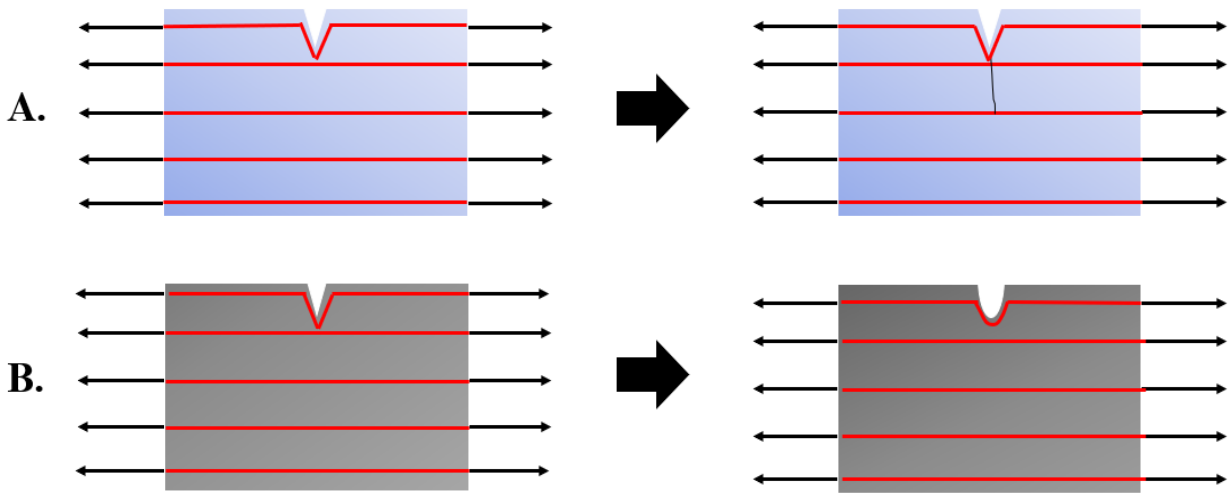

Figure 30: Influence of tensile stresses on flaws in brittle and ductile materials. A - Brittle material, B - Ductile material

2.6.6 Brittleness

A material that is termed brittle experiences very little or no plastic deformation upon fracture [6]. Brittle materials are generally defined as material with a fracture strain less than about 5%. The opposite of brittleness is toughness. Toughness is expressed graphically as the area under the stress-strain curve until the material breaks. From a physical point of view, toughness is defined as the energy required to rupture a material [21].

That is why brittle material is not very tough and does not need much energy to fail (crack). Looking at figure 31, it can be stated that material A is more brittle than material B, because the grey area under the curve (the energy required for material failure) is smaller than for material B.

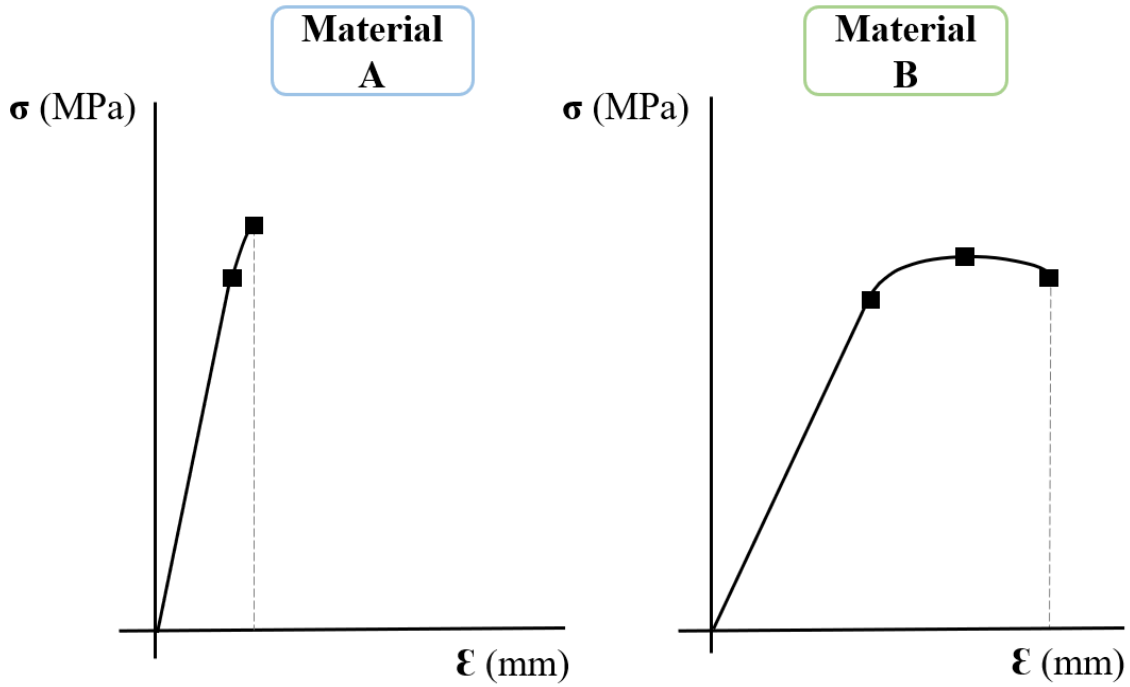

Figure 31: Toughness. Stress - strain curve for material A and B. The area under the curve represents energy required for failure of material – toughness.

Ceramic is often referred to as being brittle. The glassier the ceramic, the better the aesthetic but more fragile it gets. The brittleness of ceramics is caused by the dissociation of covalent bonds due to excessive loading [94], and also due to alkaline hydrolysis of Si-O bonds. The hydrolysis is caused by the alkaline environment, which is formed by the decomposition of potassium or sodium oxide in feldspar ceramics [6].

The ceramic material cracks with a brittle fracture, which then spreads at high speed and requires only low energy compared with ductile fracture [1]. A graphical representation of both fractures is shown in figure 32.

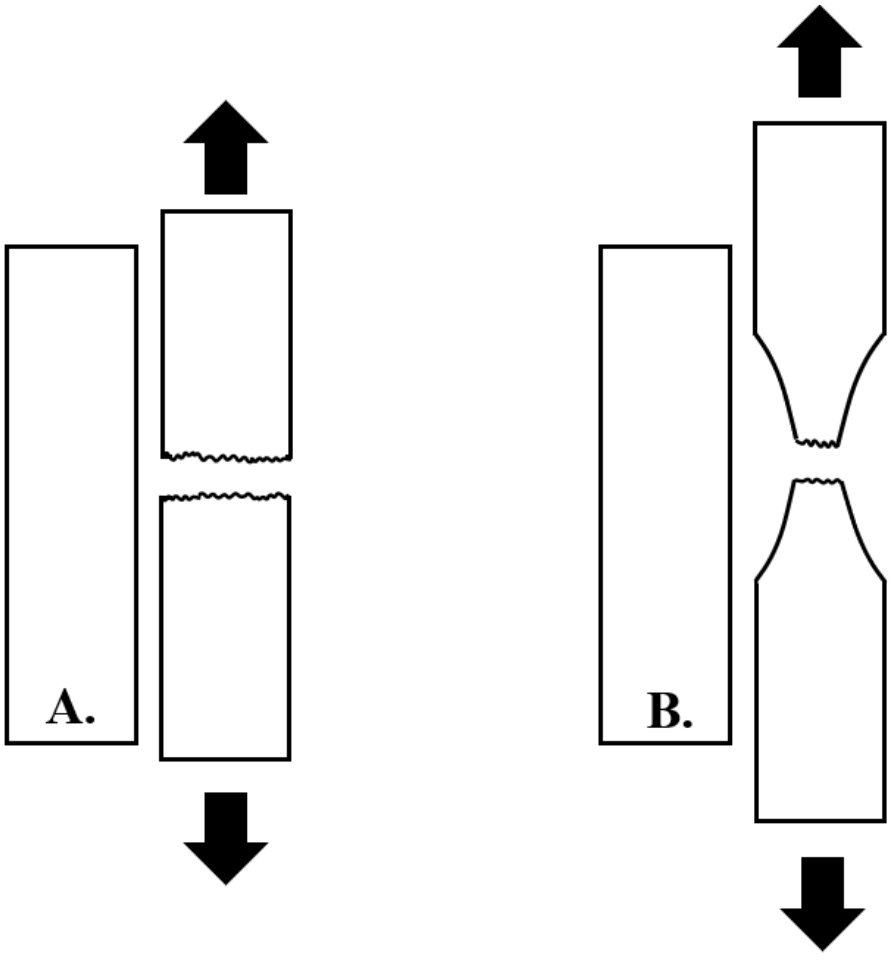

Figure 32: Brittle and ductile fracture. The materials are stressed in tension. A - brittle material, B - ductile material. Brittle fracture on the left, ductile fracture on the right.

2.6.7 Stiffness

Stiffness is defined by elastic modulus. If the interatomic bonds are closer and hard to dislocate, the elastic modulus is higher and material stiffer. Stiffness of a material related to the steepness of the stress-strain curve in the elastic region. The steeper the curve, the stiffer the material. Stiff materials are able to withstand external forces against deformation.

2.6.8 Ductility

Ductility is a mechanical property of material (especially metals) to deform plastically (permanent deformation) without fracture of material [20,21]. Dental ceramic materials are not ductile as they do not undergo significant plastic deformation before fracture.

2.6.9 Measurement methods

Due to the importance of the mechanical properties of dental ceramics, we need precise and reliable methods to measure them. There are multiple methods, each with its own strengths and weaknesses.

2.6.9.1 Strength

For ceramic and brittle materials, flexural strength is most often measured. The uniaxial bending strength test (e.g. three-point bending test) or biaxial bending test (e.g. ball on ring method) is used for the given measurement. The mechanism of these techniques is shown in figures 33, 34 and 35.

2.6.9.1.1 Uniaxial strength

Three-point bending test

In the three-point bending test, the sample (beam) of a given material is placed on two parallel support pins, which form the support of the beam of the tested material. On the other side of the specimen (beam), a load force is applied by a third pin - exactly halfway between the supporting pins. The force is applied until the material fails [21]. The stress is concentrated in the centre of the beam, under the loading point.

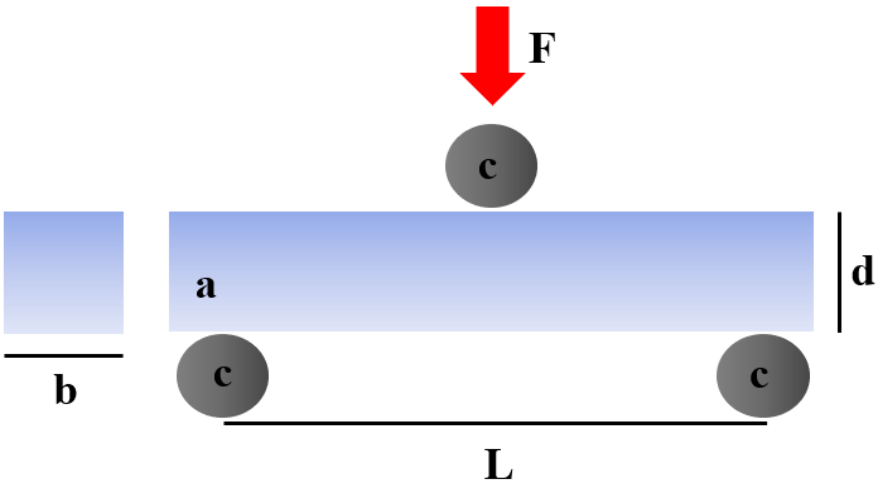

Figure 33: Graphic description of three-point bending test. a - ceramic beam sample, c - cylinders, L - distance between the supporting cylinders, b - the width of the beam, d - height of the beam, F - acting force.

Four-point bending test

In the four-point bending test, the sample (beam) of a given material is placed on two parallel support pins, which form the support of the beam of the tested material. Load force on the top side of the specimen (beam) is applied by two pins distant from each other (Fig.34). Due to two loading pins, the stress is concentrated in a larger region. The difference between the three and four-point test is the location of the area of maximum stress. Three-point bending test is better for a test of homogeneous material, while the four-point test is better four

non-homogenous material such as some composite materials. Four-point bending test with large regions of stress concentration also avoids premature failures [98].

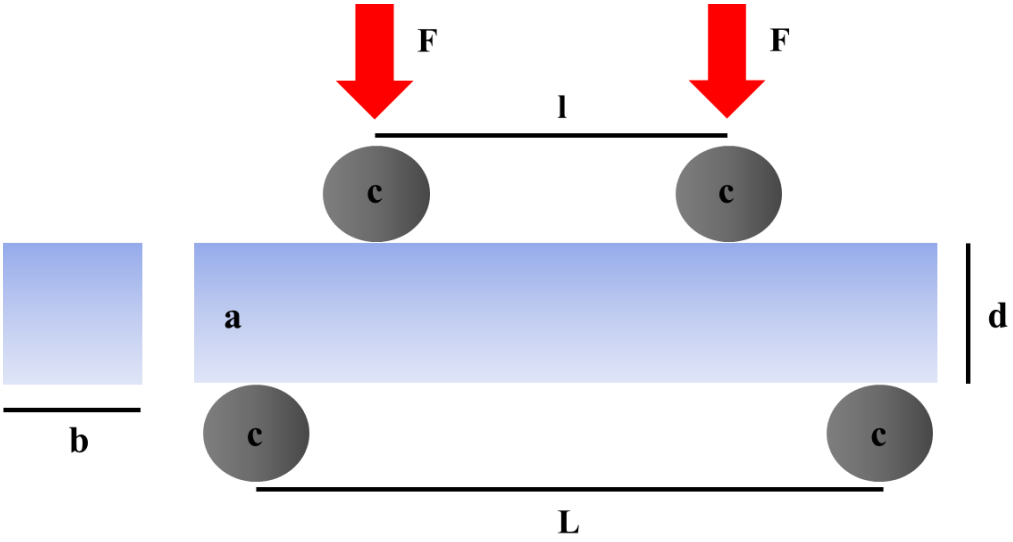

Figure 34: Graphic description of four-point bending test. a - ceramic beam sample, c - cylinders, L - distance between the supporting cylinders, l - distance between loading cylinders b - the width of the beam, d - height of the beam, F - acting force.

2.6.9.1.2 Biaxial flexural strength

Ball on ring configuration

The ball on ring method places a sample of the tested disc-shaped material on the base ring. The underside of the ceramic disk is in contact with the base ring and the upper side is in contact with a metal ball. The ball presses on the sample in the centre of the disk with a predefined force until the material fails [99]. The side facing the ball is in compression, while the side facing the ring is in tension (Fig.35).

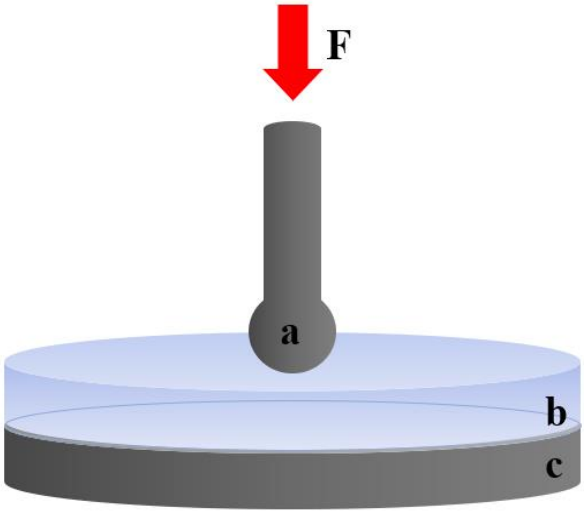

Figure 35: Graphic description of ball on ring method. a – ball applying force F to the centre of the sample, b - disc shape of testing sample, c – backing ring.

The minimum flexural strength for predominantly glass dental ceramics is reported in the literature in the range of 50-70 MPa [2,6,95]. The maximum flexural strength for polycrystalline dental ceramics based on zirconia is in the range of 900-1200 MPa [2,6,77,95]. From these data it is evident that a higher content of the crystalline phase increases the strength of the ceramic.

2.6.9.2 Hardness

Hardness can be tested in several ways, using static or dynamic tests. The best-known tests include the Martens scratch test, the Shore rebound test and the Vickers, Brinell, Knoop and Rockwell penetration tests [91]. The Vickers penetration test is then typically used in research to report the hardness of ceramic material.

Vickers Hardness Penetration test

The mechanism of the Vickers test is shown in figure 36. This method uses a quadrilateral pyramid with an apex angle of 136° [6,21,100]. The quadrilateral pyramid (indentor) is pressed with a defined force into the surface of the tested material. The hardness of the material can also be determined according to the length of the indenter diagonals and the hardness tables [101].

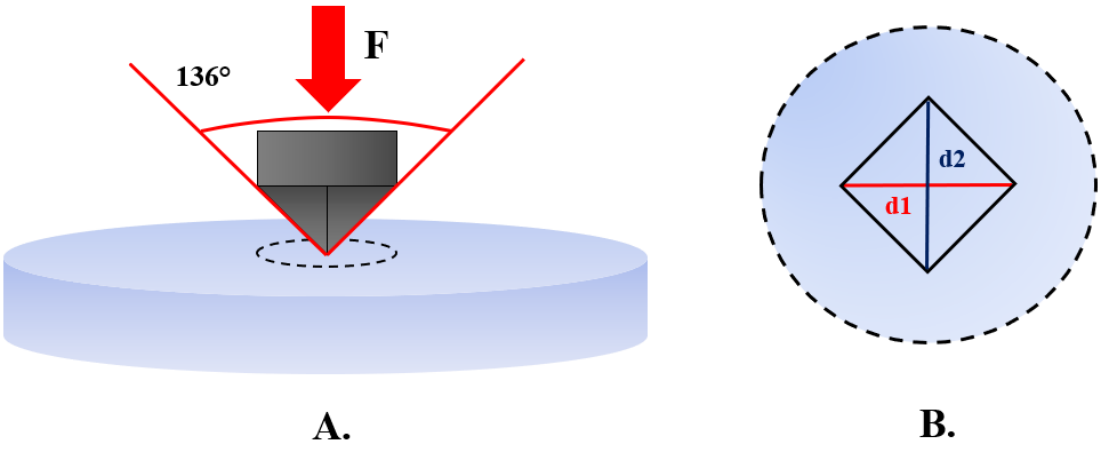

Figure 36: Graphic description of Vickers hardness penetration test. A - Vickers indenter (136° - diamond pyramid indenter) is forced into the surface of ceramic material. B - Indented surface of ceramic material with Vickers indenter – quadrilateral indentation with diagonals d1, d2.

2.6.9.3 Fracture toughness

For a measurement of fracture toughness, we use special samples (beams, discs) with an artificially created V-shaped notch, or a microcrack created by indentation using a Vickers indenter. The strength of these specimens is tested using a uniaxial or biaxial flexural test (the

side with the artificial crack faces downwards and is in tension). Demonstration of the method is described in figures 37, 38.

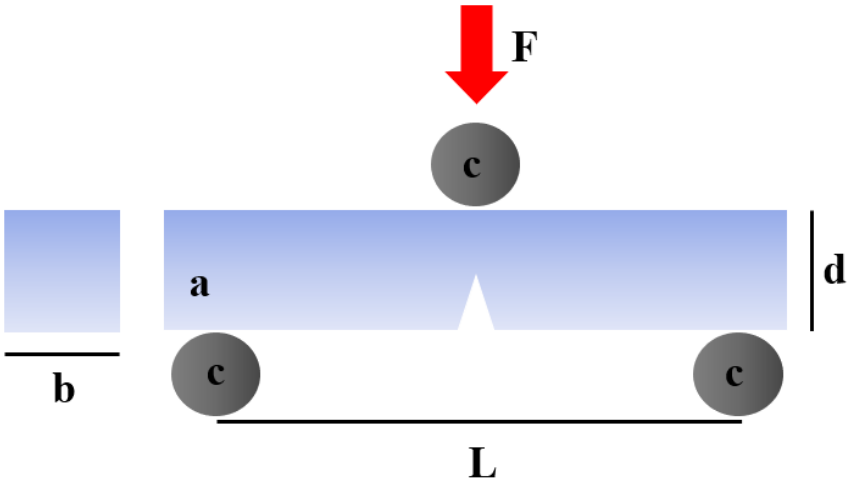

Figure 37: Measurement of fracture toughness by three-point bending test. a - ceramic beam sample with V- notch, c - cylinders, L - distance between the supporting cylinders, b - the width of the beam, d - height of the beam, F -acting force.

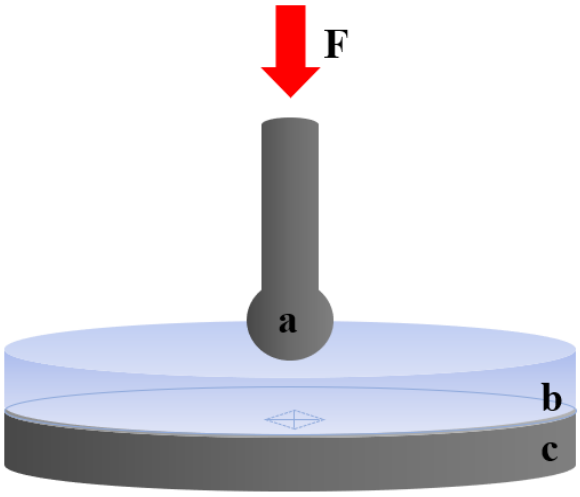

Figure 38: Measurement of fracture toughness by ball on ring configuration. a – ball applying force F to the centre of the sample with microfracture on the bottom of sample (in tension), b – disc shape of testing sample with Vickers indentation (facing downward) in tension, c – backing ring.

2.6.10 Limiting factors of strength of dental ceramic

The strength of dental materials can be influenced by many factors: the composition of dental ceramic, the existence of many flaws, or defects in material. These strength limiting factors can be caused by several aspects, and we will try to describe them briefly here:

- Defects of sub microscopic and atomic dimensions.
- Defects and stress concentrators present in the microstructure of dental ceramics.
- Glass/crystalline phase ratio. The crystals act as buffers against crack propagation. The fewer bumpers (crystals) and glassier matrix of the dental ceramic material, the less resistant the material is to crack propagation. (Fig.39).

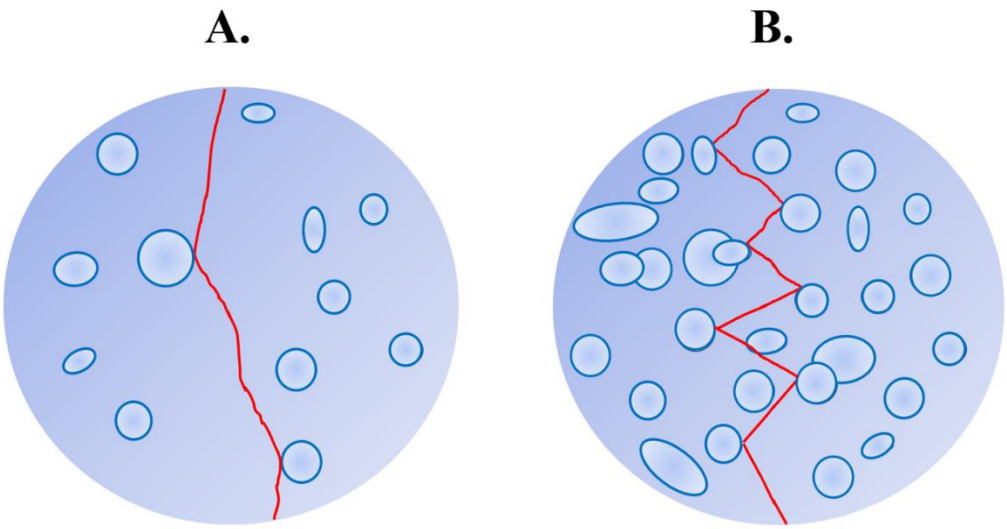

Figure 39: Glass crystalline ratio. Material A with less crystals (bumfers)- susceptible to fast crack propagation. Material B with more crystals supporting slower propagation of cracks or complete cessation.

- Surface defects, microcracks caused by grinding or cutting, using a subtractive method of machining (e.g. CAD/CAM technologies) [27], or contact with other solid bodies. From the

point of our research the most interesting are the defects caused by subtractive machining and will be described in detail in the next chapter.

- Cracks and other defects caused by incorrect technological procedure. Defects can be caused by inadequate condensation or drying during conventional shaping of dental ceramic. The defects can arise due to rapidly raising the temperature during the firing process, or rapidly decreasing temperature during the cooling process. It was found that slower (soft) cooling under the transformation glass temperature leads to reduced negative residual stresses in dental ceramic. Furthermore, a direct contact of the firing pin with glass ceramic causes localized residual stresses, potentially resulting in partial fusion of pin material into dental ceramic. These strength limiting factors can be mitigated by using fibrous pads or firing pastes [102,103].
- The strength of dental ceramics can also be affected by internal stresses caused by the differences in the coefficients of thermal expansion (CTE) of different phases [1]. It is very desirable to have a coefficient of thermal expansion of crystalline phase (disperse phase) slightly higher than a glassy matrix. The glass matrix will be placed in compression, which influences the mechanical performance of dental ceramic [22]. As mentioned in the history part (chapter 2.1), the veneering metal copings with dental porcelain had a fundamental problem of large mismatch of coefficients of thermal expansions between porcelain and metal substrate. Thanks to Weinstein (1962), we now know that for metallo-ceramic restoration, it is crucial to closely match the CTE of dental ceramic and metal substrate, and that it is also desirable to have ceramic with a little bit lower CTE than metal. Thanks to this the ceramic after cooling gets into compression, resulting in ceramic being more resistant to chipping.

2.6.11 Defects caused by subtractive machining

The use of Computer Aided Design/Computer Aided Manufacturing (CAD/CAM) processes is increasing in popularity within the dental field due to its manufacturing efficiency, as CAD/CAM systems are less time consuming and less human labor demanding [104]. The production technology for ceramic restoration primarily involves subtractive machining, which introduces some disadvantages for future ceramic restoration. This process was described in detail in the chapter: Classification by manufacturing method (2.4.2). Subtractive machining involves material removal from a ceramic block or discs by diamond particles embedded in the bur [12,105].

The principle of material removal in subtractive machining is the chipping of the material caused by microfractures. While this is welcomed during the manufacturing process, these surface quality alterations are also present at the surface of the final milled reconstruction. These defects are strength limiting for the final restoration and can negatively influence their durability [27,106–108].

The origin of the defects is well known. If the brittle ceramic is machined, there are structural changes resulting in damage of the material [109,110]. This leads to strength limiting microcracks and a zone of plastic deformation, which subsequently represents the residual stress (Fig.40.) [111]. There are two types of microfractures i.) lateral cracks, which are formed normal to the grinding direction. Lateral cracks play a dominant role in the chipping of the material, they are less severe and thus less strength limiting for the final ceramic restoration ii.) median cracks are formed predominantly parallel to the grinding direction. They are propagated to ceramic mass [27,109]. Median cracks negatively affect the strength of the material if they are more severe than pre-existing cracks in the material (Fig.40) [112–116].

Residual stress plays a big role in propagation of the cracks. It can be divided into compressive stress and wedging stress. The compressive stress is localized adjacent to the

ground groove. It helps to stabilize the cracks, but it is relatively shallow - less than the median crack length. The wedging stress is larger in comparison to the compressive zone, and negatively affects the propagation of the cracks. This means that the strength of material is influenced by severity of strength limiting microfractures and their interaction with residual stress [27].

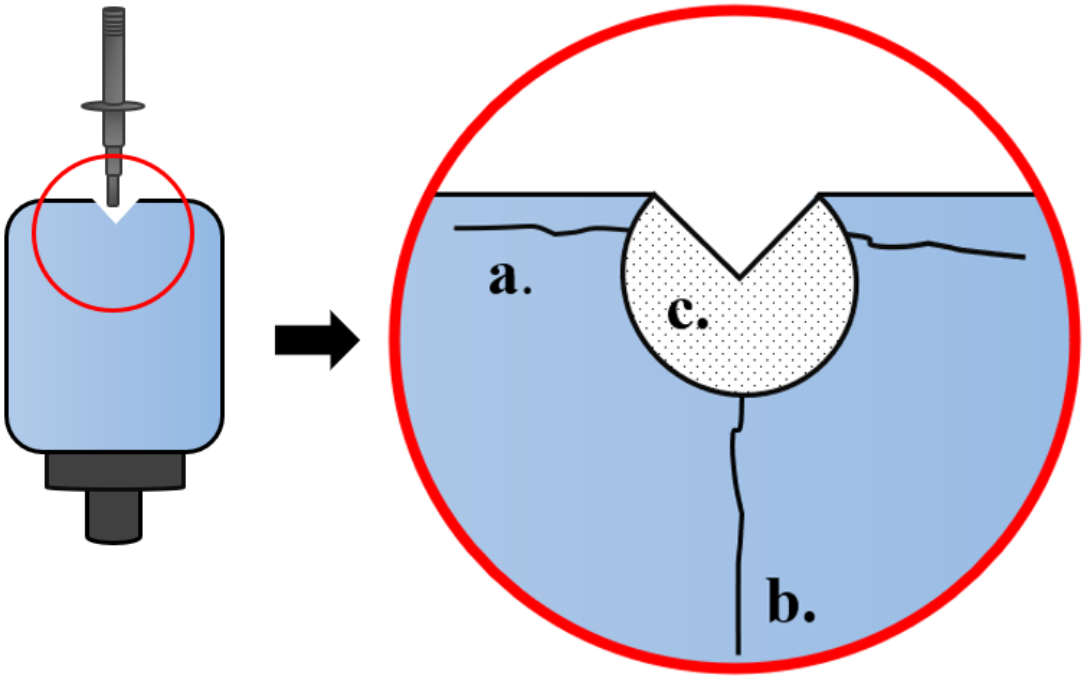

Figure 40: Graphical description of strength limiting defects caused by subtractive machining. Right - Diamond embedded bur grind sulcus in the ceramic block. Left - zoom to ground sulcus a.) lateral cracks, b.) median cracks, c.) zone of plastic deformation under the sulcus.

2.6.11.1 Negative factors

Dental restorations are steadily subjected to cyclic forces, moisture, and temperature changes in the oral environment [21,117]. These changes may further influence the promotion of the cracks previously introduced by CAD/CAM machining.

2.6.11.1.1 Use

During mastication, teeth and dental restorations are steadily subjected to cyclic forces (around 300,000 flexures per year) [21,117]. Ceramic is brittle material sensitive to the stress concentrations around pre-existing flaws and defects, so fatigue is often a mechanism of ceramic clinical failure [117].

Loading below monotonic strength of material results in slow-crack growth of defects and can lead to catastrophic failure of a restoration. This repetitive low strength loading dramatically influences the life service of ceramic restoration [118].

Microstructure changes in the material under fatigue loading and their progression are well understood: 1. nucleation of defects resumes, 2. microflows formation, 3. coalescent of microflows, 4. stable cracks, 5. unstable cracks and failure [119]. Low strength loading negatively influences propagation of pre-existing strength limiting cracks introduced by CAD/CAM machining and shortens the lifespan of ceramic restoration [27,112,120,121].

2.6.11.1.2 Heat

Strength limiting defects present on the surface of the ceramic restoration can be aggravated by thermal changes. Every day, human mouth undergoes several thermal changes from ingested food and drinks, resulting in expansive and contractile forces to any existing dental restorations [122]. When a ceramic object is transferred from hot to cold water, the surface temperature drops and is substantially lower than the specimen's average temperature while the centre of the subject is relatively warmer. This causes compressive stresses in the centre of subject and detrimental surface tensile stress, which could negatively influence the propagation of the surface cracks (Fig.41) [122,123].

As we mentioned above, the largest amount of tensile stress accumulates in the area of the crack tip (Fig.30). Ceramic material is brittle, so plastic deformation is negligible, and the

stress accumulates in the area of the crack tip. When the stress exceeds the critical limits, the crack propagates, and the material fails. Transferring the object from cold to hot water induces converse stresses. When the surface temperature is higher than the central temperature, surface compressive stresses and inner tensile occur [122,123].

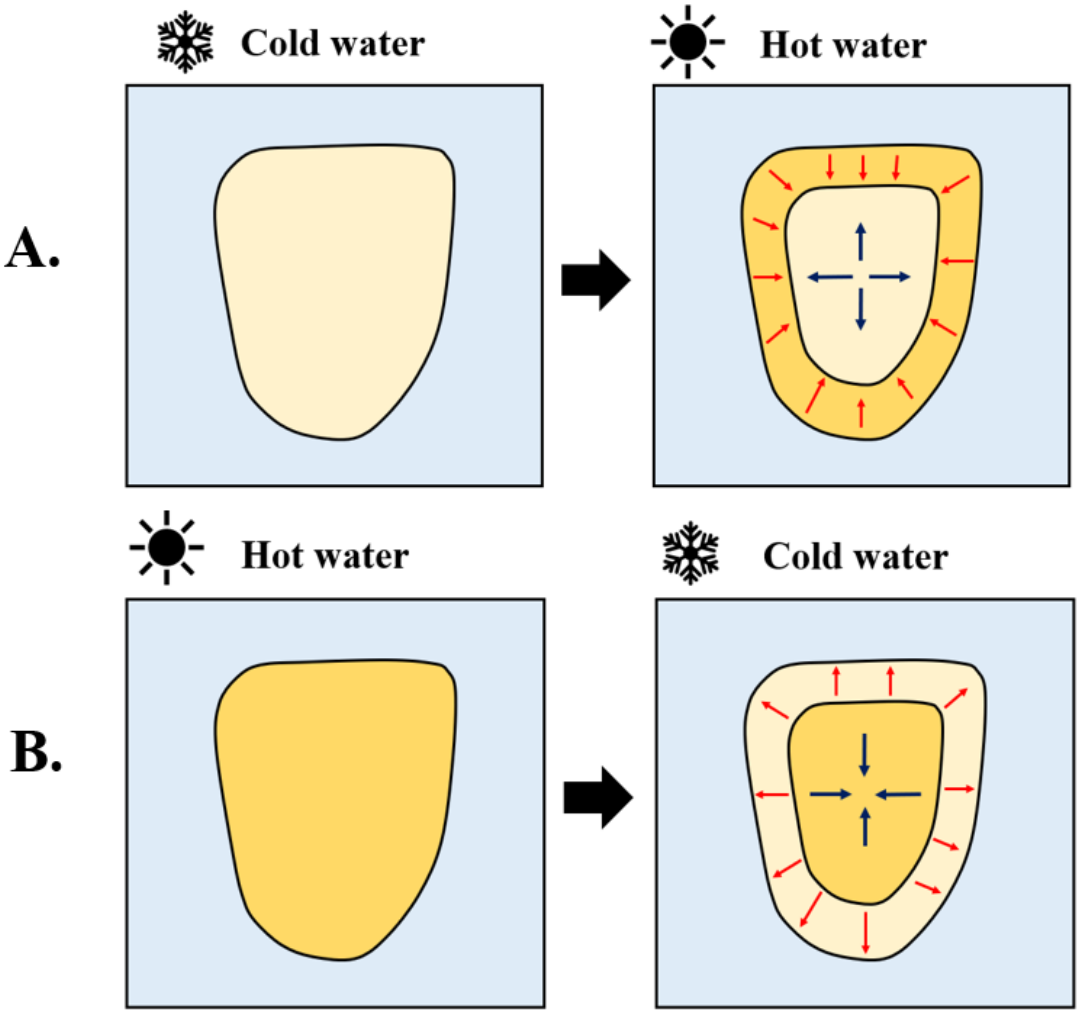

Figure 41: Graphical demonstration of stress in ceramic reconstruction during thermal changes. A - Ceramic reconstruction is transferred from cold to hot water, ceramic surface is in tension and centre in compression. B - Ceramic reconstruction is transferred from hot to cold water, surface is in compression and centre in tension.

Propagation and formation of surface defects are more likely in brittle material in tension, where rapid cooling might cause particularly detrimental effects [124]. This phenomenon is

able to negatively influence the lifespan of CAD/CAM ceramic restorations. The expansive and contractive forces from thermal loading might cause further crack extension of existing defects, and consequently reduce the strength of the restoration [124–126].

Furthermore, the presence of water molecules at the tip of a crack causes the hydrolysis of the siloxane bonds (corrosion), slowly growing the cracks [118].

2.6.11.2 Remedies

2.6.11.2.1 Crystallization process

CAD/CAM dental ceramics can be divided into two primary groups with respect to the crystallization process i) fully crystallized (one-step) or ii) partially crystallized systems (two step systems). Fully crystallized ceramics are obtained and machined in their (already) fully crystallized state and are ready to be installed after machining and polishing (belli). Partially crystallized ceramics are machined in partially crystallized form and further crystallized. The examples of partially crystallized blocks available on the market are presented in table 2.

While the partially crystallized system process is more economically demanding as it requires firing equipment and is also more time consuming, it is favourable for machining as the material is softer, it has better edge stability and causes less wear of the burs [34,127,128]. After machining, the material undergoes the heating process (crystallization), reaching its final microstructure, mechanical, physical, and optical properties [34,51,65,70,71,127,129]. Furthermore, this process has been shown to have crack-healing properties [127].

There are multiple material processes during the crystallization process:

1. **Viscous flow of glass matrix.** When glass exceeds the transition temperature during the heating, it gets into a viscous state without losing its shape [130]. This process is referred to as annealing. Another benefit of this process is that any initial residual stresses in the material are relieved [123].
2. **Change of crystallinity.** During the crystallization, the ceramic crystalline microstructure changes, final crystals grow and some dissolve. The volume of crystallinity increases.
3. **Linear shrinkage.** Due to the microstructure changes, the ceramic restoration during the heating process slightly linearly shrinks. This shrinkage is calculated in milling software for each specific ceramic material.

These processes can potentially be beneficial to the introduced defects, mitigating the resulting strength degradation.

Table 2: Representatives partially crystallized dental ceramic on the market.

Name (*Brand*)	Type of dental ceramic
IPS. Emax CAD *(Ivoclar Vivadent)*	Lithium disilicate glass ceramic
Amber Mill *(Hass)*	Lithium disilicate glass ceramic
Mazic Claro *(Vericom)*	Lithium disilicate glass ceramic
Rosseta SM *(Hass)*	Lithium disilicate glass ceramic
Vita Suprinity *(Vita Zahnfabrik)*	Lithium di-silicate glass ceramic reinforced with zirconia

2.6.11.2.1.1 Crystallization process of lithium disilicate ceramic IPS e max.CAD

Nowadays, IPS e.max® CAD is the most popular lithium disilicate material used in dentistry. This ceramic is often called “blue blocks” among dentist, due to their blue/violet colour when delivered to the dental offices or dental labs. The blue colour is caused by the valency of vanadium ions, which are added to the ceramic composition (described in detail in chapter: Lithium disilicate glass ceramic).

Blue blocks are in the partially crystalline stage and consist mainly of i) few lithium disilicate crystals ii) lithium orthophosphate which acts as nucleation agent iii) metasilicates crystals occupying the major part [34,37,71,131].

During the heating process (crystallization) as the temperature reaches 530°C [70] (650°C [132]), the metasilicate crystals grow with dendritic shape, reaching their maximum size at around 750°C. The metasilicates crystals (Li_2SiO_3) then start decomposing above 780°C up to 820°C and rod-like lithium metasilicate crystals form. It is followed by the formations of the main crystals phase (fish bone crystals) of lithium di-silicate ($Li_2Si_2O_5$) and second crystal phase lithium orthophosphate (Li_3PO_4) [37,70,131]. While $Li_2Si_2O_5$ crystals are also formed under lower temperatures in parallel with the metasilicate growth, their faster and major formation happens only after the decomposition of metasilicates crystals and their interactions with glass. $Li_2Si_2O_5$ crystals reach 70 % volume in a fully crystallized stage and can be found in two different morphologies i) rod-like/rib phase ii) oriented/spine phase.

Rod-like crystals (rib phase) are formed during the decomposition of metasilicate crystals and their subsequent interaction with silicate in a rich glass viscous matrix. Oriented crystals bundles are formed in order to keep electric neutrality - due to the omission of Li ions the Li_2SiO_3 and rearranges to $Li_2Si_2O_5$ oriented bundle (spine phase). The structure of crystals in electron microscopy (rod crystals around bundle crystals) resembles the structure of corn, therefore this formation is called corn-like shape structure [34,51,129,132]. The structural changes during the crystallization process are graphically described in figure 42.

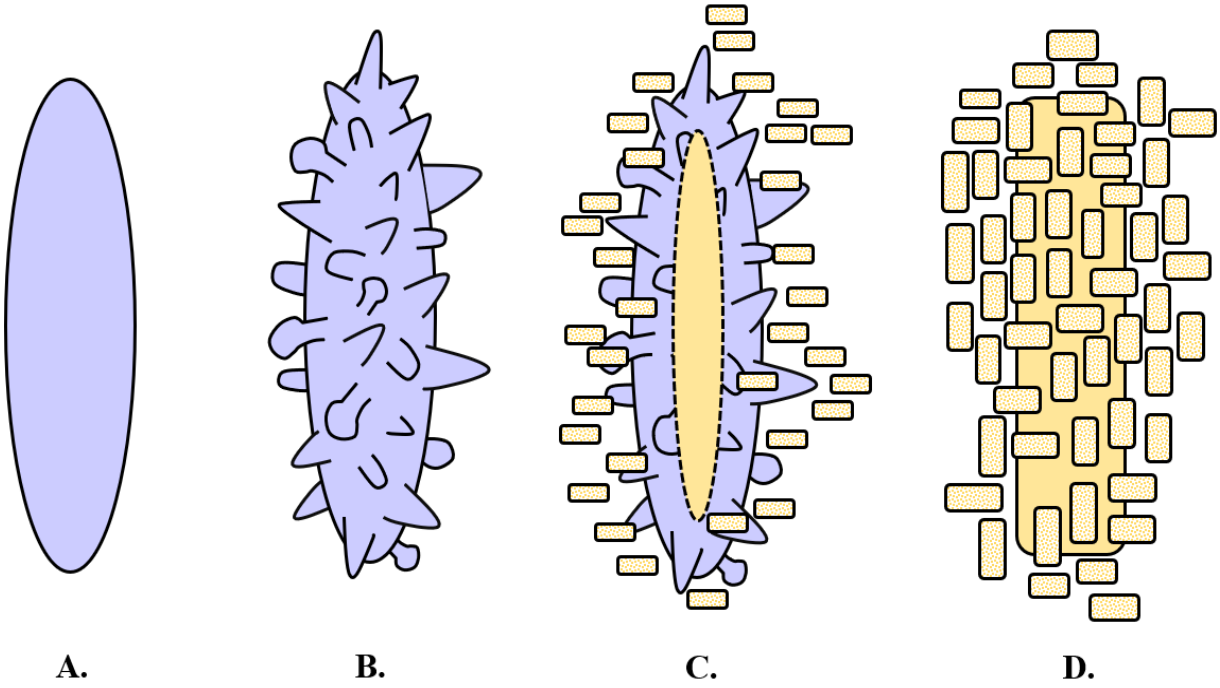

Figure 42: Graphical demonstration of formation of lithium silicate crystals during the crystallization process. A - Plate metasilicate crystal. B - Dendritic metasilicate crystal C - Dendritic metasilicate crystal in decomposition with formation of bundle and rod-like lithium di-silicate crystals D - Final lithium di-silicate crystals with bundle-crystal form in the centre and rod-like crystals form around.

3. The effect of pre-crystallization defect size on strength limitation in lithium silicate glass ceramics

This chapter explores the effects of the crystallization process on mitigating the strength-limiting defects introduced during the CAD/CAM machining and major part of the text has been published as the author's original research in [133].

3.1. Objective

The objective of this study was to explore how the size of pre-crystallization defects affects the strength of a representative lithium disilicate glass ceramic.

3.2. Hypothesis

The crystallization process mitigates the defects in terms of strength limitation, but there is a limit to this process.

3.3. Brief Introduction to the study

This study focuses on positive effects (in terms of crack healing and strength improvement) of crystallization for the partially crystallized ceramics IPS e.max® CAD. It is well known that subtractive machining introduces surface defects which negatively influence the strength and life span of future restoration (chapter 2.6.11 - Defects caused by subtractive machining).

From the chapter crystallization process it is known that there are multiple material processes during the crystallization process that can be potentially beneficial to the introduced defects resulting strength degradation. While previous work has demonstrated that the crystallization process does decrease the crack dimensions introduced during the machining, the resulting defects were still strength limiting [127]

However, only a single defect severity was considered. The effects of the crystallization process on varying defect sizes and the resulting strength degradation are thus not well understood.

The aim of this study was to determine the effect of the crystallization process of varying severe defects on partially crystallized lithium disilicate CAD/CAM ceramic. The tested hypothesis was that the crystallization process can mitigate the defects in terms of strength limitation, but there is a limit to this process.

3.4. Materials and methods

3.4.1. Test specimen manufacture

This study used partially crystallized lithium di-silicate ceramic IPS e.max® CAD blocks (Ivoclar Vivadent, Schaan, Litchenstein). In accordance with previous studies [27,134], the blocks were machined by water jet into cylinders having a nominal diameter of 10 mm. Disc shaped specimens were produced by transversely cutting the cylindrical blocks with a slow speed linear precision saw (IsoMet 5000, Buehler, USA) to produce 105-disc samples with a thickness of 1.1±0.1 mm thickness (Fig.43). The parameters used were blade speed 4000 rpm, feed rate 19 mm/min, blade thickness 0.508 mm. One side of the ceramic disc was polished to reach a consistent surface finish on which to impose defects. All disc samples were manually polished, using silicon carbide abrasive paper in a progressive polishing sequence using P-800, P-1000, P-1500, and P-2000 grits at 90 s interval for each [27]. Water served as a lubricant during this process. All polishing was completed by 2 of the researchers (Kristýna Hynková, Hai-lin Deng) to limit bias introduced by manual polishing.

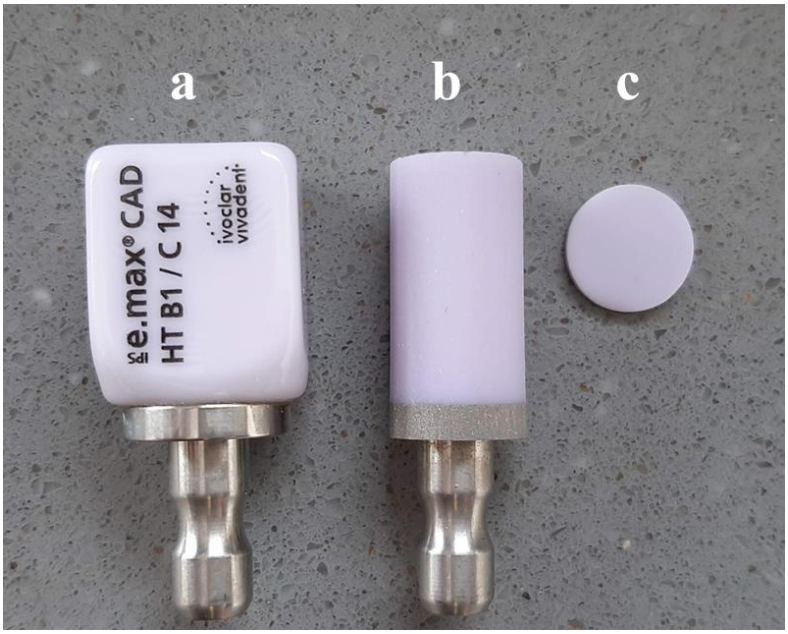

Figure 43: Manufacture of disc samples. a - Block of partially crystallized lithium di-silicate ceramic IPS e.max® CAD blocks (Ivoclar Vivadent, Schaan, Litchenstein). b - Ceramic cylinder machined by water jet. c - Ceramic disc.

3.4.2. Controlled defect generation

The samples were randomly selected to 7 groups (n=15 per group), corresponding to different static loads to be imposed through indentation. The controlled surface defects were made by indentation with a Vickers hardness indenter (Wilson® Vickers Micro-hardness Tester, Buehler, USA). To simulate varying severities of surface defects, each group used different static load of the microhardness indentation: Group CONT, control group (polish); Group IND0.1, indent with 0.1kg; Group IND0.2, indent with 0.2kg; Group IND0.3, indent with 0.3kg; Group IND0.5, indent with 0.5 kg; Group IND1, indent with 1.0 kg; Group IND2, indent with 2.0 kg (Tab.3). All static loads were held for 99 s.

Table 3 – Groups distribution.							
Group	CONT	IND0.1	IND 0.2	IND0.3	IND 0.5	IND 1	IND 2
Static Load *(kg)*	x	0.1	0.2	0.3	0.5	1	2

To make the location of indentation consistent, the approximate centre of all discs was identified using a 3D printed locator (Fig.44)

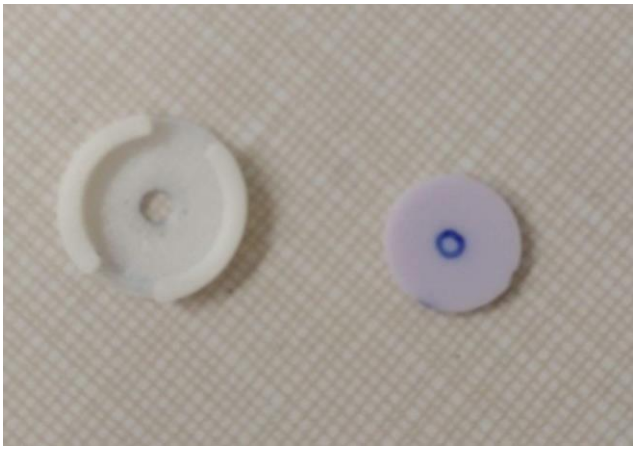

Figure 44: Process of indentation location. Left - 3D printed centre locator. Right - ceramic sample with marked centre.

Note: Here the author would like to explain briefly why the indentation control defects were used in this study to analyse CAD/CAM defects.

The grinding analysis describes in literature two mechanisms: 1. "machining" approach 2. "indentation fracture mechanics" [135]. Machining approach assumes a role of a plastic-flow mode of chip formation after the grain penetrates to a critical depth. The indentation fracture mechanism approach has been shown to be a reasonable model to describe the material removal process for dental ceramic, where the plastic-flow regime is negligible [135].

While the indentation fracture mechanics approach assumes that the damage produced by grinding can be simulated as a single crack system produced by an indenter, the machining damage differs due to different configurations of the plastic deformation zone and associated cracks, as well as the multiplicity of neighbouring damage sites [120]. Despite these discrepancies, the single indentation has been shown as a reasonable model as it provides a qualitative description of the response of machining-induced cracks [120]. These strength limiting defects were described in chapter: Defects caused by subtractive machining.

3.4.3. Crystallization process

All samples were subjected to the crystallization process in the Ivoclar Vivadent Programat EP 5000 furnace, as specified by the manufacturer. This process consisted of the following schedule: 1) preheating samples to 403°C for 6 min, 2) increasing the temperature at 90°C/min to 820°C, (550°-820°C under vacuum), 3) held for 0.1 minute, 4) increasing 30°C/min to 840°C, 5) for 7 minutes, 6) long term cooling from 700°C. As mentioned before during crystallization process the microstructure and volume changes occurred so to be consistent in determined thickness as much as possible the thickness of samples was re-measured after the crystallization. The change in thickness after crystallization was up to -0.02 mm. The thickness of samples after crystallization was used for calculations.

3.4.4. Optical microscopy

The indented surface of samples was observed with an optical microscope before and after the crystallization process. The optical microscope 50 x zoom (attached to a Wilson® Micro-hardness tester, Buehler, USA) was used to measure the cracks and indentation before and after the crystallization process (Fig.45). The sum of the horizontal/vertical crack lengths

and the horizontal/vertical dimensions of the diamond rhomb were used as a measure of cracks and central indent, respectively (Fig.45).

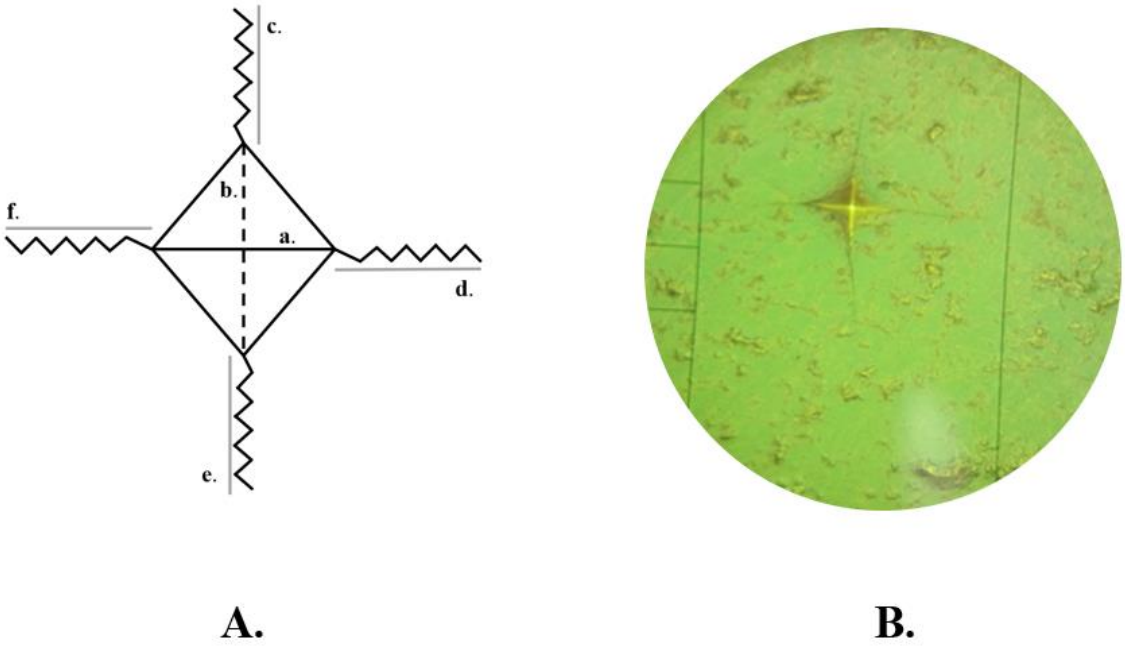

Figure 45: Control surface defect. A - Graphical description of diamond shape represents a Vickers indentation with horizontal/vertical length of a/b. The lateral microcracks propagating from the corners of the indentation are: c, d, e, f. B - Photo of control surface defect in optical microscope.

In order to not bias the data, whenever any of these values were not recognizable (e.g., at lower static indenter loads where propagating cracks could not be discerned), the datapoint was removed. As the crystallization process resulted in substantial changes to the diamond indent geometry, the measurements were performed prior to the crystallization only.

3.4.5. Atomic force microscopy

Atomic Force Microscopy (AFM) was used to further observe the effect of the crystallization process on the surface ceramic defects. Six additional samples were made and polished by the same process as described in subchapter sample preparation. These samples were distributed into three groups of two. First group was controlled (just polished) and second group was exposed to Vickers indenter with 0.5 kg static load and third was exposed to static load of 2.0 kg (Tab.4). AFM was performed before and after the crystallization process, using a Dimension Edge AFM (Bruker, USA) (Fig.46), using silicone probe Tap300-G (Ted Pella, Inc. USA) in tapping mode, a scan size of 50 × 50 μm and scan rate of 0.5 Hz. The Gwyddion software was used to visualize and analyse data from AFM.

Table 4 – Groups distribution for AFM.

Group	***First***	***Second***	***Third***
Static Load *(kg)*	X	0.5	2

Figure 46: Dimension Edge AFM (Bruker, USA)

3.4.6. Bi-axial flexural strength (BFS) determination

The BFS was measured using a ball on ring biaxial flexure configuration and a universal testing machine (ElectroPuls E 3000, Instron, USA) (Fig.47). Disc shape specimens were supported on a knife edge ring (diameter 8.3 mm) and were loaded centrally with stainless steel ball indenter (diameter 7.9 mm) at a cross head speed of 1 mm/min (Fig.48). The polished/indented surface of the samples was facing down (i.e. facing the ring) to load the affected surface in tension.

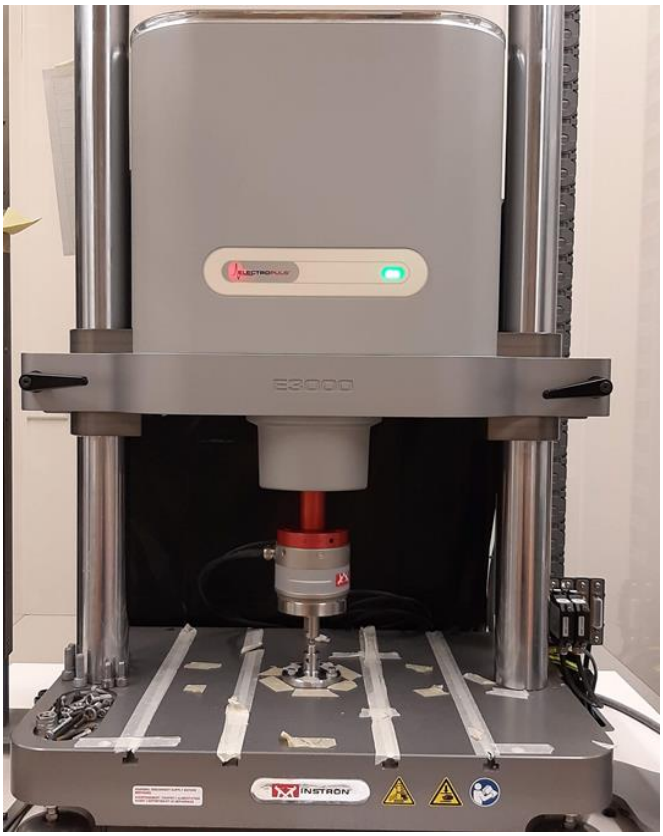

Figure 47: ElectroPuls E 3000, Instron, USA

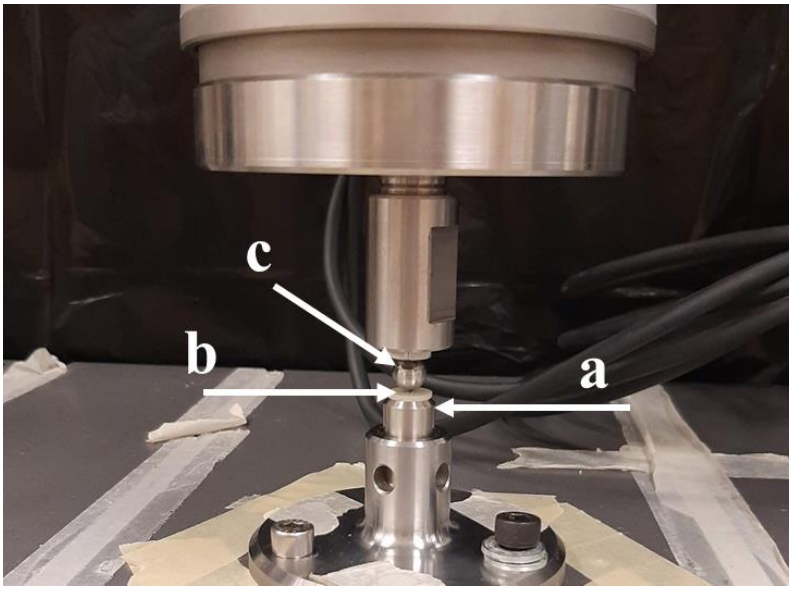

Figure 48: Ball on ring configuration, ElectroPuls E 3000, Instron, USA. a - knife edge ring, b - ceramic sample (indented surface of the samples facing the ring), c - stainless steel ball indenter.

The Timoshenko and Woinowsky Krieger formulation was utilized to calculate the resulting BFS (Eq. 1). Where *P* is force at fracture (N), *v* is Poison's ratio for the material (v = 0,215 for IPS e.max® CAD), *a* is radius of knife-edge supporter (mm), *h* is sample thickness (mm).

$$BFS = \frac{P}{h^2} \times \left[(1+v) \times \left[0.485 \times ln\ ln\ \left(\frac{a}{h}\right) + 0.52\right] + 0.48\right]$$

Eq.1. Timoshenko and Woinowsky Krieger formula. P - force at fracture, v - Poison's ratio for the material, a - radius of knife-edge supporter, h - sample thickness.

3.4.7. Statistical analysis

The Kolmogorov-Smirnov test was used to determine data normality. One-way ANOVA test was used to find out a significant difference in the mean BFS values of all the groups (CONT; IND 0.1; IND 0.2; IND 0.3; IND 0.5; IND 1; IND 2). To test significance differences between any individual group pairs the pairwise comparison Post-hoc Tukey test was used. All statistical tests were applied with significance level of $\alpha = 0.05$.

Note: All steps in the material methods part were carried out by author Kristýna Hynková.

3.5. Results

Table 5 and figure 49 box plot summarized for all the experimental groups the minimum and maximum BFS values, mean BFS and associated standard deviation. The Kolmogorov-Smirnov test did not reject normality. The one-way ANOVA ($\alpha = 0.05$) detect a significant difference ($p=0.028$). Post-hoc Tukey test ($\alpha = 0.05$) reveal a significant difference ($p<0.01$) between two groups (IND0.2 and IND2).

The biaxial flexural survival probability plot was made to further analyse the differences between the groups, as shown in figure 50. The groups with the two largest defect sizes, IND1 and IND2, exhibit outliers at lower strength values, suggesting a limit of the crystallization process, where the only samples with BFS below 300 MPa come from these two groups.

Table 5 - BFS values: mean and standard deviations.

Group	**CONT (control)**	**IND 0.1 (0.1 kg)**	**IND 0.2 (0.2 kg)**	**IND 0.3 (0.3 kg)**	**IND 0.5 (0.5 kg)**	**IND 1 (1 kg)**	**IND 2 (2 kg)**
BFS *(MPa)*	355 - 589	348 – 555	414 – 578	339 - 508	343 - 553	259 - 564	277 - 517
Mean BFS *(MPa)*	458 ± 77	441 ± 62	490 ± 52	426 ± 44	461 ± 54	428 ± 66	416 ± 64

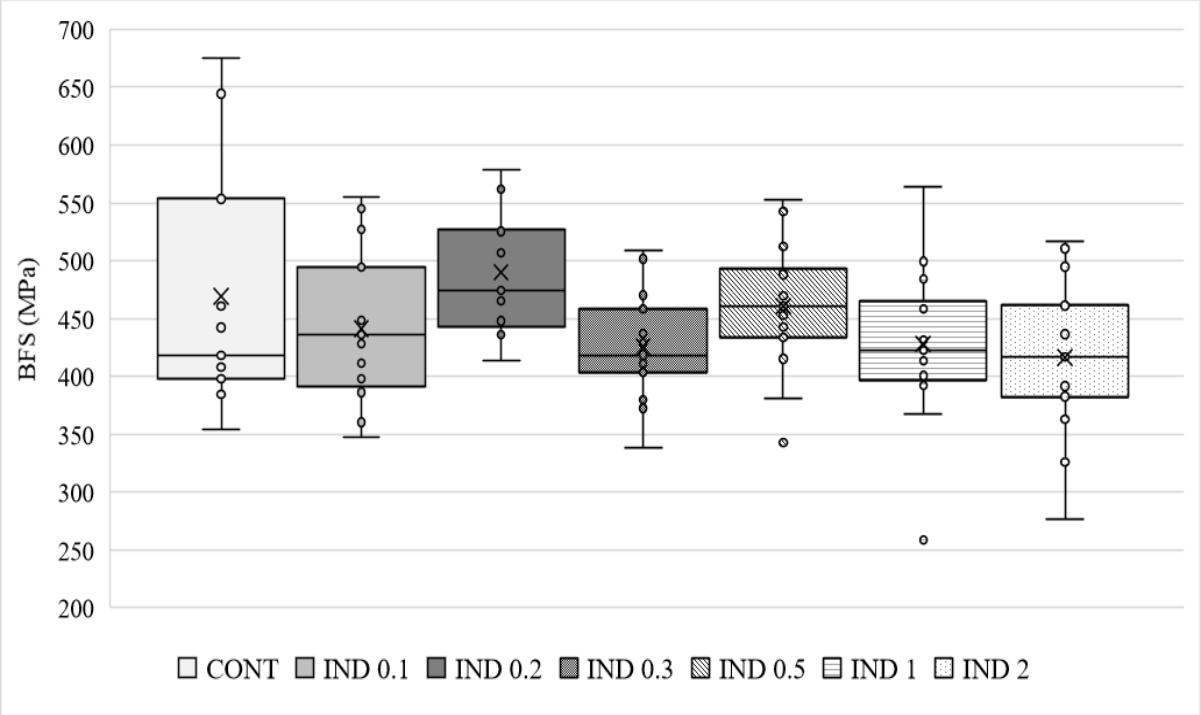

Figure 49: BFS box plot graph. Box plot graph demonstrate the BFS value with mean, standard deviation, inner and outlier points. All the groups with varying severity of the defects are present.

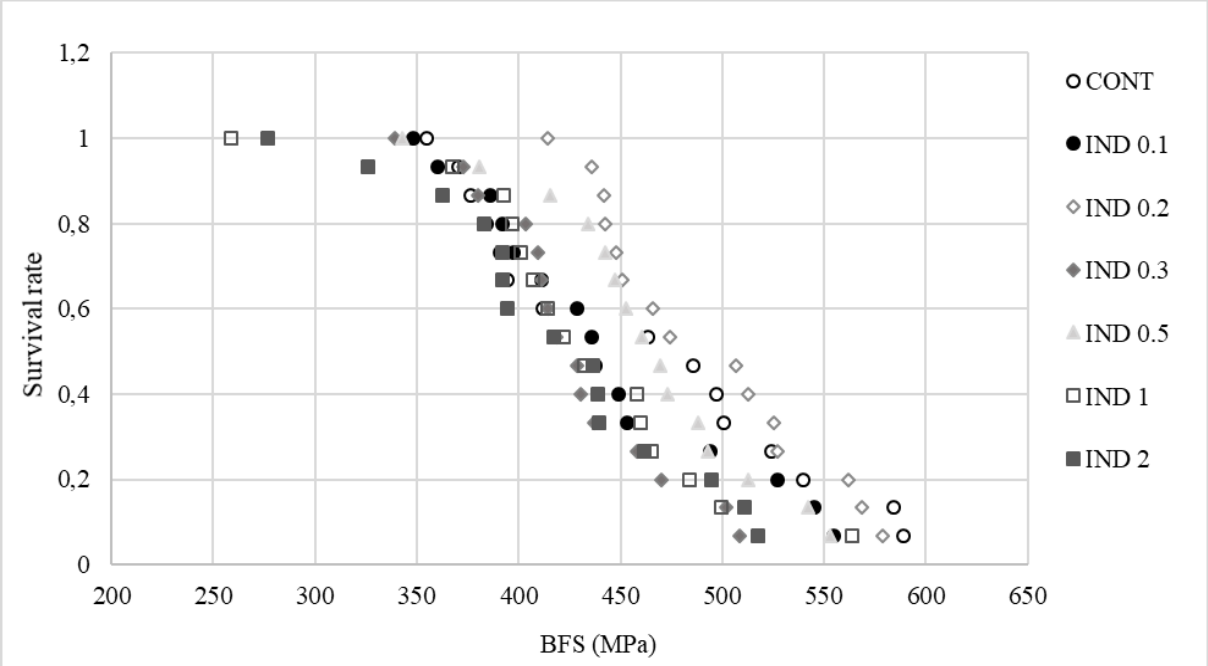

Figure 50: BFS survival probability plots. The groups with the largest surface defects IND 1 and IND 2 (1 kg and 2 kg loads) demonstrate discontinuity in the lowest BFS values, being the only ones that survived less than 300 MPa.

Figure 51 and figure 52 relate defect severity to BFS. Figure 51 focuses on the size of the diamond, while figure 52 attends to the crack dimensions propagating from the central Vickers indent. These pictures demonstrate that indentation load correlates with the defect severity, as the groups form identifiable clusters.

To review the effects of the crystallization process on the surface defects, figure 53 shows representative AFM images before and after crystallization. The samples with the 0.5 kg and 2.0 kg indentation exhibit visual changes after the crystallization. The surface control defects (indentation and the cracks) are notably smoother and shallower (Fig.53).

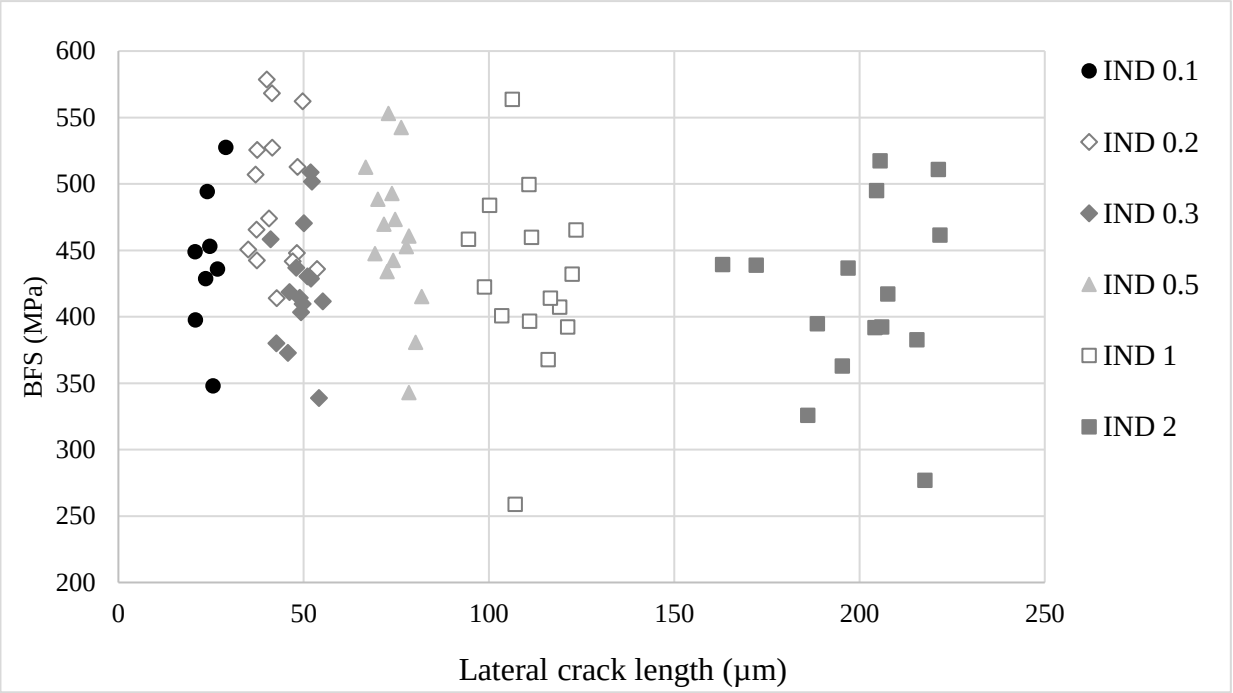

Figure 51: Diamond length against the BFS. The different indentation loads (different groups) clearly affect the diamond size of the defect. Only samples with intelligible diamond length were include.

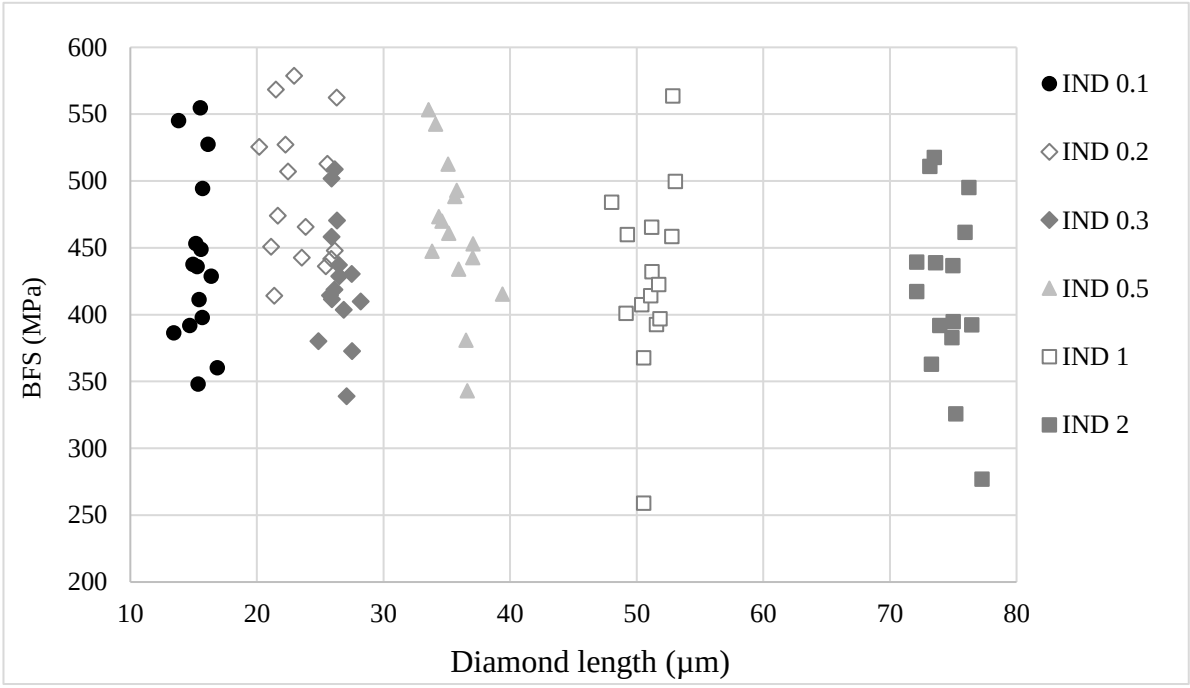

Figure 52: Lateral crack size against the BFS. The different indentation loads (different groups) clearly affect the crack length of the defect. Only samples with intelligible diamond length were included.

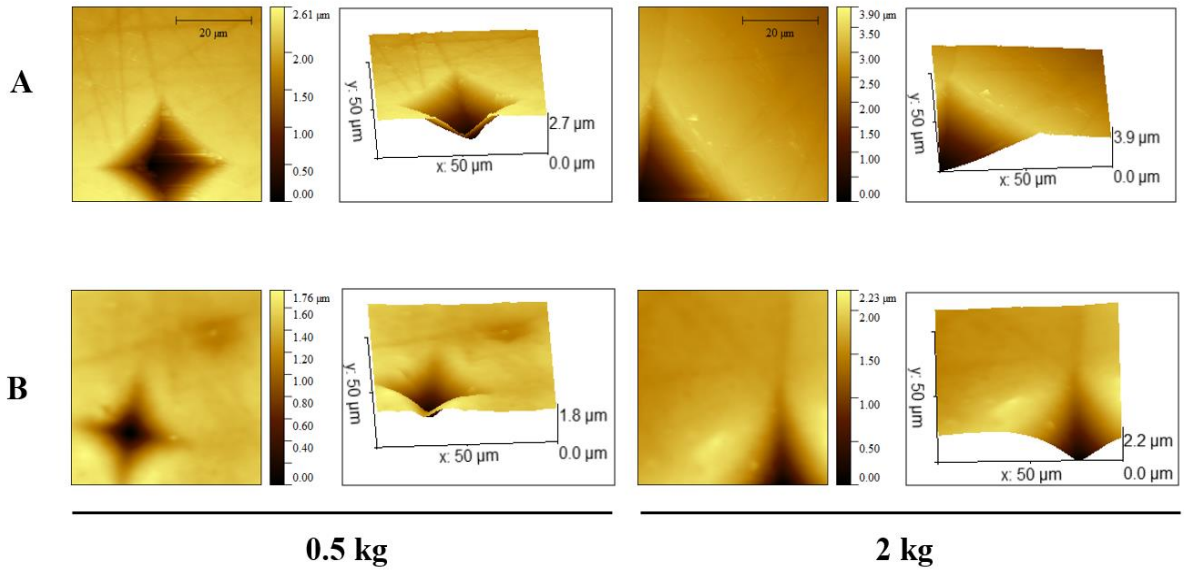

Figure 53: Atomic force microscopy (AFM) of the additional AFM group. A - Sample with 0.5 kg indentation before and after the crystallization, B - Sample with 2 kg indentation before and after the crystallization. Both pictures demonstrate that the depth of the defect was decreased, while the borders of the diamond were smoothed out.

3.6. Discussion

The defect sizes tested in this study were found to have a significant effect on resulting BFS after crystallization. Moreover, a single significant pairwise difference was found between the groups IND0.2 and IND2. Further analysis of the BFS via the survival rate (Fig.50) confirms that the only low-strength outliers come from the two groups with the largest defect sizes (IND1 and IND2). This suggests that while the crystallization helps to mitigate smaller defects, the larger defects are approaching the limits of what the crystallization mechanisms can remedy. This is consistent with previous work, where larger grinding defects do lead to decreased BFS [27,127]. While Belli et al. 2019 reports that the crystallization reduces the size of larger cracks introduced by machining, the reduced defects were still strength limiting (consistently with the results of Romanyk et al. 2019) as CAD/CAM machining damage often extends to at least 50 μm [27,107,127]. An important consideration in contextualizing current results with previous research is the fact that expansion and the resulting material failure does not follow Griffith crack expansion where the initial crack size is the only relevant factor. The failure is rather a function of crack size as well as the residual stress accumulated in the plastic zone of deformation [113,114,120]. Results from this study suggest that if the defects are sufficiently small, the crystallization process can mitigate both the crack size and the residual stress up to a point where there is no significant difference in BFS when compared to the control group.

BFS values are not the only indication of the positive effect of the crystallization process in this study. Pre and post crystallization AFM pictures show clear changes of the surface indentation defects (Fig.53). The indentation and the cracks are shallower, and the surface is noticeably smoother. It suggests that multiple material processes during the crystallization as growth of crystals and the viscos stage of glass could help to decrease the porosity of the material and to relax the residual stresses introduced during the grinding. The viscous flow of

the glass and microstructural changes can serve to reduce crack size and residual stress, mitigating the surface defects and resulting strength degradation.

This agrees with Belli et al. 2019, where the reported strengthening effect and decreased crack dimension after the crystallization process are attributed to the change of crystal structure and glass in viscous flow cause the crack shrinkage [127]. Furthermore, the included XRD analysis pre and post crystallization revealed a cristobalite crystallization on the surface of the IPS e.max CAD. This has been then suggested to create potentially beneficial compressive stresses shielding the defects and improving the strength. This study shows that when the defects are sufficiently small, all these processes can mitigate the strength-limiting effects up to the point where the microstructure governs strength.

The nature of the strength-limiting effects is well understood. A plastic zone of deformation and associated stress field developed during the grinding process plays a crucial role for both formation of the cracks and their response to the subsequent loading [120]. While an elastic component is also involved during the grinding and plays a role in formation of the cracks (e.g. suppressing the lateral cracks so that they only develop after the indenter is being removed), it is irrelevant for post-machining loading as it fully reverses after grinding. The post-machining strength thus depends on the residual stresses and the generated lateral and medial/radial cracks themselves [113]. Medial cracks do not extend back into the plastic deformation zone [136] and together with the residual fields affect the resulting material strength. Lateral cracks play a dominant role in the chipping of the material during the grinding process. The residual stresses then either help to stabilize or extend the cracks dependent on the material and machining parameters (although the crack stabilizing compressive stresses likely remain confined to a relatively thin layer [127]).

The positive effects of the crystallization process presented in this, and prior studies further motivate dental clinicians to minimize the severity of these defects (both cracks and

residual stresses). Interestingly, Addison et al. 2012 showed that this cannot be achieved simply by using new burs rather than used ones (i.e. frequently changing burs does not help) as the surface roughness rather depends on a random selection of a bur and a random machining sequence [137]. Alao et al. 2017 report that pre-crystallization polishing is significantly more effective to post-crystallization polishing in smoothing out the rough surface introduced by grinding; however, no strength data was collected preventing further understanding of how the order of manufacture operations would influence strength [138]. Belli et al. 2019 then report pre-crystallization polishing as being more effective in terms of resulting strength measurements [127]. Different crystallization cooling rates have been investigated in Wendler et al. and Lohbauer et al. [102,103]. Slower (soft) cooling under the transformation glass temperature led to reduced negative residual stresses. Furthermore, direct contact of the firing pin with glass ceramic developed localized residual stresses and also the fusion of pin material into the ceramic. Thus, different firing setups were suggested. Namely, the use of fibrous pads or firing pastes seem as good options to minimize the residual stresses near the contact with ceramic material.

3.7. Conclusion

We have demonstrated that the crystallization of partially crystallized IPS e.max® CAD ceramic can heal small indentation defects, resulting in no statistical strength difference between the control group and groups with small indentation. Post-processing steps are likely to modify strength limiting defects and residual stress states. While the positive strength effects of crystallization have been reported previously, the post-healing defects were still strength-limiting. Our study shows that if the defects are sufficiently small, the process mitigates the strength-limiting effects up to the point where the microstructure governs strength. Furthermore, the groups with larger defects do suggest that the corresponding defects approach the limits of the process and the post-processing defects are becoming strength-limiting.

4. REFERENCES

[1] Pokluda J, Kroupa F, Obdržálek L. Mechanické vlastnosti a struktura pevných látek. Brno: 1994.

[2] Giordano R, McLaren EA. Ceramics overview: classification by microstructure and processing methods. Compend Contin Educ Dent 2010;31:682–4, 686, 688.

[3] KRÁLÍK M, NOVOTNÝ V, OLIVA M. FINGERPRINT ON THE VENUS OF DOLNÍ VĚSTONICE . Antropologie 2002;XL/2:107–13.

[4] Kelly JR, Benetti P. Ceramic materials in dentistry: Historical evolution and current practice. Aust Dent J 2011;56:84–96. https://doi.org/10.1111/j.1834-7819.2010.01299.x.

[5] Zhao Z. Augustus II the Strong's Porcelain Collection at the Japanisches Palais zu Dresden: A Visual Demonstration of Power and Splendor. McGill University, 2018.

[6] Hubálková H, Krňoulová J. Materiály a technologie v protetickém zubním lékařství. vol. first. Praha: 2019.

[7] Talibi M, Kaur K, Patanwala HS, Parmar H. Do you know your ceramics? Part 1: classification. Br Dent J 2022;232:27–32. https://doi.org/10.1038/s41415-021-3818-x.

[8] Anderson TJ. History Of Dentistry: A Practical Treatise For The Use Of Dental Students And Practitioners. Philadelphia and New York : 1922.

[9] Leinfelder KF, Kurdziolek SM. Contemporary CAD/CAM technologies: the evolution of a restorative system. Pract Proced Aesthet Dent 2004;16:224–6, 228, 231.

[10] Helvey G. Classification of dental ceramics. Inside Dentistry 2013;4:62–80.

[11] Helvey G. A History of Dental Ceramics. Compendium of Continuing Education in Dentistry 2010;31.

[12] Patil M, Kambale S, Patil A, Mujawar K. Digitalization in dentistry: CAD/CAM -A review. Acta Scientific Dental Sciences 2018;2:12–6.

[13] Jain R, Takkar RR, Jain G, Takkar RR, Deora N, Jain Professor R. CAD-CAM the future of digital dentistry: a review. Annals of Prosthodontics & Restorative Dentistry 2016;2:33–6.

[14] Abdullah AO, Muhammed FK, Zheng B, Liu Y. An Overview of Computer Aided Design / Computer Aided manufacturing (CAD/CAM) in Restorative dentistry. J Dent Mater Tech 2018;7:1–10.

[15] Davidowitz G, Kotick PG. The Use of CAD/CAM in Dentistry. Dent Clin North Am 2011;55:559–70. https://doi.org/10.1016/j.cden.2011.02.011.

[16] Ottl P, Piwowarczyk A, Lauer HC, Hegenbarth EA. The Procera AllCeram system. Int J Periodontics Restorative Dent 2000;20:151–61.

[17] Mörmann WH. The evolution of the CEREC system. Journal of the American Dental Association 2006;137:7S-13S. https://doi.org/10.14219/jada.archive.2006.0398.

[18] Sannino G, Germano F, Arcuri L, Bigelli E, Arcuri C, Barlattani A. CEREC CAD/CAM chairside system. Oral Implantol (Rome) 2014;7:57–70. https://doi.org/10.11138/orl/2014.7.3.057.

[19] Ueda Y, Yamaguchi T. History of and current situation regarding dental CAD/CAM systems and future perspectives. Hokkaido J Dent Sci 2017;38:104–10.

[20] Anusavice KJ. Philips' Science of Dental Materials 12th ed. Elsevier Inc, 2012.

[21] Sakaguchi R, Powers J. Craig's Restorative Dental Materials. 14th ed. Missouri: Elsevier; 2019.

[22] Bergmann CP, Stumpf A. Dental ceramics: Microstructure, properties and degradation. Heidelberg: Springer; 2013. https://doi.org/10.1007/978-3-642-38224-6.

[23] Powers JM, Wataha JC. Dental materials. Properties and manipulation. 10th ed. London: Elsevier Health Sciences; 2014. https://doi.org/10.1016/0300-5712(84)90008-3.

[24] Khan AS, Chaudhry AA. Handbook of ionic substituted hydroxyapatites. Elsevier; 2019. https://doi.org/10.1016/c2018-0-00399-0.

[25] Ahmad I, Al-Harbi F. 3D Printing in Dentistry 2019/2020. 1st ed. Quintessence Pub Co; 2019.

[26] https://www.cncsourced.com/guides/3-4-5-axis-cnc-machine-router/ n.d.

[27] Romanyk DL, Martinez YT, Veldhuis S, Rae N, Guo Y, Sirovica S, et al. Strength-limiting damage in lithium silicate glass-ceramics associated with CAD–CAM. Dental Materials 2019;35:98–104. https://doi.org/10.1016/j.dental.2018.11.004.

[28] Manappallil J. Basic Dental Materials. 4th ed. Jp Medical Ltd; 2015. https://doi.org/10.5005/jp/books/12669.

[29] Santander SA, Vargas AP, Escobar JS, Monteiro FJ, Tamayo LFR. Ceramics for dental restorations - an introduction. DYNA (Colombia) 2010;77:26–36.

[30] Warreth A, Elkareimi Y. All-ceramic restorations: A review of the literature. Saudi Dental Journal 2020;32:365–72. https://doi.org/10.1016/j.sdentj.2020.05.004.

[31] Hynková K, Voborná I, Linke B, Levin L. Compendium of current ceramic materials used for the CAD/CAM dentistry. Acta Stomatologica Marisiensis Journal 2021;4:7–17. https://doi.org/10.2478/asmj-2021-0002.

[32] Shenoy A, Shenoy N. Dental ceramics: An update. Journal of Conservative Dentistry 2010;13:195–203. https://doi.org/10.4103/0972-0707.73379.

[33] Leung BTW, Tsoi JKH, Matinlinna JP, Pow EHN. Comparison of mechanical properties of three machinable ceramics with an experimental fluorophlogopite glass ceramic. Journal of Prosthetic Dentistry 2015;114:440–6. https://doi.org/10.1016/j.prosdent.2015.02.024.

[34] Fasbinder DJ. Materials for chairside CAD/CAM restorations. Compend Contin Educ Dent 2010;31:702–4, 706, 708–9.

[35] Atay A, Sağirkaya E. Effects of Different Storage Conditions on Mechanical Properties of CAD/CAM Restorative Materials. Odovtos - International Journal of Dental Sciences 2019;22:83–96. https://doi.org/10.15517/ijds.2020.38742.

[36] Yoshida K, Meng X, Kamada K, Atsuta M. Influence of surface characteristics of four silica-based machinable ceramics on flexural strength and bond strength of a dual-curing resin luting agent. Journal of Adhesive Dentistry 2007;9:407–14.

[37] Belli R, Wendler M, de Ligny D, Cicconi MR, Petschelt A, Peterlik H, et al. Chairside CAD/CAM materials. Part 1: Measurement of elastic constants and microstructural characterization. Dental Materials 2017;33:84–98. https://doi.org/10.1016/j.dental.2016.10.009.

[38] Sen N, Us YO. Mechanical and optical properties of monolithic CAD-CAM restorative materials. Journal of Prosthetic Dentistry 2018;119:593–9. https://doi.org/10.1016/j.prosdent.2017.06.012.

[39] Low IM. Advances in ceramic matrix composites. 2nd ed. Woodhead Publishing; 2014. https://doi.org/10.1533/9780857098825.

[40] Vichi A, Sedda M, Del Siena F, Louca C, Ferrari M. Flexural resistance of Cerec CAD/CAM system ceramic blocks. Part 1: Chairside materials. Am J Dent 2013;26:255–9.

[41] D'Arcangelo C, Vanini L, Rondoni GD, De Angelis F. Wear properties of dental ceramics and porcelains compared with human enamel. Journal of Prosthetic Dentistry 2016;115:350–5. https://doi.org/10.1016/j.prosdent.2015.09.010.

[42] Denry I, Holloway JA. Ceramics for dental applications: A review. Materials 2010;3:351–68. https://doi.org/10.3390/ma3010351.

[43] Blackburn C, Rask H, Awada A. Mechanical properties of resin-ceramic CAD-CAM materials after accelerated aging. Journal of Prosthetic Dentistry 2018;119:954–8. https://doi.org/10.1016/j.prosdent.2017.08.016.

[44] Lu T, Peng L, Xiong F, Lin XY, Zhang P, Lin ZT, et al. A 3-year clinical evaluation of endodontically treated posterior teeth restored with two different materials using the CEREC AC chair-side system. Journal of Prosthetic Dentistry 2018;119:363–8. https://doi.org/10.1016/j.prosdent.2017.04.022.

[45] Lauvahutanon S, Takahashi H, Shiozawa M, Iwasaki N, Asakawa Y, Oki M, et al. Mechanical properties of composite resin blocks for CAD/CAM. Dent Mater J 2014;33:705–10. https://doi.org/10.4012/dmj.2014-208.

[46] Sonmez N, Gultekin P, Turp V, Akgungor G, Sen D, Mijiritsky E. Evaluation of five CAD/CAM materials by microstructural characterization and mechanical tests: A comparative in vitro study. BMC Oral Health 2018;18. https://doi.org/10.1186/s12903-017-0458-2.

[47] Lambert H, Durand JC, Jacquot B, Fages M. Dental biomaterials for chairside CAD/CAM: State of the art. Journal of Advanced Prosthodontics 2017;9:486–95. https://doi.org/10.4047/jap.2017.9.6.486.

[48] Alamoush RA, Silikas N, Salim NA, Al-Nasrawi S, Satterthwaite JD. Effect of the Composition of CAD/CAM Composite Blocks on Mechanical Properties. Biomed Res Int 2018;2018. https://doi.org/10.1155/2018/4893143.

[49] Sulaiman TA. Materials in digital dentistry—A review. Journal of Esthetic and Restorative Dentistry 2020;32:171–81. https://doi.org/10.1111/jerd.12566.

[50] de Kok P, de Jager N, Veerman IAM, Hafeez N, Kleverlaan CJ, Roeters JFM. Effect of a retention groove on the shear bond strength of dentin-bonded restorations. Journal of Prosthetic Dentistry 2016;116:382–8. https://doi.org/10.1016/j.prosdent.2016.01.032.

[51] Li RWK, Chow TW, Matinlinna JP. Ceramic dental biomaterials and CAD/CAM technology: State of the art. J Prosthodont Res 2014;58:208–16. https://doi.org/10.1016/j.jpor.2014.07.003.

[52] Badawy R, El-Mowafy O, Tam LE. Fracture toughness of chairside CAD/CAM materials - Alternative loading approach for compact tension test. Dental Materials 2016;32:847–52. https://doi.org/10.1016/j.dental.2016.03.003.

[53] Bajraktarova-Valjakova E, Korunoska-Stevkovska V, Kapusevska B, Gigovski N, Bajraktarova-Misevska C, Grozdanov A. Contemporary dental ceramic materials, a review: Chemical composition, physical and mechanical properties, indications for use. Open Access Maced J Med Sci 2018;6:1742–55. https://doi.org/10.3889/oamjms.2018.378.

[54] Beuer F, Schweiger J, Edelhoff D. Digital dentistry: An overview of recent developments for CAD/CAM generated restorations. Br Dent J 2008;204:505–11. https://doi.org/10.1038/sj.bdj.2008.350.

[55] Vargas MA, Bergeron C, Diaz-Arnold A. Cementing all-ceramic restorations. The Journal of the American Dental Association 2011;142:20S-24S. https://doi.org/10.14219/jada.archive.2011.0339.

[56] Brenes DC, Duqum I, Mendonza G. Materials and systems for all ceramic CAD/CAM restorations. Dental Tribute 2016;3:10–5.

[57] Pitiaumnuaysap L, Phokhinchatchanan P, Suputtamongkol K, Kanchanavasita W. Fracture resistance of four dental computer-aided design and computer-aided manufacturing glass-ceramics. Dent J 2017;37:201–8.

[58] Ritzberger C, Apel E, Höland W, Peschke A, Rheinberger VM. Properties and clinical application of three types of dental glass-ceramics and ceramics for CAD-CAM technologies. Materials 2010;3:3700–13. https://doi.org/10.3390/ma3063700.

[59] Zhu J, Rong Q, Wang X, Gao X. Influence of remaining tooth structure and restorative material type on stress distribution in endodontically treated maxillary premolars: A finite element analysis. Journal of Prosthetic Dentistry 2017;117:646–55. https://doi.org/10.1016/j.prosdent.2016.08.023.

[60] Byeon S-M, Song J-J. Mechanical Properties and Microstructure of the Leucite-Reinforced Glass-Ceramics for Dental CAD/CAM. Journal of Dental Hygiene Science 2018;18:42–9. https://doi.org/10.17135/jdhs.2018.18.1.42.

[61] Furtado de Mendonca A, Shahmoradi M, de Gouvêa CVD, De Souza GM, Ellakwa A. Microstructural and Mechanical Characterization of CAD/CAM Materials for Monolithic Dental Restorations. Journal of Prosthodontics 2019;28:e587–94. https://doi.org/10.1111/jopr.12964.

[62] Culp L, McLaren EA. Lithium disilicate: the restorative material of multiple options. Compend Contin Educ Dent 2010;31:716–20.

[63] Lawson NC, Bansal R, Burgess JO. Wear, strength, modulus and hardness of CAD/CAM restorative materials. Dental Materials 2016;32:e275–83. https://doi.org/10.1016/j.dental.2016.08.222.

[64] Goujat A, Abouelleil H, Colon P, Jeannin C, Pradelle N, Seux D, et al. Mechanical properties and internal fit of 4 CAD-CAM block materials. Journal of Prosthetic Dentistry 2018;119:384–9. https://doi.org/10.1016/j.prosdent.2017.03.001.

[65] Zarone F, Ferrari M, Mangano FG, Leone R, Sorrentino R. "digitally Oriented Materials": Focus on Lithium Disilicate Ceramics. Int J Dent 2016;2016. https://doi.org/10.1155/2016/9840594.

[66] Elsaka SE, Elnaghy AM. Mechanical properties of zirconia reinforced lithium silicate glass-ceramic. Dental Materials 2016;32:908–14. https://doi.org/10.1016/j.dental.2016.03.013.

[67] Zhang Y, Lawn BR. Novel Zirconia Materials in Dentistry. J Dent Res 2018;97:140–7. https://doi.org/10.1177/0022034517737483.

[68] Chen XP, Xiang ZX, Song XF, Yin L. Machinability: Zirconia-reinforced lithium silicate glass ceramic versus lithium disilicate glass ceramic. J Mech Behav Biomed Mater 2020;101. https://doi.org/10.1016/j.jmbbm.2019.103435.

[69] Ramos NDC, Campos TMB, Paz ISD La, MacHado JPB, Bottino MA, Cesar PF, et al. Microstructure characterization and SCG of newly engineered dental ceramics. Dental Materials 2016;32:870–378. https://doi.org/10.1016/j.dental.2016.03.018.

[70] Sacher E, Franca R. Dental Biomaterials. vol. secound. New Jersey: 2018.

[71] Willard A, Gabriel Chu TM. The science and application of IPS e.Max dental ceramic. Kaohsiung Journal of Medical Sciences 2018;34:238–42. https://doi.org/10.1016/j.kjms.2018.01.012.

[72] Eakle WS, Bastin KG. Dental Materials Clinical Applications for Dental Assistants and Dental Hygienists. fourth. 2019.

[73] McLaren EA, Figueira J. Updating Classifications of Ceramic Dental Materials: A Guide to Material Selection. Compend Contin Educ Dent 2015;36:400–5.

[74] Rinke S, Pabel AK, Rödiger M, Ziebolz D. Chairside fabrication of an all-ceramic partial crown using a zirconia-reinforced lithium silicate ceramic. Case Rep Dent 2016;2016:1–7. https://doi.org/10.1155/2016/1354186.

[75] Rinke S, Rödiger M, Ziebolz D, Schmidt AK. Fabrication of Zirconia-Reinforced Lithium Silicate Ceramic Restorations Using a Complete Digital Workflow. Case Rep Dent 2015;2015:1–7. https://doi.org/10.1155/2015/162178.

[76] Traini T, Sinjari B, Pascetta R, Serafini N, Perfetti G, Trisi P, et al. The zirconia-reinforced lithium silicate ceramic: Lights and shadows of a new material. Dent Mater J 2016;35:748–55. https://doi.org/10.4012/dmj.2016-041.

[77] Gregg A. Helvey. Zirconia and Computer-aided Design/Computer-aided Manufacturing (CAD/CAM) Dentistry. Inside Dentistry 2008;4.

[78] IPS e.max ZirCAD englisch_aktualisiert 30112017.doc. n.d.

[79] Vágner P, Guhlke C, Miloš V, Müller R, Fuhrmann J. A continuum model for yttria-stabilized zirconia incorporating triple phase boundary, lattice structure and immobile oxide ions. Journal of Solid State Electrochemistry 2019;23:2907–26. https://doi.org/10.1007/s10008-019-04356-9.

[80] Della Bona A, Borba M, Benetti P, Pecho OE, Alessandretti R, Mosele JC, et al. Adhesion to Dental Ceramics. Curr Oral Health Rep 2014;1:232–8. https://doi.org/10.1007/s40496-014-0030-y.

[81] Passos SP, Torrealba Y, Major P, Linke B, Flores-Mir C, Nychka JA. In Vitro Wear Behavior of Zirconia Opposing Enamel: A Systematic Review. Journal of Prosthodontics 2014;23:593–601. https://doi.org/10.1111/jopr.12167.

[82] Alghazzawi TF, Lemons J, Liu PR, Essig ME, Bartolucci AA, Janowski GM. Influence of Low-Temperature Environmental Exposure on the Mechanical Properties and Structural Stability of Dental Zirconia. Journal of Prosthodontics 2012;21:363–9. https://doi.org/10.1111/j.1532-849X.2011.00838.x.

[83] Burgess JO. Zirconia: The Material, Its Evolution, and Composition. Compend Contin Educ Dent 2018;39:4–8.

[84] Meirelles L. Ceramic CAD/CAM Materials: An Overview of Clinical Uses and Considerations. ADA Professional Product Rewiev 2017;12:1–9.

[85] Campos F, Almeida CS, Rippe MP, De Melo RM, Valandro LF, Bottino MA. Resin bonding to a hybrid ceramic: Effects of surface treatments and aging. Oper Dent 2016;41:171–8. https://doi.org/10.2341/15-057-L.

[86] Ceren N, Turp V, Emir F, Akgungor G, Ayyildiz S, Şen D. Nanoceramics and hybrid materials used in CAD/CAM systems. Aydın Dental Journal 2016:55–61.

[87] Hynková K, Voborná I. Dental Ceramic - Mechanical Properties. Czech Stomatology & Practical Dentistry 2022;122:87–94.

[88] Wang L, D'Alpino PHP, Lopes LG, Pereira JC. Mechanical properties of dental restorative materials: relative contribution of laboratory tests. Journal of Applied Oral Science 2003;11:162–7. https://doi.org/10.1590/s1678-77572003000300002.

[89] Case J, Chilver L, Ross CTF. Strength of materials and structures. 4th ed. London: 1999.

[90] Somiya S. Handbook of Advanced Ceramics: Materials, Applications, Processing, and Properties: Second Edition. second. 2013. https://doi.org/10.1016/C2010-0-66261-4.

[91] Janovec J, Cejp J. Nauka o materiálu – struktura a vlastnosti materiálu a jejich zkoušení [online]. ČVUT – fakulta strojní – Ústav materiálového inženýrství. [ref.26.7.2023]. Retrieved from: http://UmiFsCvutCz/Wpcontent/Uploads/2014/08/3_2__struktura-Avlastnostni-Materialu-a-Jejich-ZkouseniPdf 2014.

[92] Chun KJ, Lee JY. Comparative study of mechanical properties of dental restorative materials and dental hard tissues in compressive loads. J Dent Biomech 2014;5:1–6. https://doi.org/10.1177/1758736014555246.

[93] Candido LM, Fais LMG, Reis JM dos SN, Pinelli LAP. Surface roughness and hardness of yttria stabilized zirconia (Y-TZP) after 10 years of simulated brushing. Rev Odontol UNESP 2014;43:379–83. https://doi.org/10.1590/1807-2577.1049.

[94] Vagkopoulou T, Koutayas SO, Koidis P, Strub JR. Zirconia in dentistry: Part 1. Discovering the nature of an upcoming bioceramic. Eur J Esthet Dent 2009;4:130–51.

[95] McCabe JF, Walls AWG. Applied of Dental Materials. 9th ed. 2008.

[96] Mettu S, Srinivas N, Reddy Sampath CH, Srinivas N. Effect of casein phosphopeptide-amorphous calcium phosphate (cpp-acp) on caries-like lesions in terms of time and nano-hardness: An in vitro study. Journal of Indian Society of Pedodontics and Preventive Dentistry 2015;33:269–73. https://doi.org/10.4103/0970-4388.165657.

[97] Hmaidouch R, Weigl P. Tooth wear against ceramic crowns in posterior region: A systematic literature review. Int J Oral Sci 2013;5:183–90. https://doi.org/10.1038/ijos.2013.73.

[98] Difference-between-3-point-and-4-point-bend-tests [online]. [ref.26.7.2023]. Retrieved from: https://AdvansesCom/Difference-between-3-Point-and-4-Point-Bend-Tests/ n.d.

[99] Shetty DK, Rosenfield AR, McGuire P, Bansal GK, Duckworth WH. Biaxial flexular test for ceramics. Amer Ceram Society Bulletin 1980;59:1194–7.

[100] O'Brian WJ. Physical properties and biocompatibility. In: Quintessence Publishing, editor. Dental material and their selection. 3th ed., Hanover Park: 2002, p. 12–24.

[101] Driml B. Zakladní vlastnosti materialů a jejich zkoušení [online]. UPOL-Katedra Fyzikalní Chemie [ref.26.7.2023]. Reitrieved from: http://ChemikalieUpolCz/ Skripta/Mvm/Zkousky_matPdf 2004.

[102] Wendler M, Belli R, Lohbauer U. Factors influencing development of residual stresses during crystallization firing in a novel lithium silicate glass-ceramic. Dental Materials 2019;35:871–82. https://doi.org/10.1016/j.dental.2019.03.002.

[103] Lohbauer U, Wendler M, Rapp D, Belli R. Fractographic analysis of lithium silicate crown failures during sintering. SAGE Open Med Case Rep 2019;7:1–8. https://doi.org/10.1177/2050313x19838962.

[104] Samra APB, Morais E, Mazur RF, Vieira SR, Rached RN. CAD/CAM in dentistry -A critical review. Revista Odonto Ciencia 2016;31. https://doi.org/10.15448/1980-6523.2016.3.21002.

[105] Rekow ED, Silva NRFA, Coelho PG, Zhang Y, Guess P, Thompson VP. Performance of dental ceramics: Challenges for improvements. J Dent Res 2011;90:937–52. https://doi.org/10.1177/0022034510391795.

[106] Abduo J, Lyons K, Bennamoun M. Trends in computer-aided manufacturing in prosthodontics: A review of the available streams. Int J Dent 2014;2014:1–15. https://doi.org/10.1155/2014/783948.

[107] Sindel J, Petschelt A, Grellner F, Dierken C, Greil P. Evaluation of subsurface damage in CAD/CAM machined dental ceramics. J Mater Sci Mater Med 1998;9:291–5. https://doi.org/10.1023/A:1008812929476.

[108] Curran P, Cattani-Lorente M, Anselm Wiskott HW, Durual S, Scherrer SS. Grinding damage assessment for CAD-CAM restorative materials. Dental Materials 2017;33:294–308. https://doi.org/10.1016/j.dental.2016.12.004.

[109] Warren PD, Pecorari C, Kolosov O V., Roberts SG, Briggs GAD. Characterization of surface damage via surface acoustic waves. Nanotechnology 1996;7:295–301. https://doi.org/10.1088/0957-4484/7/3/020.

[110] Denry IL, Holloway JA, Tarr LA. Effect of heat treatment on microcrack healing behavior of a machinable dental ceramic. J Biomed Mater Res 1999;48:791–6. https://doi.org/10.1002/(SICI)1097-4636(1999)48:6<791::AID-JBM5>3.0.CO;2-P.

[111] Chandrasekar S, Farris TN. Machining and surface finishing of brittle solids. Sadhana - Academy Proceedings in Engineering Sciences 1997;22:473–81. https://doi.org/10.1007/BF02744484.

[112] Rice RW MJThe nature of strength controlling machining flaws in ceramics. NBS Special Publication: The Science of Ceramic Machining and Surface Finishing II. Washington DC: US Government Printing Office; 1979. The nature of strength controlling machining flaws in ceramics. NBS Special Publication: The Science of Ceramic Machining and Surface Finishing II. Washington DC: 1979.

[113] LAWN BR, EVANS AG, MARSHALL DB. Elastic/Plastic Indentation Damage in Ceramics: The Median/Radial Crack System. Journal of the American Ceramic Society 1980;63:574–81. https://doi.org/10.1111/j.1151-2916.1980.tb10768.x.

[114] MARSHALL DB, LAWN BR, EVANS AG. Elastic/Plastic Indentation Damage in Ceramics: The Lateral Crack System. Journal of the American Ceramic Society 1982;65:561–6. https://doi.org/10.1111/j.1151-2916.1982.tb10782.x.

[115] Lawn B, Wilshaw R. Indentation fracture: principles and applications. J Mater Sci 1975;10:1049–81. https://doi.org/10.1007/BF00823224.

[116] Lawn BR, Swain M V. Microfracture beneath point indentations in brittle solids. J Mater Sci 1975;10:113–22. https://doi.org/10.1007/BF00541038.

[117] Wiskott HW, Nicholls JI, Belser UC. Stress fatigue: basic principles and prosthodontic implications. Int J Prosthodont 1995;8:105–16.

[118] Kelly JR, Cesar PF, Scherrer SS, Della Bona A, van Noort R, Tholey M, et al. ADM guidance-ceramics: Fatigue principles and testing. Dental Materials 2017;33:1192–204.

[119] Suresh S. Fatigue of materials. Cambridge university press, 1998. Cambridge university press; 1998.

[120] Marshall DB, Evans AG, Khuri Yakub BT, Tien JW, Kino GS. NATURE OF MACHINING DAMAGE IN BRITTLE MATERIALS. Proc R Soc Lond A Math Phys Sci 1983;385:461–75. https://doi.org/10.1098/rspa.1983.0023.

[121] Fraga S, Amaral M, Bottino MA, Valandro LF, Kleverlaan CJ, May LG. Impact of machining on the flexural fatigue strength of glass and polycrystalline CAD/CAM

ceramics. Dental Materials 2017;33:1286–97. https://doi.org/10.1016/j.dental.2017.07.019.

[122] Addison O, Fleming GJP, Marquis PM. The effect of thermocycling on the strength of porcelain laminate veneer (PLV) materials. Dental Materials 2003;19:291–7. https://doi.org/10.1016/S0109-5641(02)00046-5.

[123] Kingery WD, Bowen HK, Uhlmann DR. Thermal and compositional stresses. Introduction to ceramics. 2nd ed. New York: 1976.

[124] Callister WD RD. Materials Science and Engineering : An Introduction. 8th ed. New York: Wiley; 2009. https://doi.org/10.1007/BF01184995.

[125] Anusavice KJ, Lee RB. Effect of Firing Temperature and Water Exposure on Crack Propagation in Unglazed Porcelain. J Dent Res 1989;68:1075–81.

[126] Gale MS, Darvell BW. Thermal cycling procedures for laboratory testing of dental restorations. J Dent 1999;27:89–99. https://doi.org/10.1016/S0300-5712(98)00037-2.

[127] Belli R, Lohbauer U, Goetz-Neunhoeffer F, Hurle K. Crack-healing during two-stage crystallization of biomedical lithium (di)silicate glass-ceramics. Dental Materials 2019;35:1130–45. https://doi.org/10.1016/j.dental.2019.05.013.

[128] Ivoclar Vivadent. IPS e.max CAD Scientific Documentation. 2005 n.d.

[129] Zhang Y, Kelly JR. Dental Ceramics for Restoration and Metal Veneering. Dent Clin North Am 2017;61:797–819. https://doi.org/10.1016/j.cden.2017.06.005.

[130] Celtra Duo, Developed to make a difference, brochure for the dental laboratory. Dentsply Sirona. 2017 n.d.

[131] Ritzberger C, Schweiger M, Höland W. Principles of crystal phase formation in Ivoclar Vivadent glass-ceramics for dental restorations. J Non Cryst Solids 2016;432. https://doi.org/10.1016/j.jnoncrysol.2015.04.034.

[132] Zhang P, Li X, Yang J, Xu S. The crystallization and microstructure evolution of lithium disilicate-based glass-ceramic. J Non Cryst Solids 2014;392–393. https://doi.org/10.1016/j.jnoncrysol.2014.03.020.

[133] Hynková K, Deng H, Voborná I. The effect of pre-crystallization defect size on strength limitation in lithium silicate glass ceramics. Ceramics-Silikáty 2023;67.

[134] Romanyk DL, Guo Y, Rae N, Veldhuis S, Sirovica S, Fleming GJ, et al. Strength-limiting damage and its mitigation in CAD-CAM zirconia-reinforced lithium-silicate ceramics machined in a fully crystallized state. Dental Materials 2020;36:1157–565. https://doi.org/10.1016/j.dental.2020.09.012.

[135] Malkin S, Bitter JE. Grinding mechanisms and strength degradation for ceramics. Journal of Manufacturing Science and Engineering, Transactions of the ASME 1989;111:167–74. https://doi.org/10.1115/1.3188746.

[136] Evans AG, Wilshaw TR. Quasi-static solid particle damage in brittle solids-I. Observations analysis and implications. Acta Metallurgica 1976;24:939–56. https://doi.org/10.1016/0001-6160(76)90042-0.

[137] Addison O, Cao X, Sunnar P, Fleming GJP. Machining variability impacts on the strength of a “chair-side” CAD-CAM ceramic. Dental Materials 2012;28:880–7. https://doi.org/10.1016/j.dental.2012.04.017.

[138] Alao AR, Stoll R, Song XF, Abbott JR, Zhang Y, Abduo J, et al. Fracture, roughness and phase transformation in CAD/CAM milling and subsequent surface treatments of lithium metasilicate/disilicate glass-ceramics. J Mech Behav Biomed Mater 2017;74:251–60. https://doi.org/10.1016/j.jmbbm.2017.06.015.

5. LIST OF FIGURES

Figure 1: Composition of dental ceramic.

Figure 2: Creation of crystals in glassy matrix.

Figure 3: Classification of dental ceramic by glass/crystalline content.

Figure 4: Photo of intraoral scanner (CEREC Omnicam AC).

Figure 5: Virtual crown fit in virtual software block.

Figure 6: Graphical demonstration of selective laser sintering.

Figure 7: Graphical demonstration of binder jetting.

Figure 8: Graphical demonstration of nanoparticle jetting.

Figure 9: Milling axis.

Figure 10: Graphical demonstration of subtractive machining.

Figure 11: Graphical demonstration of hot-pressing process.

Figure 12: Preparation of ceramic slurry.

Figure 13: Application of dental ceramic layers.

Figure 14: Graphical demonstration of stacking-sintering process.

Figure 15: Photo of VITA Mark II block.

Figure 16: Graphical demonstration of ceramic block with integrated shades gradients.

Figure 17: Boxing graph - flexural strength.

Figure 18: Boxing graph - elastic modulus.

Figure 19: Boxing graph - fracture toughness.

Figure 20: Photo of Empress CAD.

Figure 21: Propagation of crack.

Figure 22: Photo of IPS e.max CAD.

Figure 23: Illustration of yttria stabilized zirconia.

Figure 24: Transformation toughening mechanism.

Figure 25: Uniaxial dry pressing.

Figure 26: Cold isostatic pressing.

Figure 27: Graphical description of MDP monomer bond with zirconia ceramic.

Figure 28: Stress (σ) – strain (ε) curve of hypothetical material.

Figure 29: Elastic and plastic deformation.

Figure 30: Influence of tensile stresses on flaws in brittle and ductile materials.

Figure 31: Toughness.

Figure 32: Brittle and ductile fracture.

Figure 33: Graphic description of three-point bending test.

Figure 34: Graphic description of four-point bending test.

Figure 35: Graphic description of ball on ring method.

Figure 36: Graphic description of Vickers hardness penetration test.

Figure 37: Measurement of fracture toughness by three-point bending test.

Figure 38: Measurement of fracture toughness by ball on ring configuration.

Figure 39: Glass crystalline ratio.

Figure 40: Graphical description of strength limiting defects caused by subtractive machining.

Figure 41: Graphical demonstration of stress in ceramic reconstruction during thermal changes

Figure 42: Graphical demonstration of formation of lithium silicate crystals during the crystallization process.

Figure 43: Manufacture of disc samples.

Figure 44: Process of indentation location.

Figure 45: Control surface defect.

Figure 46: Dimension Edge AFM (Bruker, USA)

Figure 47: ElectroPuls E 3000, Instron, USA

Figure 48: Ball on ring configuration, ElectroPuls E 3000, Instron, USA.

Figure 49: BFS box plot graph.

Figure 50: BFS survival probability plots.

Figure 51: Diamond length against the BFS.

Figure 52: Lateral crack size against the BFS.

Figure 53: Atomic force microscopy (AFM) of the additional AFM group.

6. LIST OF TABLES

Table 1: Example of market representatives of CAD/CAM dental ceramic.

Table 2: Representatives partially crystallized dental ceramic on the market.

Table 3: Groups distribution.

Table 4: Groups distribution for AFM.

Table 5: BFS values: mean and standard deviations.

7. LIST OF EQUATIONS

Equation 1. Timoshenko and Woinowsky-Krieger formula.

8. CONTRIBUTIONS

List of publications published during the course of my study:

1. **Hynková K., Sarao SK., Voborná I., Levin L. Effect of assessor's sex on visual color matching in dentistry: A systematic review of the literature. Journal of Esthetic and Restorative Dentistry. 2022;34(2):383-396.**

This study systematically discusses whether an individual's gender has an influence on the choice of colour for future reconstruction. It also includes other factors that can influence the choice of colour such as light, training, experience, surrounding environment and so on. This systematic study was developed during a research internship at the University of Alberta in Canada.

2. **Hynková K., Voborná I., Linke B., Levin L. Compendium of current ceramic materials used for the CAD/CAM dentistry. Acta Stomatologica Marisiensis Journal. 2021;4(1):7-17.**

This study reviews and introduces readers to the current CAD/CAM ceramic materials on the market, their composition, suitable indications, optical and mechanical properties. This review article was developed during a research internship at the University of Alberta in Canada.

3. **Hynková, Kristýna, Mutlu Özcan, and Iva Voborná. Composition and mechanical properties of contemporary CAD/CAM glass ceramics. Italian journal of Dental Medicine. 2020;5/4:64- 69.**

This study introduces the main three groups of glass CAD/CAM ceramic materials, explains and reviews the important mechanical properties and compares them with the mechanical properties of main hard dental tissues such as dentin and enamel. This study was developed by cooperation with Zürich University.

4. **Hynková K., Voborná I. Dental ceramic – mechanical properties. Czech Stomatology & Practical Dentistry. 2022;122(3):87-94.**

This article describes the main mechanical properties of dental ceramic and the available testing methods which can be used to measure these properties.

5. Hynková K., Pospíšilová L., Voborná I. Manual toothbrushes – bristles quality. Czech Stomatology & Practical Dentistry.2023;123(1):11-17.

This original study focuses on the quality of toothbrushes bristles of different brands of toothbrushes available on Czech market.

6. **Hynková K., Deng H., Voborná I. The effect of the pre-crystallization defect size on the strength limitation in lithium silicate glass ceramics. Journal Ceramics - Silikáty. 2023;67(2):135-141 doi: 10.13168/cs.2023.0010.**

This original study focuses on how the size of pre-crystallization defects affects the strength of a lithium disilicate glass ceramic. This original study was developed during a research internship at the University of Alberta in Canada.

9. ACKNOWLEDGEMENT

I would like to express my thanks to my supervisor MDDr. Iva Voborná PhD. for her supervision and guidance throughout doctoral studies.

I would like to thank Palacký University Olomouc for financial support during my two-year research internship at University of Alberta. For provision of laboratories and equipment for research study I would like to thank the University of Alberta School of Dentistry.

Words cannot express especially my gratitude to my parents who encouraged me not only through the doctoral studies but in all my life. Thank you very much for everything.

10. UNDERTAKING

I, Kristýna Hynková, honestly declare that I carried out this dissertation independently and that I have listed all used literature and other sources.

……

Signature

In Olomouc

……

Date